VOLTAGE GATEABLE IONIC PORES INDUCED BY ALAMETHICIN IN BLACK LIPID MEMBRANES

Thesis by

Moisés Eisenberg-Grünberg

In Partial Fulfillment of the Requirements

For the Degree of

Doctor of Philosophy

California Institute of Technology

Pasadena, California

1972

(Submitted September 12, 1972)

To

Mela and David

ACKNOWLEDGMENTS

After being at Caltech for the last five years, I feel that I owe an enormous amount of gratitude to a very large number of people, so large a number that I cannot mention them all here, but their help has nonetheless been essential and much appreciated. To all of them, muchas gracias.

I especially want to thank Dr. Max Delbrück for his excellent advice and patience with me as his student. Dr. Carver Mead, for a lab, the design of the channel statistics analyser, and keeping me on the track with his incisive counsel. And Dr. James Hall, dear friend and colleague, who shared with me the research and its ups and downs.

A la Universidad de Chile agradezco el patrocinio de mis estudios y en especial a mi profesor y amigo, Dr. Guillermo Contreras, cuyo impulso inicial hizo realidad mi carrera en Biofisica.

I am indebted to the Rockefeller Foundation for their continuous financial support.

ABSTRACT

The strongly surface-active polypeptide antibiotic alamethicin (m.w. ~ 1700) interacts with artificial black lipid membranes to form voltage gateable ionic channels with five discrete conductance states. The channels fluctuate between these states with transition rates which depend little on the applied voltage. Within any conductance state, the behavior is approximately ohmic and similar to bulk solutions. When added on one side only, alamethicin confers upon a phosphatidyl-ethanolamine-decane black film a pronounced asymmetry. The alamethicin channels are only slightly ion selective, their rate of formation is strongly dependent on the alamethicin concentration, on the voltage across the membrane and on the ionic strengths.

TABLE OF CONTENTS

I. INTRODUCTION

I.1 Statement of the Problem

The operation of the nervous system depends in part on the excitable membranes surrounding most of the cells which form part of it. Electrical, chemical, and pharmacological evidence indicates that the ionic permeability through the nerve cell membrane, which underlies its excitability, is due to the existence of channels, or pores, of at least two kinds, namely, the sodium channel and the potassium channel.

The detailed experimental study of single ionic pores in some artificial systems is quite easy, but it is next to impossible in biological preparations. Therefore, with the hope that the understanding of single pore mechanisms in an artificial system will aid in the understanding of ionic pores in general, we propose to characterize a particular type of voltage gateable ionic pore induced by the cyclic polypeptide antiobiotic alamethicin, in black lipid films of well defined components. We do not pretend to imply that the alamethicin pore in artificial membranes is a model of, say, the potassium channel in nerve membranes, but rather that the study of ionic pores in these *in vitro* membrane systems is a possible aid to the understanding of pore forming systems.

We will show that even such a relatively simple artificial system is fairly complicated. We feel that our investigation, together with those of other groups currently working on different aspects of alamethicin-membrane interactions, will advance the understanding of

the molecular mechanisms that underlie this particular kind of ionic pore.

I.2 General Background on Biomembranes

With the advent of the microscope in the XVII Century, and Robert Hooke's observations, the notion that living organisms are constituted of one or more cells, each surrounded by a boundary, appeared. Nevertheless, the idea of a cell membrane as we know it today, remained an unproven concept, and most of today's concrete knowledge of biomembranes has been developed since the advent of electron microscopy. Many reviews have been written on the topic of biological membranes, and it is not my intention to attempt to write another. For recent reviews I refer the reader to Singer and Nicolson (1972), Chapman (1970), Branton (1969), and Stoeckenius and Engelman (1969).

The principal constituents of biological membranes are lipids and proteins. New analytical techniques have allowed the identification of most of the lipid components of biological membranes (Rouser, Nelson, Fleischer and Simon, 1968). Membrane proteins, on the other hand, are much less known. In some cases, such as the myelin sheath, the protein composition has been determined (Eng, Chao, Gerstl, Pratt, and Tavaststjerna, 1968). In many enveloped viruses, the protein composition has also been determined to the extent of the number of components, their molecular weight and the sugar and amino acid contents (Burge and Strauss, 1970). But the isolation of membrane proteins in native form and pure has yet to be done.

Current models on membrane structure (Singer and Nicolson,

1972) seem to indicate that at least part of a biological membrane is a lipid bilayer (in a liquid crystalline state), in which proteins are embedded, either partially or, in some cases, bridging across the thickness of the bilayer. This is schematically represented in fig. 1. The amphiphilic nature of the lipid molecules makes them particularly suited for building a double layer. The hydrophobic interactions between the fatty acid chains of adjacent and juxtaposed lipid molecules form an oily permeation barrier that isolates the aqueous media on the two sides of the membrane, from each other.

The lipid bilayer part of the biological membrane is in a rather dynamical state and lateral diffusion of molecules in the plane of the membrane occurs (Frye and Edidin, 1970). Lipid-protein complexes probably form structural units. Thus we can conceive of membranes as mosaics of units diffusing laterally with different rates depending on their size and other properties.

Although this type of model has a wide popularity, the evidence to support it is indirect, and several other models for the structure of biological membranes are in circulation. For instance, Rouser (1971), proposes a membrane made of units, each of which has, from the outside to the inside of the membrane, six layers, namely: lipid, protein, lipid, lipid, protein, lipid. All of the subunits would align so to make the overall membrane six-layered. In this case, the lipid molecules would be lying with their hydrocarbon tails parallel to the plane of the membrane, and hydrophobic and hydrophilic interactions between lipid and protein, and lipid with lipid would be rather specific. The model is a consequence of quantitative analytical study

Fig. 1. Schematic representation of a membrane structure. The lipids are in a bilayer configuration. Some proteins may bridge across the thickness of the membrane. The hydrocarbon chains are in a fairly liquid state and the membrane is in a dynamic state. Proteins can diffuse laterally. (Not in scale.)

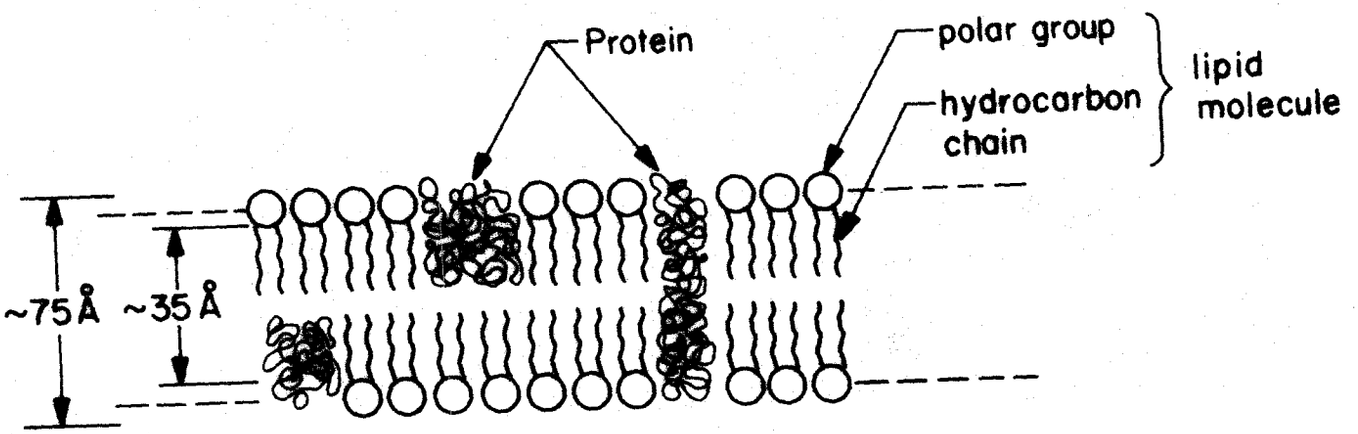
Protein
polar group
hydrocarbon chain
lipid molecule
~75Å
~35Å

FIG. 1

of membrane composition, and imagination, and it explains the known properties of red blood cell membranes and myelin sheath. Its weakest point is the very unfavorable situation of having the top layers of lipid with part of their hydrocarbon chains in contact with the aqueous phase. Perhaps one should postulate that the hydrocarbon part of the extreme outer and inner lipids actually penetrates the neighboring protein layer into a less polar region.

Biological membranes perform an enormous variety of functions. The biological function that is most closely related to our model system, and which motivated the study of the model, is the excitability of the membrane of the nerve fiber and its synaptic processes.

I.3 Ionic Pores in Biological Membranes

The study of the electrical properties of the giant axon of the squid, under the voltage clamp technique, by Hodgkin, Huxley and Katz (1952), and subsequent formulation of their observations on the ionic currents involved, in terms of a mathematical model, Hodgkin and Huxley (1952), marks a turning point in the understanding of excitation phenomena in membranes, since with their model, the properties of the action potential and its propagation follow immediately if the permeabilities of Na^+ and K^+ are known as functions of voltage and time. Although this model was not based on molecular mechanisms that govern the ionic permeabilities of the axonic membrane (and no such model could be constructed even today because these mechanisms are not known), it is quite likely that its success in explaining the experimental observations means that the model contains some information on the

physical events. Thus, we may take the separation of the parameters of the Na^+ conductance from those of the K^+ conductance in the Hodgkin-Huxley equations as a hint that the ionic movements of Na^+ and K^+ across the excitable membrane are independent of each other.

Hille (1970), reviews with admirable clarity the evidence on the independence of the pathways for the Na^+ and K^+ across the squid and lobster axons and in frog myelinated nerve fibers. The emerging picture is that the Na^+ channel is a gated pore which exists in two states, open or closed. Its conductance in the open state lies in the range 10^{-10} to 6×10^{-10} mho, as measured by several different methods. The density of Na^+ channels, ranges from about 3 channels/μ^2 in squid giant axons to about 300 channels/μ^2 in the node of frog myelinated fiber. More recent estimates, using radioactively labelled tetrodotoxin (a specific toxin that binds to the sodium channel with a large affinity and in a 1:1 stoichiometry), indicates that there are approximately 5 to 100 Na^+ channels/μ^2 in different axons of giant squid and lobster (B. Hille, personal communication).

The shifts of the sodium conductance along the voltage axis, with increasing Ca^{++} concentration and decreasing pH, at the outside of the frog myelinated fiber node, suggests that there are areas of fixed negative charge near these ionic channels. The block of the sodium permeability by protons at low pH, suggests the presence of an essential ionized acid group at the sodium channel with a pK_a of 5.2. Recent experiments show that the pK_a increases as the potential across the membrane is made more negative inside the fiber's node. Assuming that the distribution of protons in the electric field follows a Boltz-

man distribution, these experiments can be interpreted as saying that the titratable acid group is about one quarter of the way inside of the sodium channel (Hille, personal communication).

These Na^+ channels, finally, are not totally Na^+ selective, but they let other ions go through, although with lesser permeability. The following cations with their permeabilities relative to that of sodium is parentheses, have been measured: Li(1), K(1/13), NH_4 (1/6), guanidinium (1/7), hydrazine (3/5), hydroxylamine (1) (Hille, 1970).

Probably the most specific features of the Na^+ channel are the time course of its conductance after a voltage step and its high affinity for tetrodotoxin, a drug which drastically blocks its conductance.

The characteristics of the potassium channels are not well known. It is likely that these channels are narrower than the Na^+ channels and that their conductance is about 10^{-12} mho in the squid axon. The K^+ channels have a membrane density of about 50 times that of the sodium channels, and they can be blocked by tetraethylammonium, but the inhibiting site is at the inside for the axon membrane and at the outside for the frog myelinated nerve fiber node.

Although the existence of sodium and potassium channels of axons and node of Ranvier from frog myelineated fibers is backed by extensive evidence, these are not the only ones. Many other biological membranes show excitability phenomena due to the existence of several ionic channels.

I.4 General Background on Model Membranes

Mueller, Rudin, Tien, and Wescott (1962), first reported on a novel *in vitro* membrane system, known as black lipid film.

Some lipid, or a mixture of lipids, dissolved in a non-polar solvent, usually an alkane (octane to hexadecane), or chloroform-methanol-tocopherol, can be spread in a small orifice (~ 1 mm diameter) drilled through an electrically insulating partition separating two aqueous compartments. The lipid solution spread in that way, will spontaneously form a thin film, about 50 to 75 Å thick, in equilibrium with a torus of the bulk solution that remains attached to the rim of the orifice (see sec. III.1). The black lipid film is in the lipid bilayer configuration with the polar groups of the lipids facing the water phases and the hydrocarbon chains and solvent molecules forming a fairly liquid layer.

Even though the molar fractions of the lipid components and the solvents are known for the membrane forming solution, they are not necessarily the same in the black film. Andrews, Manev and Haydon (1970), have studied this phenomenon for a system of glyceryl-mono-oleate in alkane solvents of different lengths and came to the conclusion that the molar ratio of hydrocarbon chains from the lipid to the solvent molecules increases with the length of the solvent, in such a way that with hexadecane as the solvent, there is practically none of it in the black film. With n-decane as the solvent, the molar ratio is about 0.5.

Black lipid films resemble biological membranes in the bilayer configuration of their lipids, in their thickness, in their permeability to water and in their electrical capacitance. But, these artificial

membranes have a very low conductance, namely, between 10^{-8} mho/cm^2 to 10^{-6} mho/cm^2, when formed between aqueous salt solutions. In contrast, biomembranes have conductances of the order of 10^{-3} mho/cm^2. Nevertheless, the addition of certain molecules can raise the conductance of these black films to levels comparable with those of biological membranes. Further, some of these modifiers confer ionic selectivity on the lipid film.

This type of model membrane has the following desirable qualities. One can know the components with a great degree of precision. The monitoring of electrical properties is easily accomplished. There are many parameters that can be experimentally varied (composition of membrane, nature of ionic environment, temperature, etc.). And lastly, due to the fact that the bare membrane has such a low conductance, we know that conductance changes induced by the addition of modifiers are directly caused by the modifier reaching the membrane.

A variation on the Mueller and Rudin planar membrane is its spherical counterpart, where a sphere of black lipid film in equilibrium with a cap of bulk lipid solution, separating the aqueous media of the inside and outside, can be maintained in buoyancy in a sucrose density gradient. Pagano and Thompson (1967), first described this type of membrane system. Even though the monitoring of its electrical properties is more cumbersome, this system has the advantage of allowing optical probing both parallel and perpendicular to the membrane surface. Yguerrabide and Stryer (1972), have studied the fluorescence spectroscopy, at different orientation angles relative to the plane of the bilayer, of several probes incorporated into spherical black lipid

films and thus obtained information on the alignment and degree of orientation of the emission transition moments.

Perhaps a membrane model system closer to the biological membrane is the lipid vesicle. When lipid water mixtures are sonicated, they form closed vesicles of lipid bilayers of either one single shell or many shells, inside each other (Huang, 1969). These can be further separated by chromatography in Sepharose 4B according to their size. The multilamellar vesicles come out first as a sharp peak, followed by a wide peak of the single bilayer vesicles. Their size correlates with the elution position, with a diameter range from 1300 Å to about 250 Å.

The homogeneity of the preparation, the knowledge of the total surface of the bilayer and the large surface to volume ratio make the lipid vesicle suited for magnetic resonance experiments, for studies of ionic fluxes across the bilayer, and for the studies of thermal transitions of bilayer membranes. On the other hand, they are not suitable for electrical measurements because of their very small size. Further, Sheetz and Chan (1972), have shown that the curvature of these lipid vesicles, and also similar vesicles made from sonicated ghosts of red blood cells (Sheetz, 1972) significantly alters the bilayer structure of the membranes, for the small size vesicles.

To a great extent, the bilayer vesicle and the black lipid film are complementary model systems.

A great deal of work has been done on these artificial lipid membrane systems, especially related to the action of modifiers. For reviews on these subjects, I refer the reader to Bangham (1968),

Mueller and Rudin (1969), Delbrück (1971), Haydon (1970), and Haydon and Hladky (1972).

Modifiers which give the artificial membrane system different electrical properties from those of the bare membrane can be classified according to their mechanisms of action. Among them, carriers and uncouplers will be briefly discussed in what follows and pore formers will be dealt with in the next section.

Black lipid films are very impermeable to small cations and anions (Na^+, K^+, Ca^{++}, Cl^-, etc.). In particular this is also true for I^-. But, in the presence of I_2 and I^- simultaneously, the electrical conductivity of a black film increases substantially (Läuger, Lesslauer, Marti, and Richter, 1967; Finkelstein and Cass, 1968). These authors suggest that the premeant species might be an I_3^-, I_5^-, or even higher order polyiodide anion, therefore, its larger size would allow its negative charge to become more delocalized and thus increase its partition coefficient relative to the membrane.

A number of macrocyclic antibiotics that show profound influence on ion transfer across biological membranes (Moore and Pressman, 1964; Pressman, 1968; Harris, 1968) are very effective in enhancing cation transfer across black lipid membranes (Mueller and Rudin, 1967). In particular, valinomycin (a cyclic dodecadepsipeptide) and the macrotetralide antibiotics (nonactin, monactin, etc.), induce, in a black film, cationic conductance increases which are proportional to both the antiobiotic and the salt concentrations, and are highly selective. (Eisenman, Ciani, and Szabo, 1968; Tosteson, Andreoli, Tieffenberg, and Cook, 1968; Gotlib, Buzhinsky, and Lev, 1968). The permeabilities

induced by valinomycin to a few monovalent cations are, in order of decreasing selectivities $H^+ > Rb^+ > K^+ > Cs^+ > Na^+ = Li^+$ (Eisenman et al., 1968).

The mechanism of the specificity of the molecules is suggested by the determination of their structure. Kilbourne, Dunitz, Pioda and Simon (1967), described the crystal structure of nonactin-K^+ as resembling the seam of a tennis ball with the unhydrated K^+ ion at the center of the ball, 8-coordinated to oxygens. The selectivity originates from the closeness of the fit and hence the relative strengths of the chelation for the various ions. The valinomycin-K^+ complex has been studied by several groups (Ivanov, Leone, Abdulaev, Senyavina, Popov, Ovchinikov, and Shemyakin, 1969; Pinkerton, Steinrauf, and Dawkins, 1969; Duax, 1972). A picture similar to that derived for nonactin has emerged.

The mechanism of ion transfer by these selectivity inducing macrocyclic antibiotics, has been studied (Eisenman et al., 1968; Läuger and Stark, 1970; Stark, Ketterer, Benz, and Läuger, 1972; Hall, Mead, and Szabo, 1972). It can be described as a carrier mechanism. The carrier molecule (nonactin, valinomycin) binds the unhydrated carried cation at one interface, and makes a membrane soluble carrier-ion charged complex, that moves across the bilayer under the influence of the electric field, releases the ion in the other side, and returns uncharged to repeat the cycle. Clearly, any one of these processes could be rate limiting. Translocation of the ion-carrier complex across the membrane is likely to be the step most strongly dependent on voltage. For translocation to take place, the carrier-ion complex must

surmount an energy barrier resulting from the low dielectric constant of the thin slab of hydrocarbon phase, at the center of the bilayer. The barrier shape can be an important factor in determining the detailed voltage dependence of transmembrane ionic flows. Hall et al. (1972), have shown that a single flat topped, symmetric barrier shape, spanning about 1/3 of the hydrocarbon layer, accurately describes the experimental results on the basis of a carrier model.

Uncouplers of oxidative phosphorylation in mitochrondria have also been studied with black lipid films. All uncouplers have been shown to increase the conductance of phospholipid membranes, and many of them produce a resting potential in the presence of a pH gradient. Hopfer, Lehninger, and Thompson (1968), and Liberman and Topaly (1968), studying the effects of 2-4 dinitrophenol (DNP) on black lipid films suggested that these uncouplers may indeed be good proton carriers. Finkelstein (1970); and Lea and Croghan (1969), suggested that for these weak acids, HA, which dissociate into $H^+ + A^-$, a better interpretation of the uncoupler mechanism might be that the weak acid HA, was acting as a carrier for the anion, A^-, the permeant species being the HA_2^- complex. Nevertheless, failure to obtain an accurate square dependence of the conductance on the DNP concentration (Lieberman, Mochova, Skulachev, and Topaly, 1968) and the characteristics of DNP induced conductance in black lipid films of charged phospholipids (Hopfer, Lehninger, and Lennarz, 1970) have led McLaughlin (1972) to study the effects of DNP on the surface charge of neutral black lipid films. Thus, by requiring that DNP, in addition to acting as a carrier, also binds to the surface of the black film and introduces a

screening effect, Finkelstein's (1970) model can quantitatively explain all of the experimental results observed.

Conductance changes in black lipid films in the presence of proteins have been reported (Del Castillo, Rodríguez, Romero, and Sánchez, 1966; Barfort, Arquilla, and Vogelhut, 1968). These authors have observed conductance changes brought about by the simultaneous presence of an antigen and its specific antibody. The presence of either one alone had no effect. Unfortunately there is little data suggestive of a particular mechanism of the conductance increase.

I.5 Pore Formers in Black Lipid Membranes

I.5.1 EIM (Excitability Inducing Material)

EIM is a proteinaceous extract from Aerobacter cloacae ATCC 961 (Kushnir, 1968) whose chemical composition is as yet unknown. Mueller and Rudin (1963) first reported on the excitability induced by EIM in black lipid films made from crude extracts of beef brain lipids dissolved in chloroform, methanol and tocopherol. Steady state current-voltage characteristics of the EIM doped lipid membranes showed that the zero volt conductance was typically between 3 to 5 orders of magnitude higher than that of the bare black lipid membrane, depending on the amount of EIM added and the type of lipid used. At higher voltages, the conductance drastically diminished to values of 1/5 to 1/100 of the zero volt conductance, with an accompanying n-shaped negative resistance region. Such behavior predicts the possibility of inducing regenerative transitions between the low and high conductance states following current pulses.

Mueller and Rudin (1963) have in fact observed these regenerative transitions. They assume that EIM induces channels in the membrane, each of which has two conductance states, with voltage dependent rates for the forward and backward transitions between the states. The relative number of channels in each state is determined by the difference in the free energy between the states which is postulated to be a function of the applied membrane potential.

Mueller and Rudin (1963), constructed a theoretical model that could explain all of the transition kinetics of these excitable artificial systems. Their predictions proved to be true when Bean, Shepherd, Chan, and Eichner (1969) showed that the addition of EIM to black lipid films induces increases in conductance which occur in discrete steps of about 4×10^{-10} mho, suggesting the presence of individual conducting channels.

Ehrenstein, Lecar, and Nossal (1970), subsequently showed that, after the addition of sufficiently small amounts of EIM, the current through the black lipid membrane fluctuates between discrete levels. Thus, they were able to have membranes with only two levels, only three levels, and so forth. They interpreted these levels as reflecting conductance channels that can be in two states, high or "open" state, and low or "closed" state. Thus, a membrane with four levels reflects the existence of three channels, the lowest level being that of all-three channels simultaneously in the low conductance state. The conductance step between neighboring levels was measured and it gave values between 2.2 and 3.5×10^{-10} mho, independent of the voltage, from 0 to 80 mV. The conductance of the lowest level relative to the bare membrane

conductance, was also voltage independent and it gave a value of 4×10^{-10} mho per channel, in agreement with Bean et al. (1969).

Ehrenstein et al. (1970), measured the average fraction of the time that these EIM induced channels remained in the high conductance state, and they showed that it was a function of the voltage, such that at zero voltage it was 1, but at a higher voltage, corresponding to the low conductance in the steady state, it was 0. Moreover, this distribution closely followed the voltage dependence of the steady state conductance.

A statistical study of the behavior of membranes containing four EIM induced channels (Ehrenstein et al., 1970) showed that, if one assumes that the channels are identical and statistically independent, the mean conductance, and the distribution of the fraction of time that a given number of channels spends in the open state, could be well explained.

Bean (1972) has recently shown that this picture is complicated by the existence of more than two conductance states of the EIM channel. The number of states, as well as their conductances, depends on the type of black lipid film used. Thus, in sphingomyelin-tocopherol-chloroform-methanol membranes, a single channel can exist in four conductance states about equally spaced. In dipalmitoyl lecithin and oxidized cholesterol in nonane, there are three states, the second one very close to the lowest.

Measurement of the conductance of the EIM channel and its intermediate conductance states as a function of NaCl activity in the aqueous media showed a linear relationship (Bean, 1972).

Mueller and Rudin (1968) have shown that the presence of an ionic gradient across an EIM containing black lipid film develops a resting potential of a sign and magnitude expected for a perfect cation selective membrane (59 mV/decade of gradient). The addition of polycations such as Protamine shifts this to an anionic resting potential. Careful titration on the amount of protamine added leads to bistable states, and voltage oscillations at constant current occur under those conditions.

I.5.2 Gramicidin A

Gramicidin A is a linear pentadecapeptide antibiotic containing alternating L and D residues (Sarges and Witkop, 1964). The end groups are blocked by formylation of the amino terminus and by amide-bond linkage to ethanolamine at the carboxy terminus (Sarge et al., 1964).

Hladky and Haydon (1970) first reported the observation of discrete conductance steps induced by gramicidin A on black lipid films of glycerolmonooleate in n-decane. These conductance steps had ohmic conductance on the order of 2.4×10^{-11} mho, at a concentration of 1.0 M NaCl in the aqueous phase. The conductance of these discrete steps showed a square root dependence on the NaCl concentration in the aqueous phase. The duration of the conductance steps was between 100 msec. and two seconds (there might be faster fluctuations that would not be resolved by their apparatus). The frequency of the conductance steps increased with voltage, and the conductance for K^+ was about twice the conductance for Na^+.

Electrolytes other than NaCl and KCl have also been studied.

The conductance relative to that of Na^+ are: H^+ (14), Li^+ (0.24), Na^+ (1), K^+ (1.8), Rb^+ (2.9), Cs^+ (2.9), Ca^{++} (0.01), (Myers and Haydon, 1972).

These data suggest that gramicidin A produces pores across the black lipid membrane.

Urry (1971), and Urry, Goodall, Glickson, and Mayer (1971) have proposed a left handed $\pi_{(L,D)}$ helical structure for gramicidin A with a lipophilic exterior, provided by the non-polar side chains, and a polar interior. This structure has the capability of forming a transmembrane structure by dimerization through hydrogen bonding at the formyl end. Different helices can be postulated, depending on the number of residues per turn, and consequently different diameter of their inner hydrophilic pore.

A helix with 6.3 residues per turn and 4 Å diameter pore size seemed the most favorable one, in view of the selectivity towards potassium (Hladky and Haydon, 1970). The length of a dimer, in that case, would be between 25 and 30 Å. Since this is somewhat shorter than the thickness of the non-polar region of a black lipid film, it was suggested that the membrane might thin around the gramicidin A dimer to allow the pore formation (Urry et al., 1971).

The dimer model for the channel is in agreement with the following observations. First, the conductance of gramicidin A treated lipid films depends on the square of the antibiotic concentration (Goodall, 1970). Second, one can chemically connect the amino ends by replacing the formyl groups from two gramicidin molecules, by one malonyl moiety, thus obtaining a complete transmembrane structure.

The induced conductance in black lipid films is simply proportional to the malonyl gramicidin A (Urry et al., 1971). Thirdly, deformylated gramicidin A has no effect on the conductance of lipid films.

Hladky and Haydon (1972) have studied the gramicidin A induced conductance of black lipid films of different thicknesses. Glycerylmonooleate alkane membranes have hydrocarbon region thicknesses of 31 Å, 40 Å, and 47 Å for the alkanes hexadecane, tetradecane, and decane, respectively (Fettiplace, Andrews, and Haydon, 1971). The single channel conductance of gramicidin A in the three membranes is the same. On the other hand, the mean duration of a single channel decreases (2.2 sec., 1.3 sec. and 0.4 sec., from the thinner to the thicker membrane).

When small amounts of gramicidin A are present in a glycerylmonooleate-decane black film, the number of open channels, n, fluctuates about a mean value, $\bar{n}$. If one assumes that the opening and closing of the channels occur as statistically independent events and that the number N of total gramicidin A molecules is much larger than $\bar{n}$, then the probability of finding a certain number of channels open at a given time should be given by the Poisson distribution. Hladky and Haydon (1972), have, in fact, found a distribution with a mean of 0.787, which agrees with a Poisson distribution up to $n = 4$.

Goodall (1972) reported on the kinetics of the conductance induced by gramicidin A on black phospholipid films of different charge. Although the kinetic data were rather confusing and seem to indicate that Gouy-Chapman double layer theory would have to be invoked, it provided indirect evidence that the conductance is larger for thinner membranes.

An interesting experiment that confirms the prediction that gramicidin A forms a transmembrane structure like a pore has been reported by Krasne, Eisenman and Szabo (1971). These authors report that planar black lipid membranes made of 2% w/v glyceryldipalmitate in n-decane undergo a phase transition at about 42°C. Above this temperature, the films are in the usual highly liquid hydrocarbon phase, below 42° they are frozen. This effect has been studied extensively by many authors (c.f., Philips, Williams, and Chapman, 1969), and these transitions are usually referred to as Chapman transitions. Krasne et al. (1971), observed that the conductance of black lipid films with gramicidin A, are the same above and below the Chapman transition in contrast with the finding that the conductance of black lipid membranes with nonactin and valinomycin (carriers) are four orders of magnitude less in the frozen membrane than in the melted one.

I.5.3 Alamethicin

Alamethicin (antibiotic U-22,324) was discovered in the culture broth of the fungus Trichoderma viride (Meyer and Reusser, 1967). Recently, Payne, Jakes, and Hartley (1970) have deduced its very curious primary structure. It is an 18 amino acid cyclized polypeptide, not cyclized into a simple ring but by a bond between the γ-carboxyl group of glutamic acid-17 and the imino group of proline-1. The structure thus becomes a ring of 17 amino acids with a pendant C-terminal glutamine residue (Fig. 2). Among its amino acids there are seven α-aminoisobutyric acid (α-Aib) residues. α-Aib is a very uncommon amino acid found only once before in another antibiotic (Kenner and Sheppard, 1958).

Fig. 2. Primary structure of alamethicin. Notice the unusual bond between the γ-carboxyl group of Glu-17 and the imino group of Pro-1 that closes the ring. The hydrophobic side chains have been drawn pointing outward from the center of the ring, and thus leaving a more hydrophilic interior. The carboxyl end of Glu-18 is free and ionizable with a pH of 5.5. Glu-18 has a great flexibility compared with the rest of the ring.

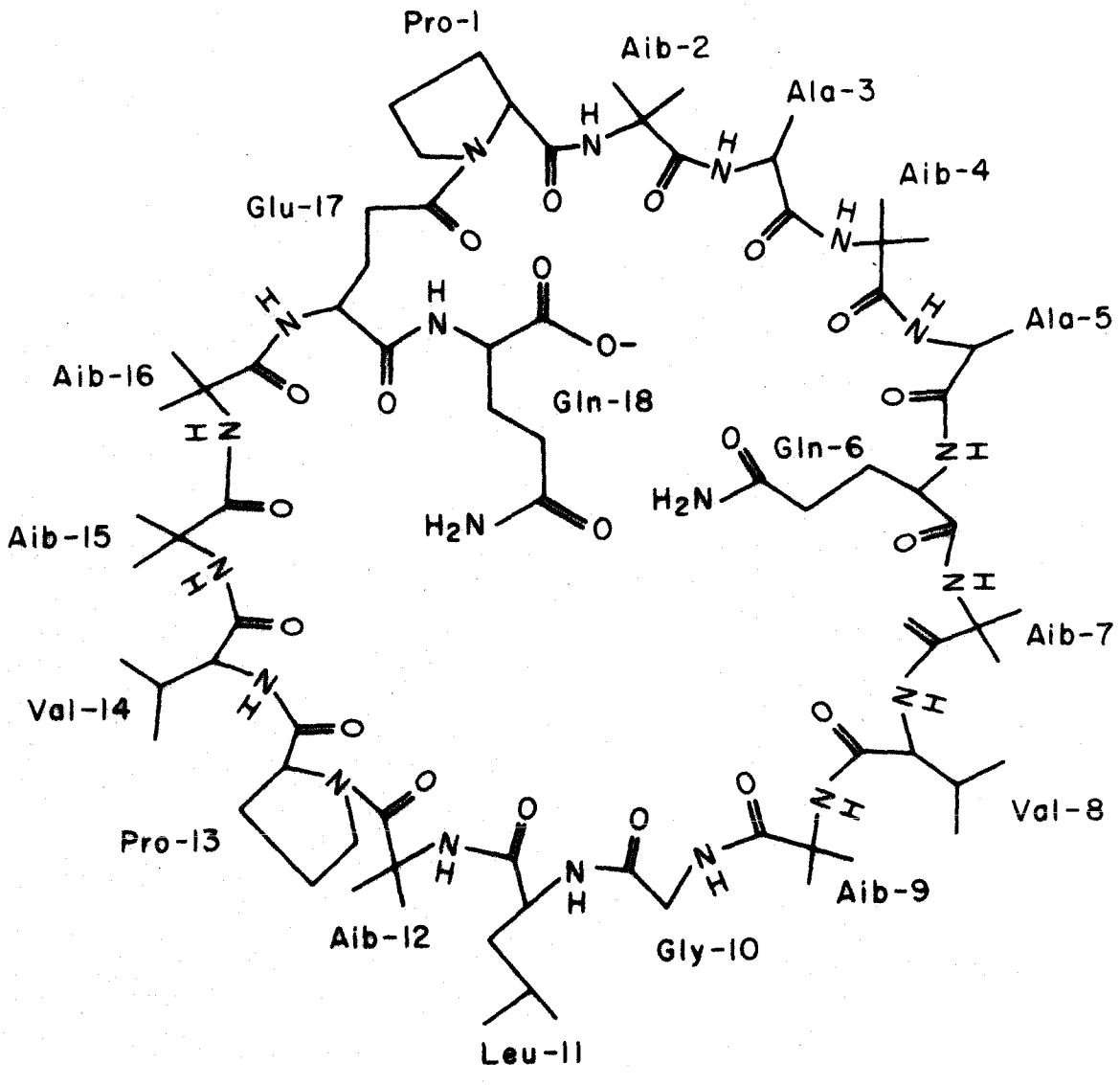
Pro-1
Aib-2
Ala-3
Aib-4
Glu-17
Ala-5
Aib-16
Gln-18
Gln-6
Aib-15
Aib-7
Val-14
Val-8
Pro-13
Aib-9
Aib-12
Gly-10
Leu-11

FIG. 2

The amino acid analysis of alamethicin (Payne et al., 1970) gave non-integral quantities for α-Aib and alanine, per polypeptide molecule. The authors concluded that the sample of alamethicin was probably a mixture of two or more forms. The predominant form containing two alanine and seven α-aminoisobutyric acid residues, whereas in the remaining molecules, an alanine residue at position-3 or position-5 is replaced by an α-Aib residue. These forms differ only slightly. McMullen (1970) has reported the separation of two additional components by thin layer chromatography analyses, but lack of discrimination in the ultracentrifugal analysis (McMullen and Stirrup, 1971) suggest that this is a microheterogeneity typical of polypeptides synthesized by non-ribosomal routes (Reusser, 1967).

Mueller and Rudin (1968) first reported on the interaction of alamethicin with black lipid membranes. The membrane systems they used were mixed brain lipids—tocopherol-chloroform-methanol, lecithin-decane, sphingomyelin-tocopherol-chloroform-methanol, or oxidized cholesterol-octane.

These authors reported that the addition of alamethicin at one side of a black film in the presence of 0.1 M NaCl induced conductance increases that depended exponentially on voltage (e-fold/5 mV) asymmetric about zero volts, higher for positive voltages at the side to which alamethicin had been added. The conductance depended on the sixth power of both the alamethicin and the salt concentrations.

In the presence of salt gradients across the black membrane, alamethicin showed cationic resting potentials of the order of 10 to 30 mV/decade of concentration gradient, but not intracationic specific-

ity (although Mueller and Rudin do not specify which ions they tested). Furthermore, the salt gradients induced a negative slope resistance, as expected for a steeply voltage dependent conductance with a non-zero resting potential.

The addition of protamine to an alamethicin doped black lipid film in symmetric salt solutions increased the zero volt conductance by a factor of about 40 and gave rise to a negative resistance, in the absence of a resting potential (Mueller and Rudin, 1968). They have interpreted these effects as resulting from phase boundary potential changes accompanying adsorption of basic proteins to the membrane water interphase.

The system described by Mueller and Rudin (1968) contains some of the elements found for the EIM system (see above), with the important difference that in the latter the system intrinsically rests in the high conductance state and voltage will drive it to the low conductance state, whereas in the alamethicin system the voltage dependence is reversed.

Experiments performed on alamethicin modified black films by Mueller and Rudin (1968), with current pulses and observation of the time dependence of the voltage across the membrane, essentially showed what might be expected from the steady state i-v curves for the different conditions mentioned above. Thus, by careful titration of the amount of protamine added to an alamethicin doped black membrane under a salt gradient, it was possible to obtain reversible switching between two stable resting potentials in response to current stimuli, single action potentials and subthreshold responses to current stimuli, as well

as spontaneous rhythmic firing when the current was maintained at a critical level (Mueller and Rudin, 1968).

The kinetics of the conductance increase following voltage pulses was also reported by Mueller and Rudin (1968). They claimed that the kinetic order of the reaction was six, and that the maximal rate of conductance change depended on the sixth power of the alamethicin concentration. An instantaneous change of sign of the clamped voltage across the alamethicin doped black lipid films showed that the reversed membrane current underwent a marked decline before building up to its starting level, suggesting that the conducting system exists in some well defined polarized state across the membrane.

Cherry, Chapman, and Graham (1972) have also published observations on the interaction of alamethicin with black lipid membranes. They confirmed some of Mueller and Rudin's results and have added a few new observations.

Most striking is their finding that the alamethicin induced conductance of black films does saturate for increasing salt concentration above 0.001 M KCl and above 0.1 M NaCl.

Further, they observed an alamethicin induced, voltage independent conductance, apart from the voltage-dependent conductance reported by Mueller and Rudin (1968). This conductance we can best define as the zero-volt conductance. Cherry et al. (1972) have found this zero-volt conductance to be proportional to the sixth power of the alamethicin concentration, for a lecithin-squalene-decane black membrane.

The voltage dependent conductance was exponential but with different rates than those previously reported. Namely, for KCl and $CaCl_2$, an e-fold increase in conductance every 4.5 mV and every 2.1 mV. This is steeper than the e-fold/5 mV reported by Mueller and Rudin.

The pH dependence of the conductance of alamethicin induced in egg lecithin-cholesterol-decane-chloroform membranes was found to be negligible.

Finer, Hauser, and Chapman (1969), and Hauser, Finer, and Chapman (1970) have studied the interaction of alamethicin with phospholipid membrane systems by nuclear magnetic resonance techniques. They report on unsonicated and sonicated phospholipid-alamethicin suspension in D_2O. Their high resolution nmr seems to be not high enough to draw any conclusions from the unsonicated system. On the other hand, in the sonicated system, where vesicles of small size are formed, they were able to obtain resolved nmr spectra and to draw a number of far-reaching conclusions. Sheetz and Chan (1972) have shown that sonicated vesicles of small size are intrinsically in a distorted bilayer configuration, due to the small radius of curvature. Consequently, these are not necessarily applicable to flat black lipid films. Some qualitative properties of the interactions found by Hauser et al. (1970) follow.

It is apparent that alamethicin interacts more strongly with the negatively charged phosphatidylserine than with the neutral phosphatidylcholine sonicated vesicles. This is an indication that alamethicin is not negatively charged when interacting with phospholipids, in particular with membranes.

Regardless of the precise site of localization of the alamethicin molecules relative to the lipid bilayer, alamethicin must be decreasing the hydrocarbon chains' mobility to some extent. Hauser et al. (1970) have measured the percent of immobilized hydrocarbon chains as a function of the ratio of phospholipid to alamethicin molecules in their sonicated system. Since the partition of the alamethicin between the lipid and the aqueous phases is unknown, they obtain only an upper limit. The strikingly high values they have reported are 600 and ~ 10 lipid molecules with immobilized hydrocarbon chains per alamethicin molecule for phosphatidylserine and phosphatidylcholine, respectively.

Recent evidence on PMR of lecithin-alamethicin dispersions in D_2O (unsonicated) in the Fourier transform mode to increase resolution (Lau and Chan, personal communication) show that the Chapman transition of these systems, as compared with the one without alamethicin, has been somewhat broadened as it would be expected from an interfacially bound impurity.

The sedimentation of alamethicin has been studied in low dielectric solvents such as ethanol, and in aqueous solutions (McMullen and Stirrup, 1971). These measurements show that alamethicin is quite soluble in ethanol, ethanol containing up to 50% water, and ethanol containing 10% aqueous NaCl up to 0.5 M solution. This is evidenced by the constancy of the sedimentation coefficient ($\overline{s}_{20^\circ,w} = 0.363$) and the calculated molecular weight ($\overline{m.w.}$ = 1760; theoretical mol. weight = 1691), for alamethicin concentrations ranging from 0.1% to 1.0% w/V in those solvents.

These results have to be contrasted with those obtained for alamethicin in 0.2 ionic strength phosphate buffer at pH 8. Sedimentation coefficients show that at 0.6 and 0.8% w/v concentration of alamethicin, the aggregation number of alamethicin monomers is 16.2 and 16.8. At alamethicin concentrations of about 0.2% w/v it is estimated to be around 6 monomers per micelle.

Urea has some disaggregation effect, although limited. Furthermore, at 0.2% w/v alamethicin concentration in phosphate buffer, there is a strong micellization dependence on the buffer's ionic strength, from about 3 alamethicin molecules per aggregate at an ionic strength of 0.006 to an aggregation number of 15 at ionic strength of 1.2.

McMullen and Stirrup (1971) have also measured the critical micellar concentration of alamethicin in water solutions of 0.05 M KCl and dilute NaOH at pH 8.0 and at 30°C. They obtain a value of 2.4 μM, meaning that the monomeric form of alamethicin in the salt conditions indicated has a saturation value of 2.4×10^{-6} M, beyond which additional alamethicin molecules will micellize.

Direct evidence for the pore inducing property of alamethicin in black lipid films has been reported (Gordon and Haydon, 1972), These authors have measured discrete conductance states in alamethicin doped glycerylmonooleate-hexadecane black films. At constant voltage across the membrane, the current rises from the bare membrane conductance level and fluctuates rapidly (< 6 msec.) between discrete levels for a period, to return again to the bare membrane current level.

The grouping of the fluctuations in the way described is characteristic at low levels, and the frequency of occurrence of these

groups depends on the concentrations of the salt and alamethicin in a manner that was not reported.

The current levels are not equally spaced and the conductance steps between the bare membrane and the first level, between the first and second current level, and so forth, are: 1.0, 1.8, 2.1, 2.3, and 2.8 x 10^{-9} mho at 2.0 M KCl in the aqueous phase, and 210 mV across the membrane.

Although data are not given, Gordon and Haydon mention that the current-voltage characteristics of the conductance states are nearly ohmic but curve somewhat toward the current axis. The conductances of the discrete steps are approximately proportional to the electrolyte concentration for NaCl and KCl in the 1.0 M to 2.0 M range.

Similar to what was found for gramicidin A, the conductance levels are independent of the thickness of the membrane. This conductance mechanism does not show significant ion specificity.

With respect to current fluctuations, Gordon and Haydon point out that the likelihoods of finding the current at the different levels are not equal. In one case, where five levels are shown, levels three and four are more probable than the rest.

These authors interpret their results as indicative of the formation of two-dimensional aggregates of alamethicin on the surface of a membrane, such that under an applied voltage, each of these aggregates yields clusters of pores situated closely adjacent to each other.

I.5.4 Other Pore Formers

Recent evidence on discrete conductance steps in some protamine doped lecithin-squalene-decane black films (Boheim, 1972) indicate that these protamines may also be pore formers.

In the case of protamines the channels seem to have cation or anion selectivity depending on the state of the hydrocarbon phase of the black membranes, as evidenced by the selectivity shift induced by temperature changes. The analysis of bistability and selectivity shifts of the protamine pores, induced by its interaction with alamethicin, at concentrations where the alamethicin cannot by itself produce pores, led Boheim to the formulation of a model which suggests that alamethicin has a specific orientation relative to the membrane which is field sensitive, possibly due to the existence of an electric dipole moment.

Even though individual conductance steps have not been seen for any other membrane modifier, strong voltage dependent conductance and kinetic behavior of the antibiotics nystatin (Finkelstein and Cass, 1968) and monazomycin (Muller, 1971) strongly suggest that they are also pore formers in black lipid films.

II. MATERIALS AND METHODS

Chromatographically pure phosphatidyl ethanolamine (PE) and phosphatidyl glycerol (PG), from bacterial sources, were purchased from Analabs Inc. (North Haven, Conn.), Supelco Inc. (Bellefonte, Penn.), Calbiochem (La Jolla, Calif.), and General Biochemicals (Chagrin Falls, Ohio). n-Decane was obtained from Eastman (Rochester, N.Y.) and Aldrich Chemical Co. (Milwaukee, Wis.). All the salts, of ultra-pure quality, were purchased from Mann Research Lab. (Orangeburg, N.Y.) and Alfa Inorganics, Ventron (Beverly, Mass.). Glycerol, analytical reagent grade, was obtained from Malinckrodt (St. Louis, Mo.).

Alamethicin was kindly provided by Dr. G. B. Whitfield, from the Upjohn Co. (Kalamazoo, Mich.). This sample was from the same batch of alamethicin that was used by Payne, Jakes, and Hartley (1970), for their determination of its primary structure. They concluded that this material was probably composed of two or more fractions which differ in their relative contents of alanine and α-aminoisobutric acid (see Introduction).

Nonactin was kindly provided by Ms. Barbara Stearns from the Squibb Institute (New Brunswick, N.J.).

The water was distilled and bottled by Arrowhead Puritas (Los Angeles, Calif.), and passed through a "Deeminazer" demineralizer from Crystalab (Hartford, Conn.). The conductivity of this distilled, demineralized water was typically about 5×10^{-7} mho/cm.

Membrane forming solution was made by dissolving PE (or PG) in n-decane at 2.5% weight/volume at 65°C for 1 min. under nitrogen; it was brought back to room temperature for use, and to -20°C for storage. Stock solutions of salts were prepared at high concentration and diluted as required. Alamethicin stock solutions in water were made to 10^{-3}, 10^{-4}, and 10^{-5} gr/ml; all of them were stored at 2°C. The 10^{-3} gr/ml solution of alamethicin in water was dissolved at 2°C, stirring continuously overnight.

The experimental apparatus consisted mainly of three components, namely, the chamber itself, the supporting assembly, and the electrical equipment.

Several types of membrane set-ups were used. A typical one is shown schematically in fig. 3. Two chambers are separated by a vertical septum with a small cylindrical orifice. One chamber has a quartz window to allow visual monitoring of membrane formation through a stereo microscope (Wild Inc., Switzerland). The combined volumes of the chambers were between 5 ml and 20 ml. The diameter of the orifice varied between 0.25 mm and 2.5 mm, and the thickness of the septum was always about two thirds of the diameter of the orifice. A narrow cylindrical feeder channel (~ 0.065 mm diameter), drilled into the septum, connected the orifice with a polyethylene tube containing the membrane forming solution. This solution could be moved in and out using a Hamilton 10 µl syringe (Whittier, Calif.). In this way the area of the thin film could be controlled (fig. 3). The life-time of the black lipid membranes was maximized when the orifice was cylindrical, as described above. Moreover, with such an orifice shape, the area of black film

Fig. 3. (Left) Longitudinal cross-section of typical set-up. A. Quartz window, 1½ in. diameter by 1/8 in. thick. B: Septum with membrane forming orifice and feeder channel. C: Chamber. D: Aluminum housing. E: Aluminum plug to tighten set-up assembly. F: 4/40 nylon screw, with fitted gage 27 needle, to connect feeder channel to syringe. G: Membrane forming orifice.
(Right) Transversal cross-section of septum. F,G: same as left. H: Polyethylene tubing. I: 10 microliter syringe. J: Feeder channel.

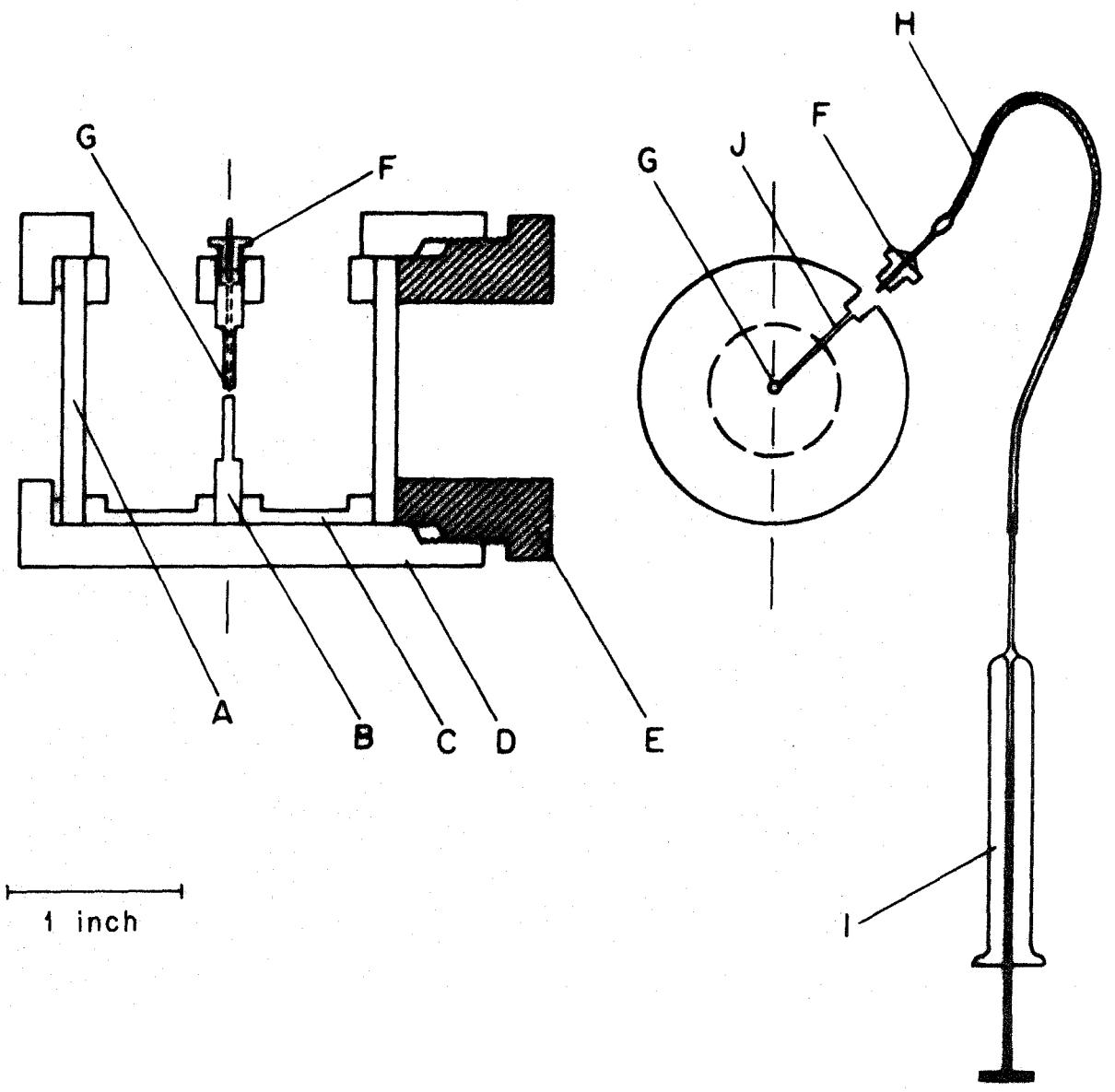

FIG. 3

could be easily controlled quantitatively with the amount of membrane forming solution moved through the feeder channel (White, 1971). The preferred material for the set-up was Teflon, but other plastics such as polyvinylchloride (PVC) and Delrin (DuPont), were also used with good results. The cleaning procedure for the set-ups consisted of ultrasonication in alkaline soap, such as Alconox (New York, N.Y.), followed by thorough rinsing in distilled water, chloroform, ethanol and demineralized distilled water. (Chloroform rinse was avoided for PVC parts.)

The set-ups had close fitting metal jackets through which water from a constant temperature bath could be circulated; the jackets also provided electrical shielding. Temperature was monitored with a Stolab 911 PL electronic thermometer (Stow Lab., Inc.; Hudson, Mass.). A well at the bottom of each chamber held a cylindrical Teflon coated magnet, 2 mm in diameter by 7 mm long, which stirred the chamber contents by means of a set of motor driven magnets under the set-up. The magnets rotated at about 1300 rpm. The stirring mechanism was mechanically isolated from the membrane set-up. The mechanical support is shown schematically in fig. 4, it consisted of a lead pedestal (ab. 35 lb) resting on a small motorcycle innertube. This system provided excellent isolation from external vibrations, and had a natural frequency of vibration of about 0.7 Hz.

A block diagram of the electrical set-up is depicted in fig. 5.

We used silver-silver chloride electrodes, made by passing a 1 mA current through a 0.9 mm diameter, 2 cm long, silver wire used as the anode, submerged in a 0.5 M solution of hydrochloric acid for 20 min. One pair of electrodes delivered any current necessary to maintain a

Fig. 4. Schematic cross-section of membrane set-up with mechanical isolation and stirring works. A: Membrane forming set-up. B: D.C. motor. C: Small motorcycle innertube. D: Lead pedestal. E: Magnet mounted on pulley, freewheeling around shaft. F: Teflon coated magnetic bar, 2mm diameter by 7mm long.

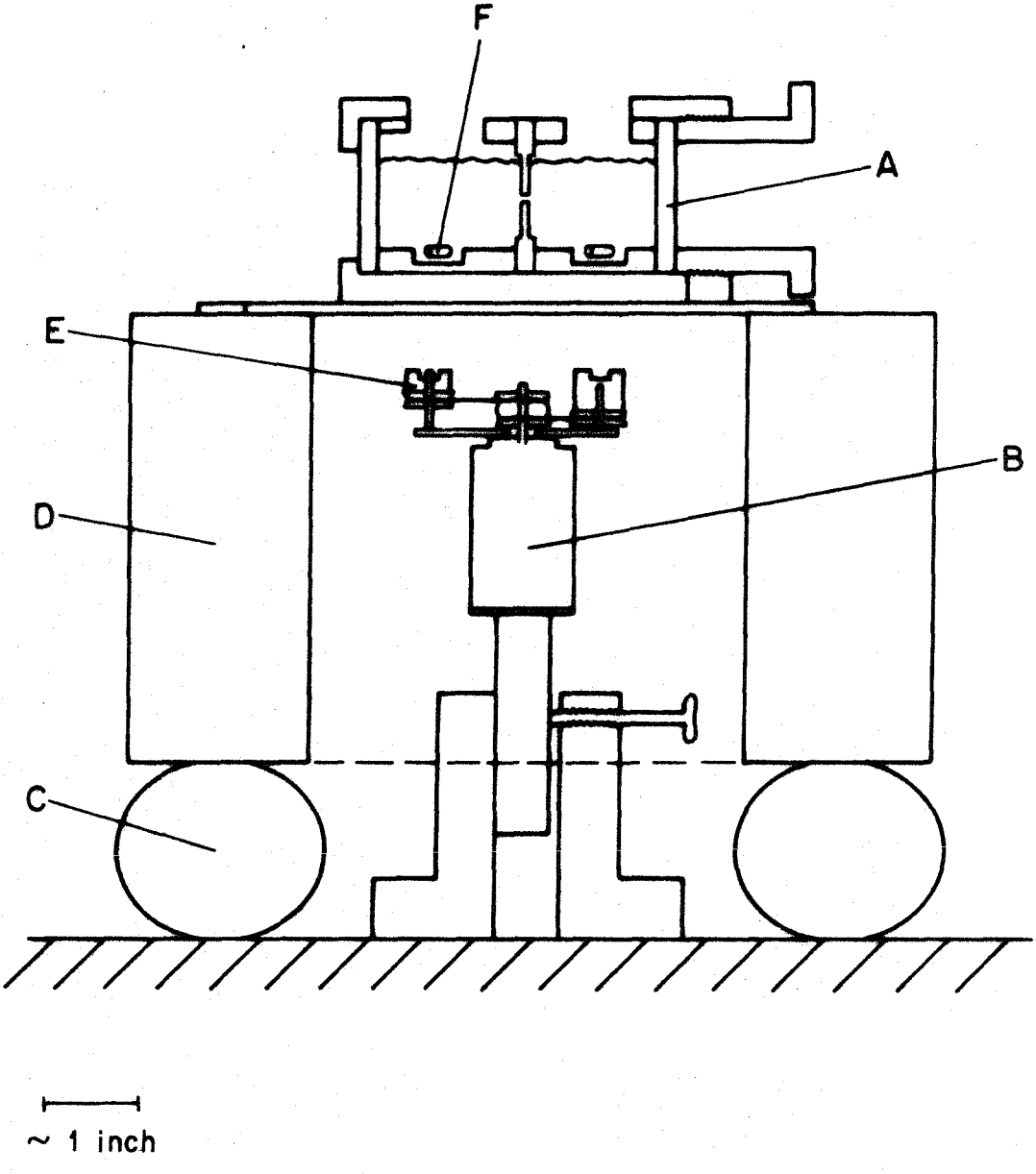

FIG. 4

Fig. 5. Block diagram of the electrical set-up.

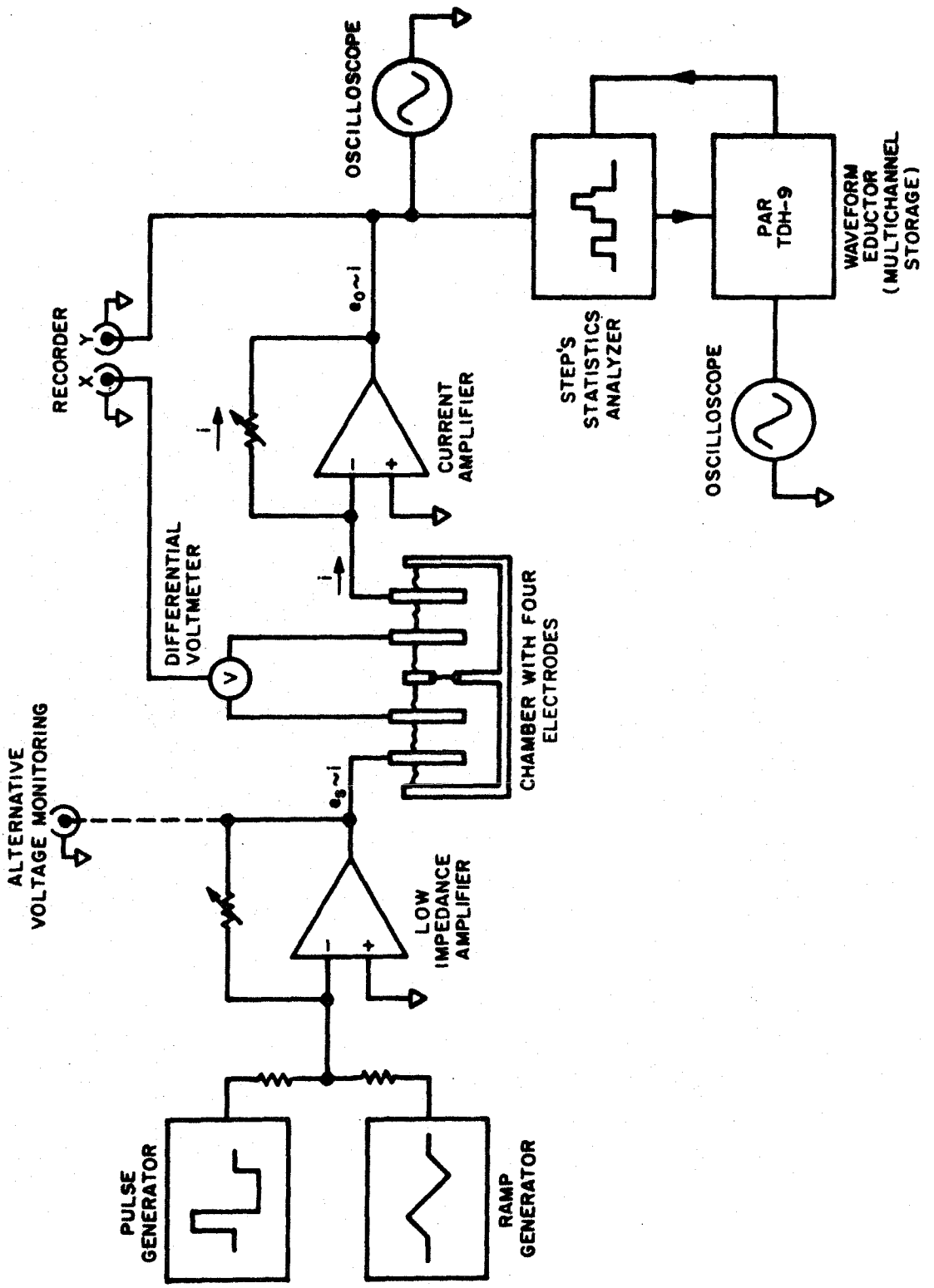
OSCILLOSCOPE
RECORDER
X
Y
$e_o \sim i$
CURRENT AMPLIFIER
i
STEP'S STATISTICS ANALYZER
PAR TDH-9
WAVEFORM EDUCTOR (MULTICHANNEL STORAGE)
OSCILLOSCOPE
DIFFERENTIAL VOLTMETER
V
CHAMBER WITH FOUR ELECTRODES
ALTERNATIVE VOLTAGE MONITORING
$e_s \sim i$
LOW IMPEDANCE AMPLIFIER
PULSE GENERATOR
RAMP GENERATOR

FIG. 5

desired voltage. To avoid polarization effects, another pair was used for voltage measurement, it went directly into a differential voltmeter of 10^{14} Ω input impedance. Schematics for this voltmeter are given in fig. 6.

The voltage across the two chambers was prescribed at all times. In other words, the voltage source had a very low impedance. For taking current-voltage curves we used a voltage ramp, where the voltage as a function of time was a sawtooth as shown in fig. 7A. The limits, V_+ and V_-, could be independently preset from 0 to +1 V and -1 V, respectively; the rate, $\frac{dV}{dt}$, could be varied from 0.45 $\frac{mV}{sec}$ to 300 $\frac{mV}{sec}$. Schematics of the ramp generator and current amplifier are shown in fig. 8. This instrument was designed by Huebner and Bruner (1972), and we have added minor modifications. The other type of prescribed voltage was a programmed pulse controlled by a pulse generator. In this case, the voltage as a function of time was adjustable in several parameters, as shown in fig. 7B. V_0, V_1, and V_2 could be independently preset from -500 mV to +500 mV, t_1 and t_2 could also be independently preset from 0.1 msec to any desired duration. The schematics of the pulse generator are shown in fig. 9.

The monitoring of conductance steps, their amplitude as well as their time dependence, was achieved by a special logic circuit designed to operate in conjunction with a Princeton Applied Research Waveform Eductor model TDH 9 (Princeton, N.J.). Schematics are shown in fig. 10. (An explanation of the operation of this apparatus is found in the Appendix 1.) Briefly, the current was sampled for only 3 μsec, at fixed intervals in time (usually 10 msec), and stored in a 100-channels multi-

Fig. 6. Schematics of differential voltmeter.

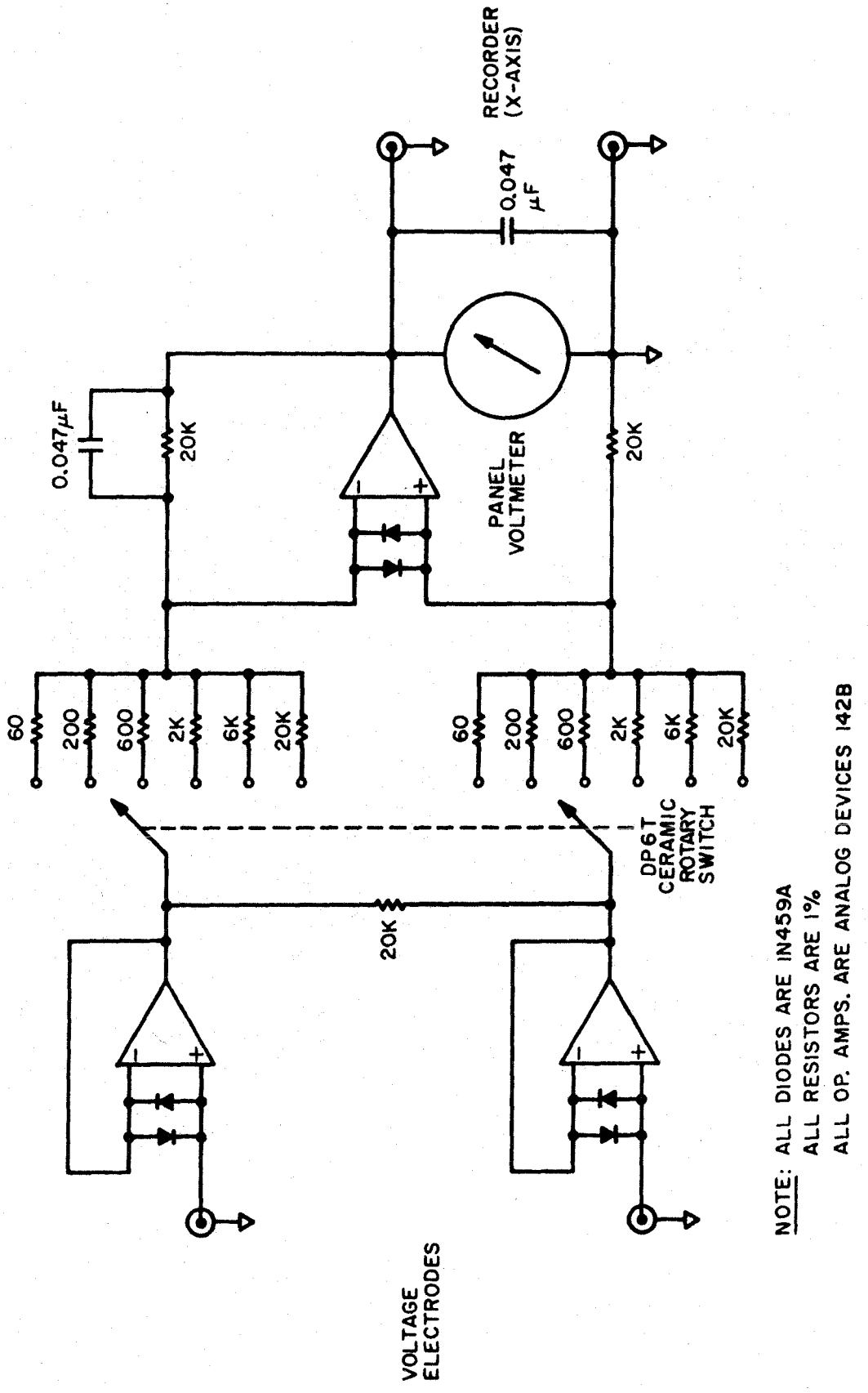

NOTE: ALL DIODES ARE IN459A
ALL RESISTORS ARE 1%
ALL OP. AMPS. ARE ANALOG DEVICES 142B

FIG. 6

Fig. 7. A. Voltage program of ramp generator. V_+ and V_- can be independently set from 0 to +1 V and -1 V, respectively. $\frac{dV}{dt}$ can be set from 0.45 mV/sec to 130 mV/sec. B. Voltage program of pulse generator. V_0, V_1, and V_2 can be independently set from -500 mV to +500 mV; t_1, t_2 can be independently set from 0.1 msec to any desired length. Arrows indicate beginning of named functions. Enable will set the prescribed V_0 and maintain it in standby. Trig. refers to the initiation of the pulse by the triggering switch. Zero brings the voltage to 0V. The figure shows a single cycle, but this full pulse can be continuously recycled.

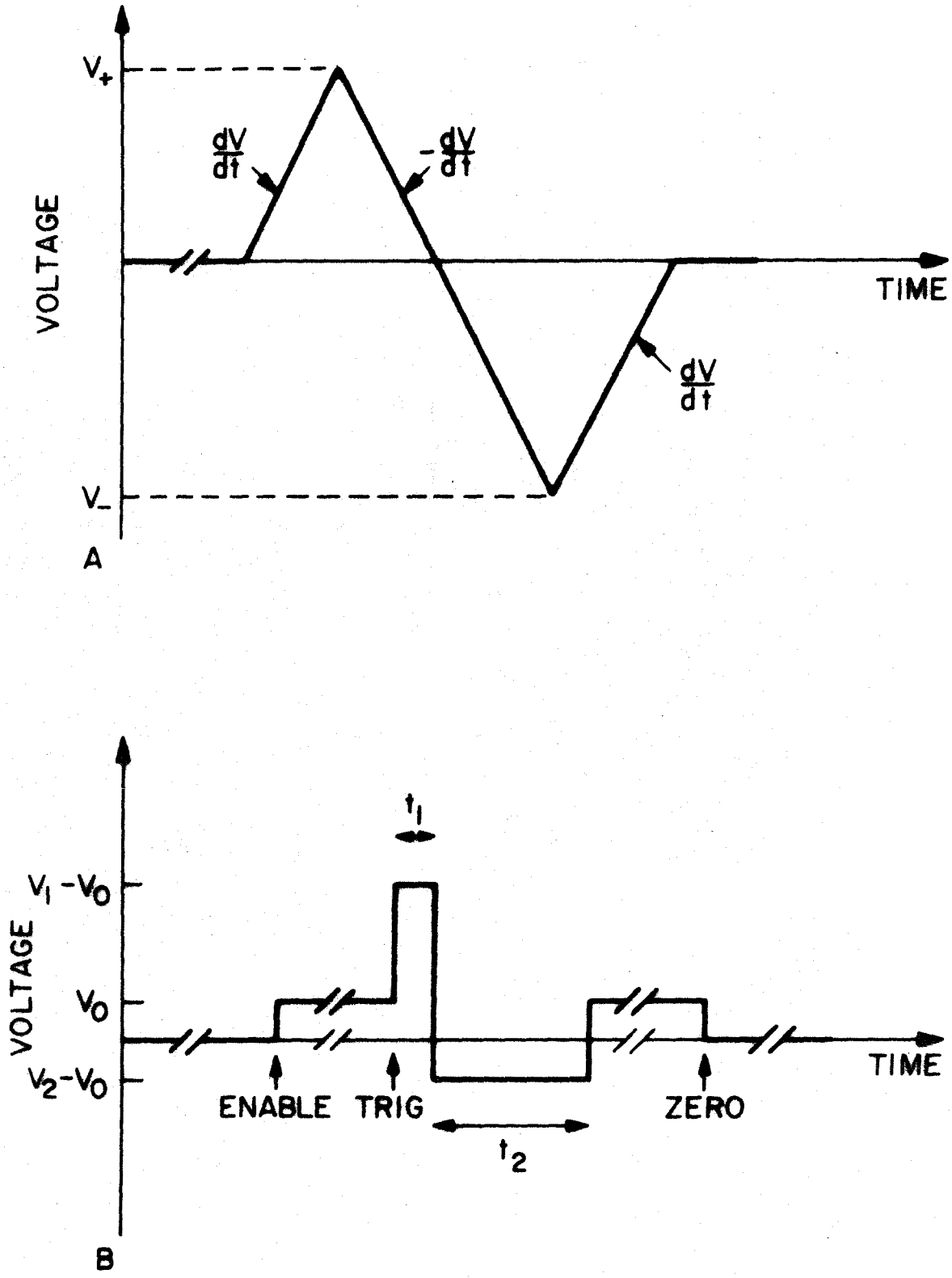
V+
V-
VOLTAGE
TIME
dV/dt
-dV/dt
dV/dt
A
t1
V1 -V0
V0
V2-V0
VOLTAGE
ENABLE
TRIG
ZERO
TIME
t2
B

FIG. 7

Fig. 8. Schematics of ramp generator and current amplifier (modified from Huebner and Bruner, 1972).

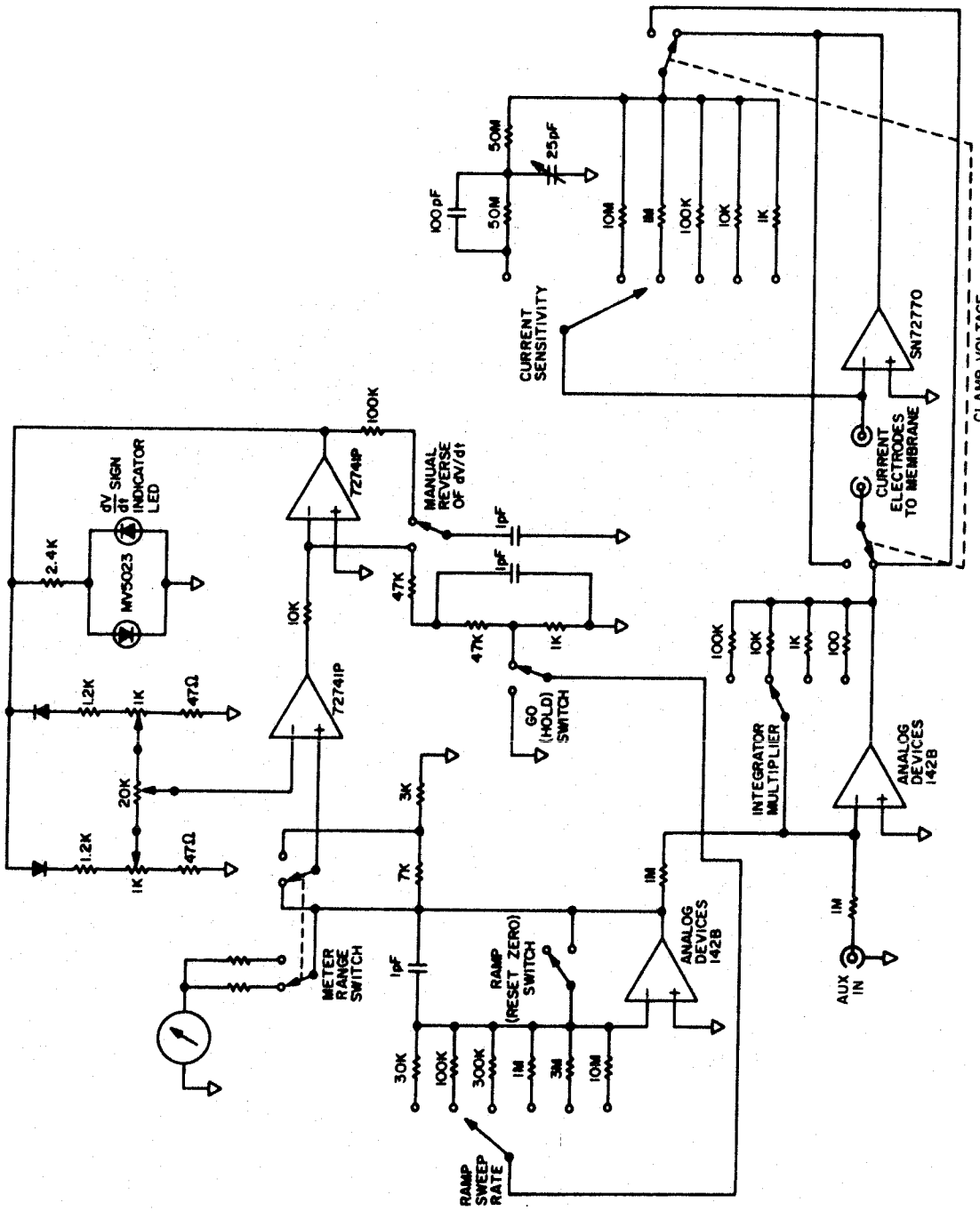
100pF
50M
50M
25pF
10M
1M
100K
10K
1K
CURRENT SENSITIVITY
SN72770
CLAMP VOLTAGE (CLAMP CURRENT) SWITCH
CURRENT ELECTRODES TO MEMBRANE
100K
MANUAL REVERSE OF dV/dt
1pF
1pF
47K
47K
1K
GO (HOLD) SWITCH
dV SIGN dt INDICATOR LED
MV5023
2.4K
1.2K
1K
47Ω
20K
1.2K
1K
47Ω
10K
7274IP
7274IP
100K
10K
1K
100
INTEGRATOR MULTIPLIER
ANALOG DEVICES 142B
3K
7K
1M
1pF
METER RANGE SWITCH
RAMP (RESET ZERO) SWITCH
ANALOG DEVICES 142B
1M
AUX IN
30K
100K
300K
1M
3M
10M
RAMP SWEEP RATE

FIG. 8

Fig. 9. Schematics of pulse generator.

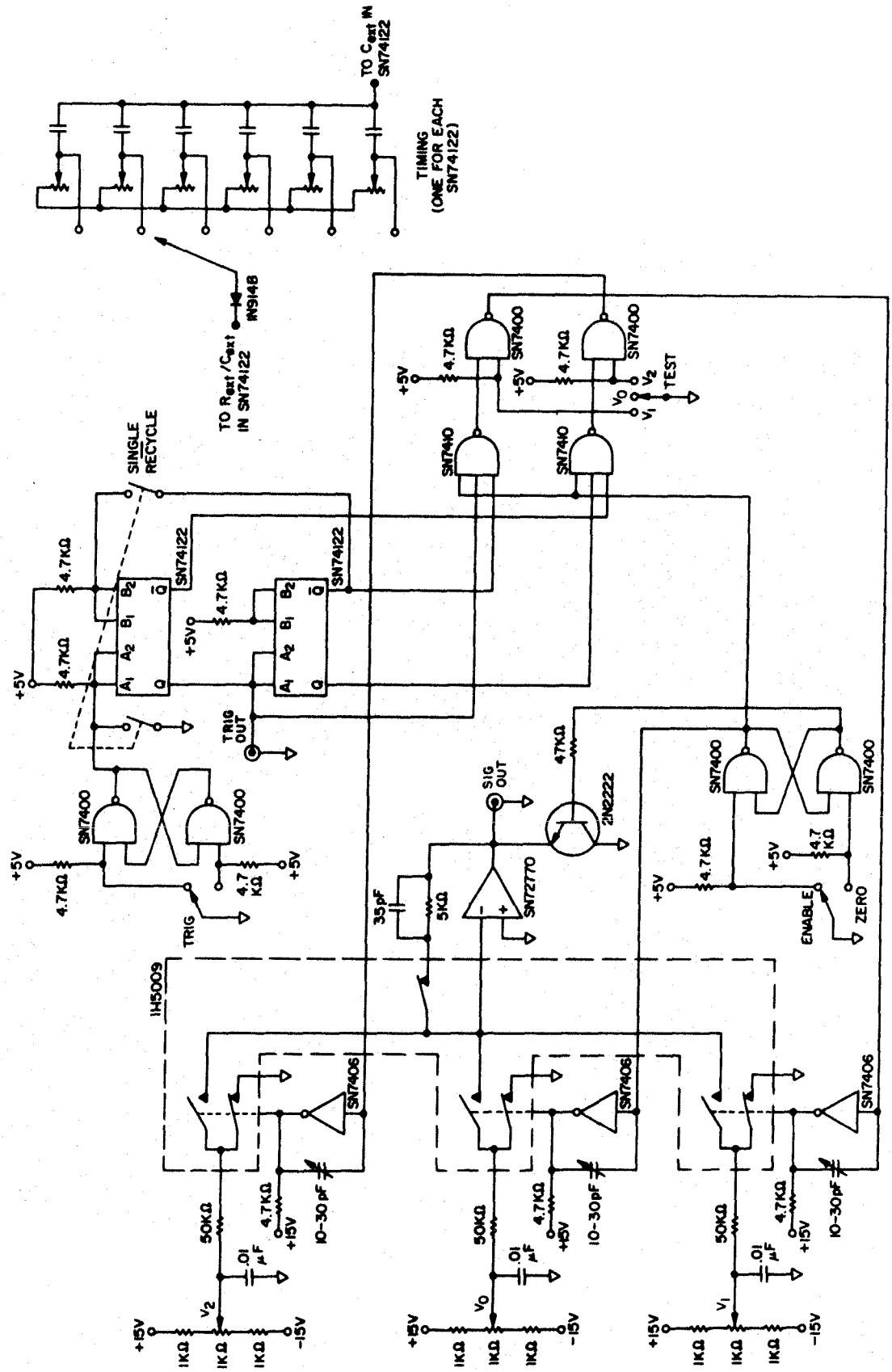
TO C_{ext} IN SN74122
TIMING (ONE FOR EACH SN74122)
TO R_{ext}/C_{ext} IN SN74122
IN9148
SINGLE RECYCLE
SN74122
SN7400
SN7440
SN7406
SN72770
2N2222
TRIG
TRIG OUT
SIG OUT
ENABLE
ZERO
TEST
IH5009
4.7KΩ
47KΩ
5KΩ
50KΩ
1KΩ
35pF
.01 μF
10-30pF
+5V
+15V
-15V

FIG. 9

Fig. 10. Schematics of step statistics analyzer.

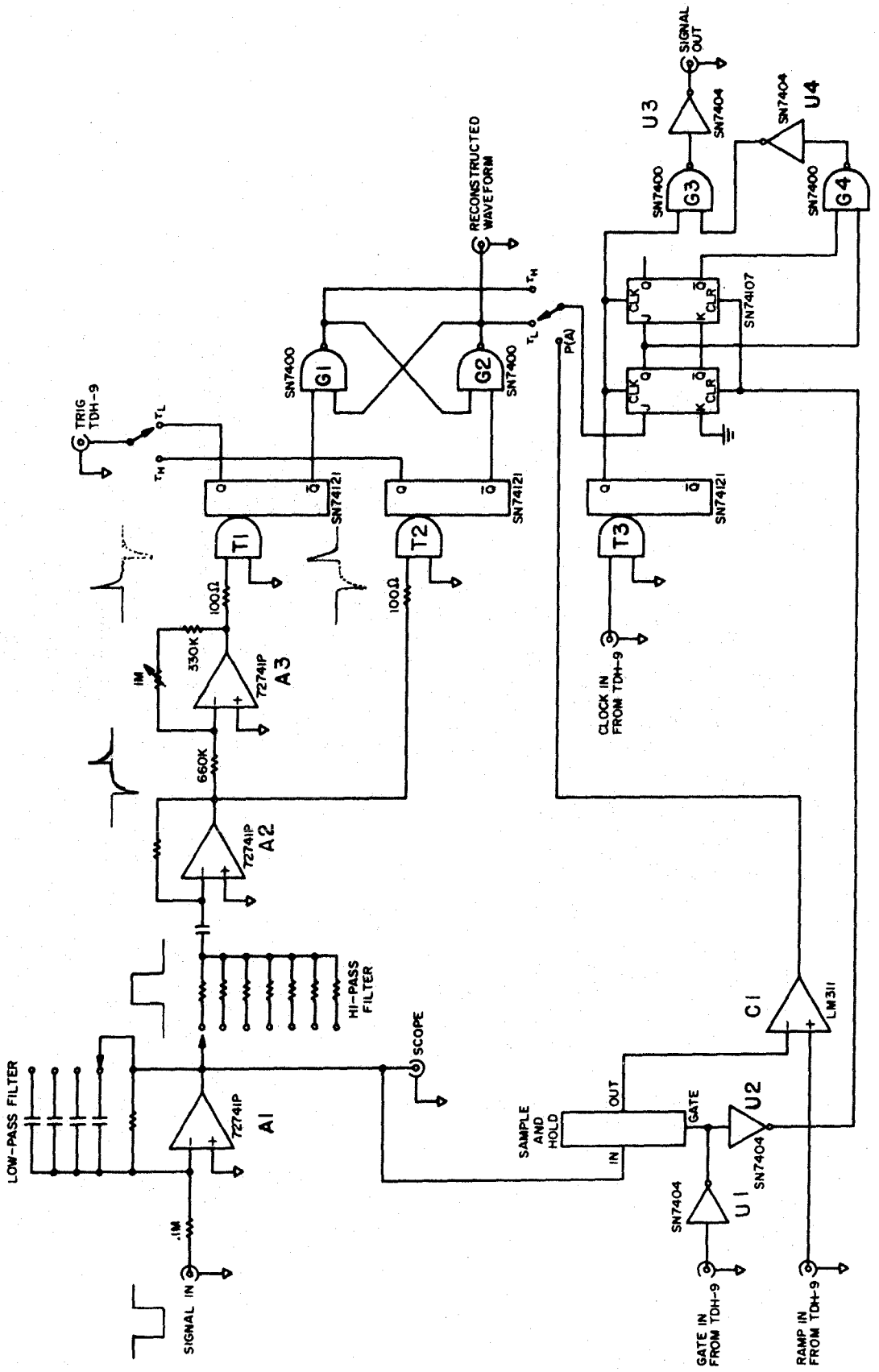
LOW-PASS FILTER
SIGNAL IN
.1M
A1
72741P
HI-PASS FILTER
SCOPE
660K
A2
72741P
330K
1M
A3
72741P
100Ω
100Ω
T1
T2
T3
SN74121
SN74121
SN74121
TRIG TDH-9
TL
TH
RECONSTRUCTED WAVEFORM
G1
G2
SN7400
SN7400
P(A)
CLOCK IN FROM TDH-9
SAMPLE AND HOLD
IN
OUT
GATE
U2
SN7404
U1
SN7404
GATE IN FROM TDH-9
C1
LM311
RAMP IN FROM TDH-9
U3
SN7404
SIGNAL OUT
G3
SN7400
U4
SN7404
G4
SN7400
SN74107
CLK
J
K
CLR

FIG. 10

channel analyser. The stored voltage of each channel, thus represented the relative probability of the current level corresponding to that channel during the total time of sampling (usually 30 sec to 2 min). Typically, when full scale was set to cover 5×10^{-10} A, the resolution power was 5×10^{-12} A per channel. Results were directly plotted on an x-y recorder (Hewlett Packard 7034A) and displayed by an oscilloscope (Tektronix type 502).

III. RESULTS

All experiments were done at room temperature (22 ± 1°C) unless otherwise stated.

III.1 Unmodified Black Lipid Membrane

The formation of the film was achieved by first filling the orifice through the feeder hole with the membrane forming solution, with both chambers already filled with the aqueous salt solution. At this stage the PE-decane forms a blob which plugs the hole in the septum separating the two chambers. With the blob in place, the conductivity was checked to make sure that there were no electrical leaks between the two chambers, and the current and voltage offsets were balanced to zero. By suction through the feeder channel, one could remove some of the membrane forming solution, and a small disc of this solution appeared, concentric to the perimeter of the orifice, while the rest of the bulk solution remained attached to the inner wall of the cylindrical hole, as a torus. This disc was monitored by reflected light through a low power microscope and showed colored interference fringes indicating that it is a film a few thousand Angström thick. After a few minutes, a spontaneous nucleation spot appeared as a non-reflecting black region in the disc, and this black area grew, swallowing as it were, the colored disc. This is schematically illustrated in fig. 11.

When the material in which the membrane is formed is not sufficiently hydrophobic, for example Delrin or PVC, membrane stability is improved by preconditioning the orifice. This is accomplished by wet-

Fig. 11. Schematic representation of membrane formation. (a) Filling the orifice with membrane forming solution. (b) Blob of solution plugging the orifice. (c) Extraction of excess solution yields a colored disc, a few thousand Angström thick, concentric to the perimeter of the orifice. The amount of lipid solution removed will control the area of the thin film. (d) Spontaneous appearance of a non-reflecting nucleation spot which grows, swallowing as it were the colored disc. (e) Final stage, black lipid film, about 70 Å thick, in equilibrium with torus of lipid solution.

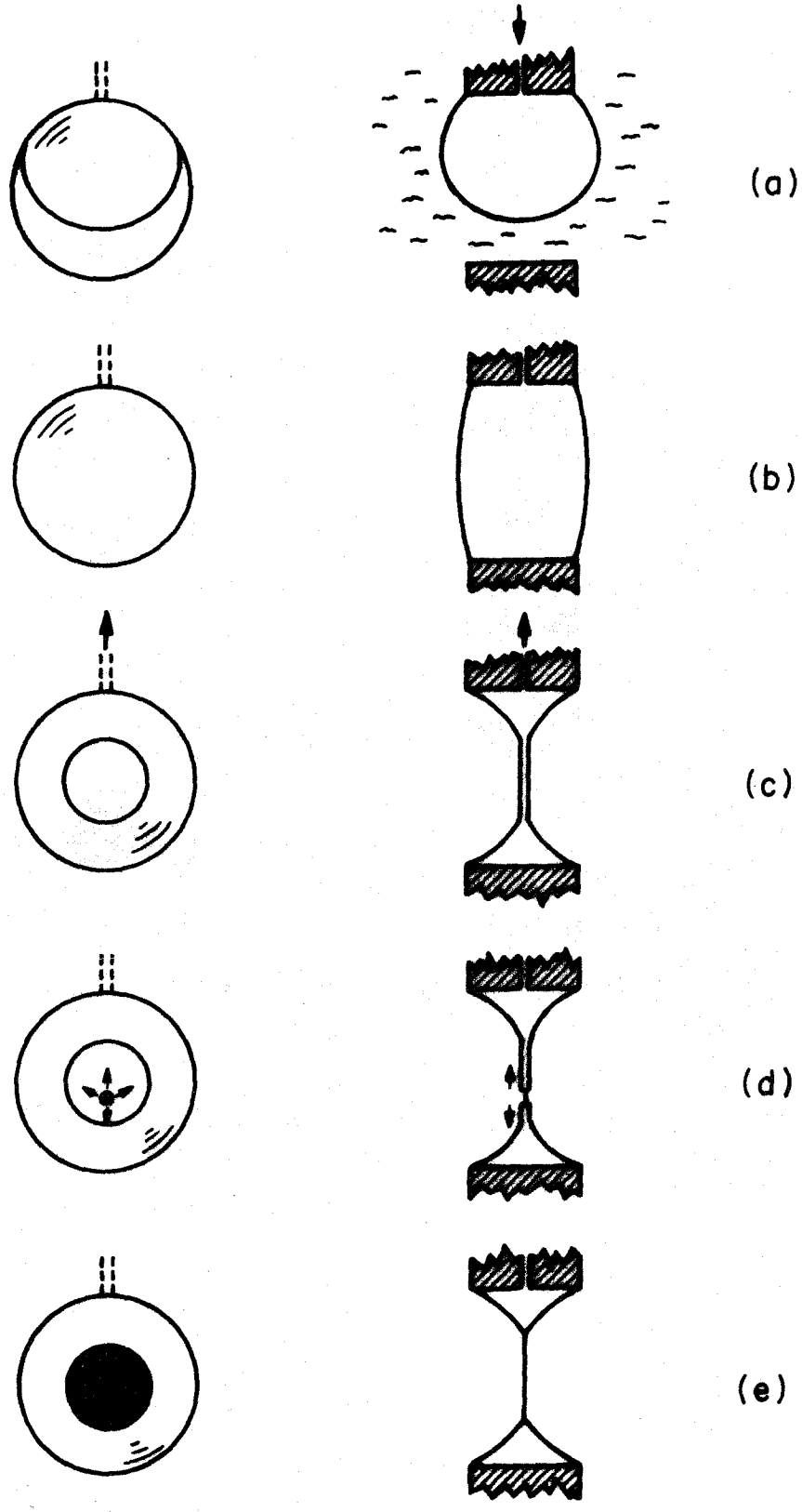

FIG. 11

ting it with membrane forming solution and drying under nitrogen prior to the addition of the aqueous phases.

Typical current-voltage (i-V) curves of an unmodified PE-decane black membrane are shown in fig. 12. The aqueous solution was tenth molar sodium chloride; curves A, B, and C were taken at 4.5, 13.3, and 45 mV/sec, respectively, as indicated in the lower part of fig. 12.

The conductance of the system with the aqueous solutions in the chambers and no membrane in the orifice is about 10^{-4} mho, for 0.1 Molar NaCl, much larger than that of the black membrane, which is about 10^{-10} mho for a square millimeter of area. Thus, all the applied voltage drop is effectively across the membrane, which also represents the main capacitance of the circuit.

The current is given by

$$i = \frac{V}{R} + C\frac{dV}{dt} + V\frac{dC}{dt} \qquad (1)$$

where

i : current through membrane

V : voltage across membrane

R : resistance of membrane

C : capacity of membrane

t : time

Since the voltage ramp generator provides a constant dV/dt, one obtains from the i-V curves, a direct measure of the membrane capacity as well as of conductance. However, one must exercise caution in drawing conclusions about the capacity and conductance of bare

Fig. 12. (Top) Current-voltage curves of a PE-decane black film. Area of black film: 9×10^{-3} cm^2; aqueous solutions: 10^{-1} M NaCl; (Bottom) Voltage vs. time, indicating the different rates dV/dt, of ramp A: 4.5 mV/sec, B: 13.3 mV/sec, C: 45 mV/sec. Arrows show capacitance effects at fast voltage sweep rates. Inflection points as the voltage is increasing may reflect a rapid voltage dependent thinning. Effective negative resistance as the voltage decreases might be due to relaxation. The difference between the i-V curves at the three distinct sweep rates is indicative of the deviation from steady state conductance, probably largely pronounced due to the high resistance of the membrane.

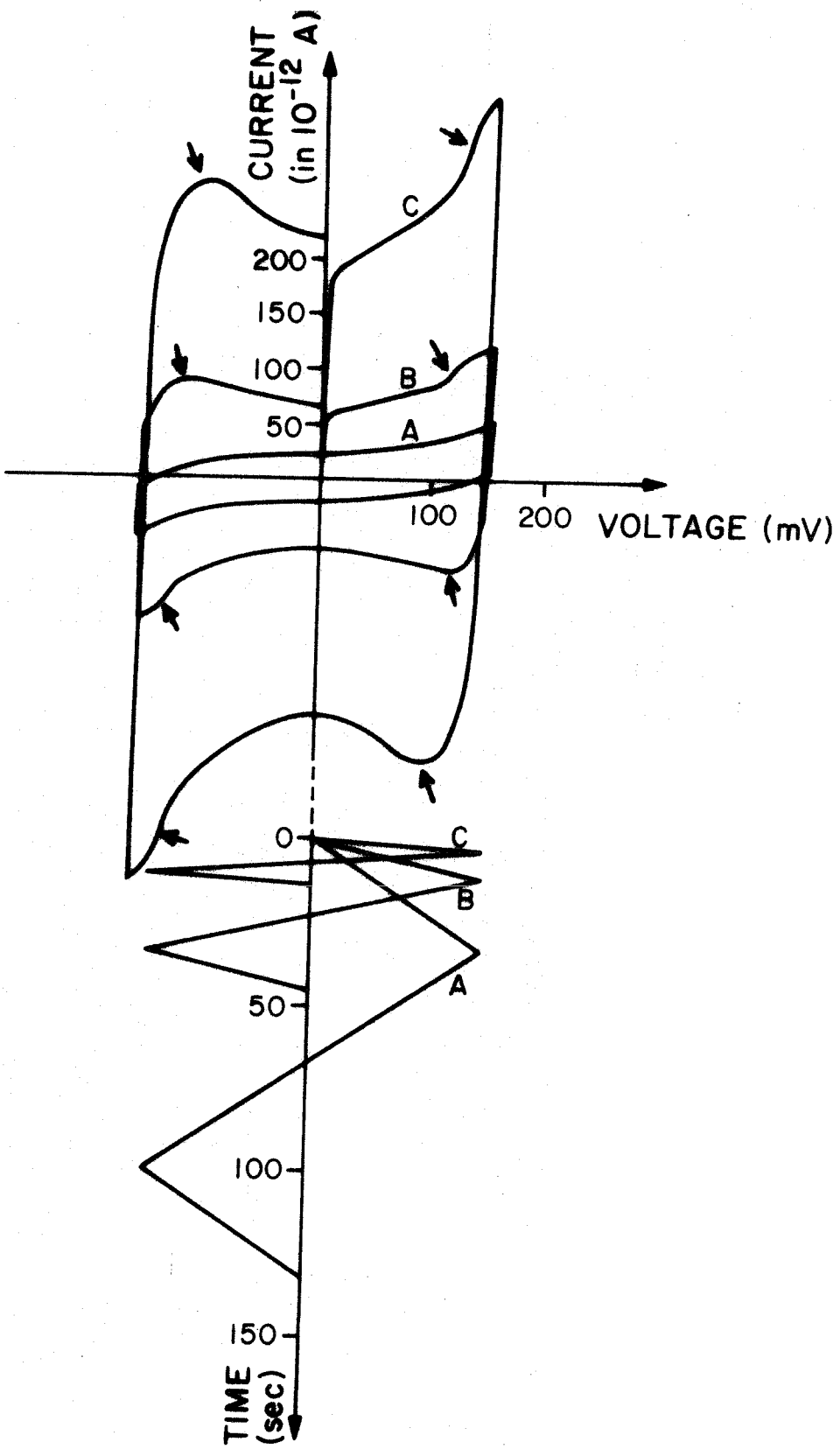
CURRENT (in 10^{-12} A)
200
150
100
50
C
B
A
100
200
VOLTAGE (mV)
0
C
B
A
50
100
150
TIME (sec)

FIG. 12

membranes directly from these i-V curves. As shown in fig. 12, one can see that the curves are not entirely as expected for a pure voltage independent capacitance in parallel with a non-linear resistance. Fig. 13 illustrates what would be expected in this latter case. With the membrane, additional effects arise when the rate of change of the voltage is increased beyond 4.5 mV/sec. Inflexion points appear at high voltages, while the voltage is increasing, and an apparent "negative resistance" at high voltage when the voltage is decreasing (see arrows in fig. 12).

If one calculates the capacity of the membrane from eq. (1) at the zero volt current, one obtains the same result from all three dV/dt values shown in fig. 12, namely 4.9×10^{-9} F, or, since the area of that particular black lipid film was 0.9 mm^2, a membrane capacitance of 5.4×10^{-7} F/cm^2. From the slope of the i-V curve in fig. 12, one can measure the membrane conductance near zero voltage to be 10^{-8} mho/cm^2. It is known from measuring the conductance of bulk membrane forming solution (se in fig. 11c), that the torus surrounding the black membrane can contribute a significant fraction of the observed current.

The capacity of the membrane, as calculated from the zero voltage current and the voltage change rate dV/dt, is plotted against the calculated area of black film, as observed through a calibrated reticle in the microscope, in fig. 14.

III.2 Alamethicin Doped PE-decane Black Membrane

III.2.1 General Remarks

Addition of alamethicin to the aqueous phase on one side of an

Fig. 13. "Gedanken" experiment showing the expected i-V curves for a non-linear resistor in parallel with a voltage independent capacitor, for the same voltage rates as in Fig. 12.

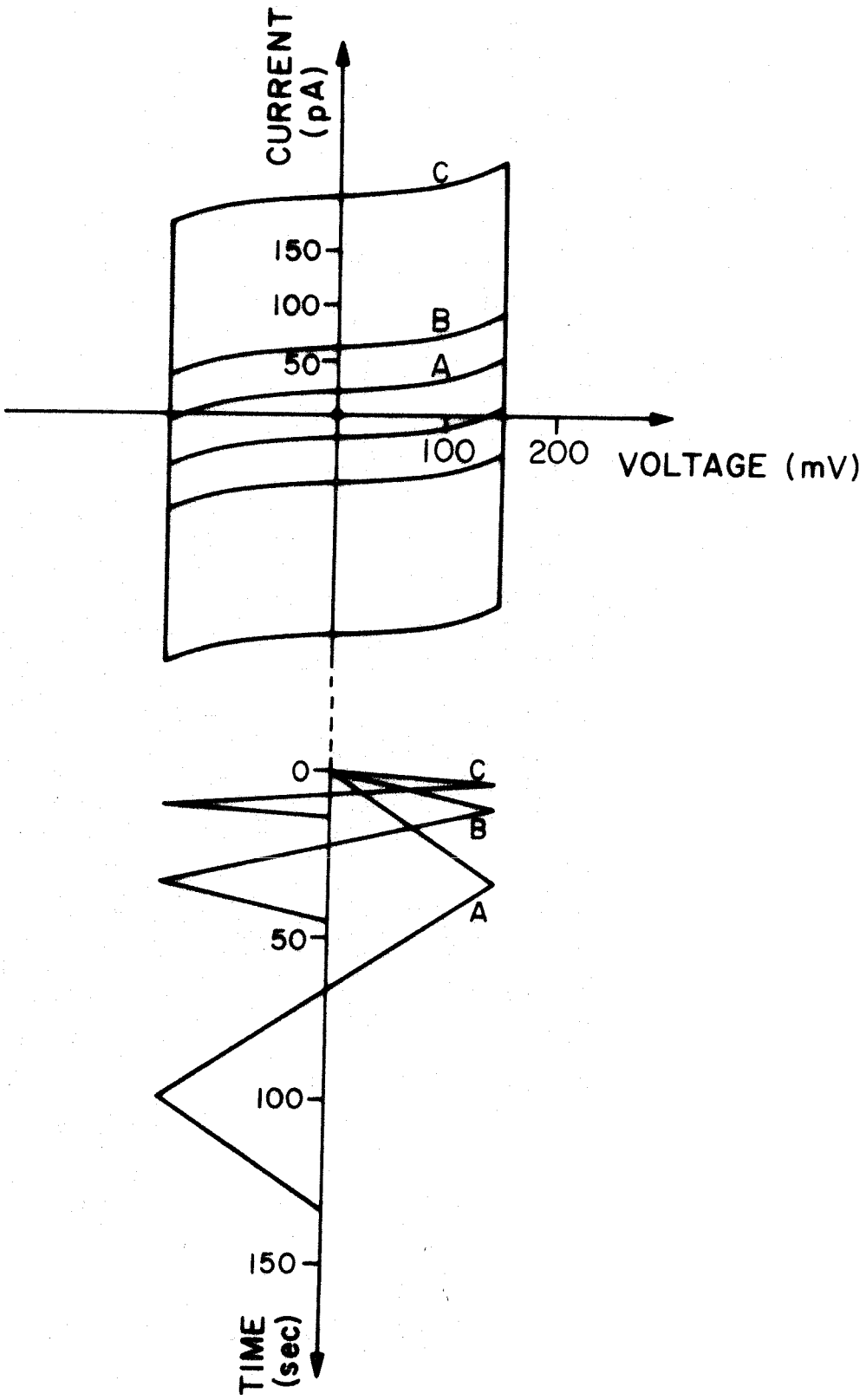
CURRENT (pA)
C
150
100
B
50
A
100
200
VOLTAGE (mV)
0
C
B
A
50
100
150
TIME (sec)

FIG. 13

Fig. 14. Electrical capacity of black PE-decane membrane versus area of the black film. The capacity is calculated from the zero voltage current, i_o, at a given voltage change rate, dV/dt, namely: $C = i_o / \frac{dV}{dt}$. The area is calculated from the diameter of the black film as measured with a calibrated reticle in the microscope's eyepiece.

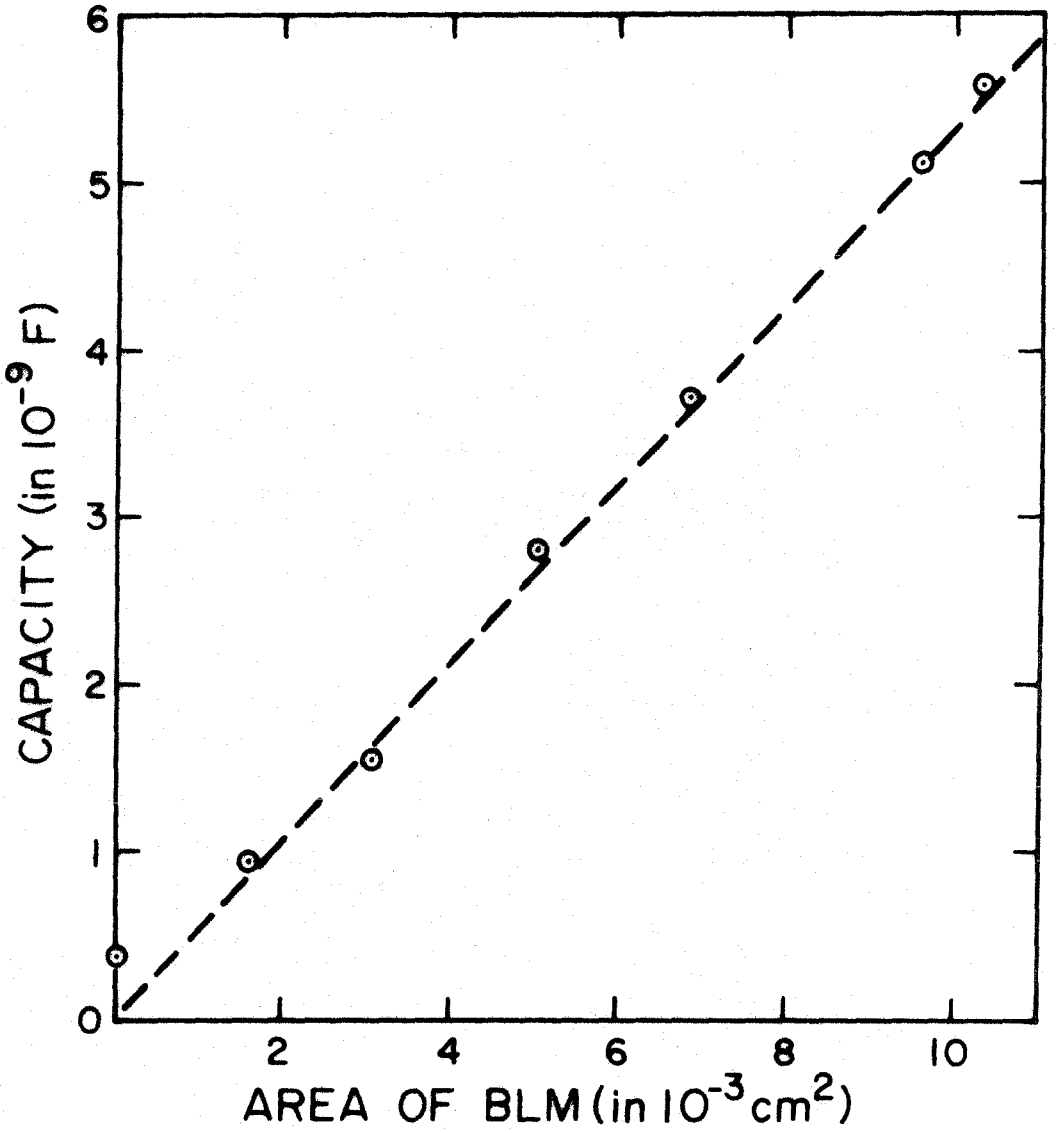

FIG. 14

already formed PE-decane black film induces a sharp conductance increase at a voltage depending on the concentration of both alamethicin and salt, on the type of salt (NaCl, KCl, etc.), and on the area of black membrane. This conductance increase occurs when the test side, to which alamethicin has been added, is positive relative to the other side, grounded, as it is shown in fig. 15. (At very high alamethicin concentrations the high conductance occurs even when the test side is negative, but this high conductance disappears as the voltage of the test side becomes increasingly negative. This phenomena gives rise to a negative resistance region, as shown in fig. 36. (See section III.2.12 and Discussion)).

Fig. 15 shows a typical i-V curve of an 8.5×10^{-3} cm^2 area of PE-decame black film in 0.1 M NaCl, and 3×10^{-6} gr/ml alamethicin on the test side. In the high conductance state the probability of breaking the membrane increases if large currents are allowed to flow through it.

The onset of the high conductance is not continuous, but occurs in discrete steps which begin at some threshold voltage region and rapidly increase in number to produce an average current which appears to rise exponentially with voltage.

III.2.2 Evidence for Discrete Conductance States

If the voltage is held constant at some point in the threshold range, and the current is monitored as function of time, one can see discrete conductance levels differing by steps of relatively uniform size but irregular duration. Fig. 16 shows an oscilloscope display

Fig. 15. i-V curve of a PE-decane black membrane, 8.5×10^{-3} cm^2 in area, in 0.1 M NaCl and 3×10^{-6} gr/ml alamethicin on the test side. dV/dt = 4.5 mV/sec. The arrows indicate the direction of the voltage sweep. The finite current at zero voltage, of opposite signs for opposite dV/dt are due to the capacity of the membrane.

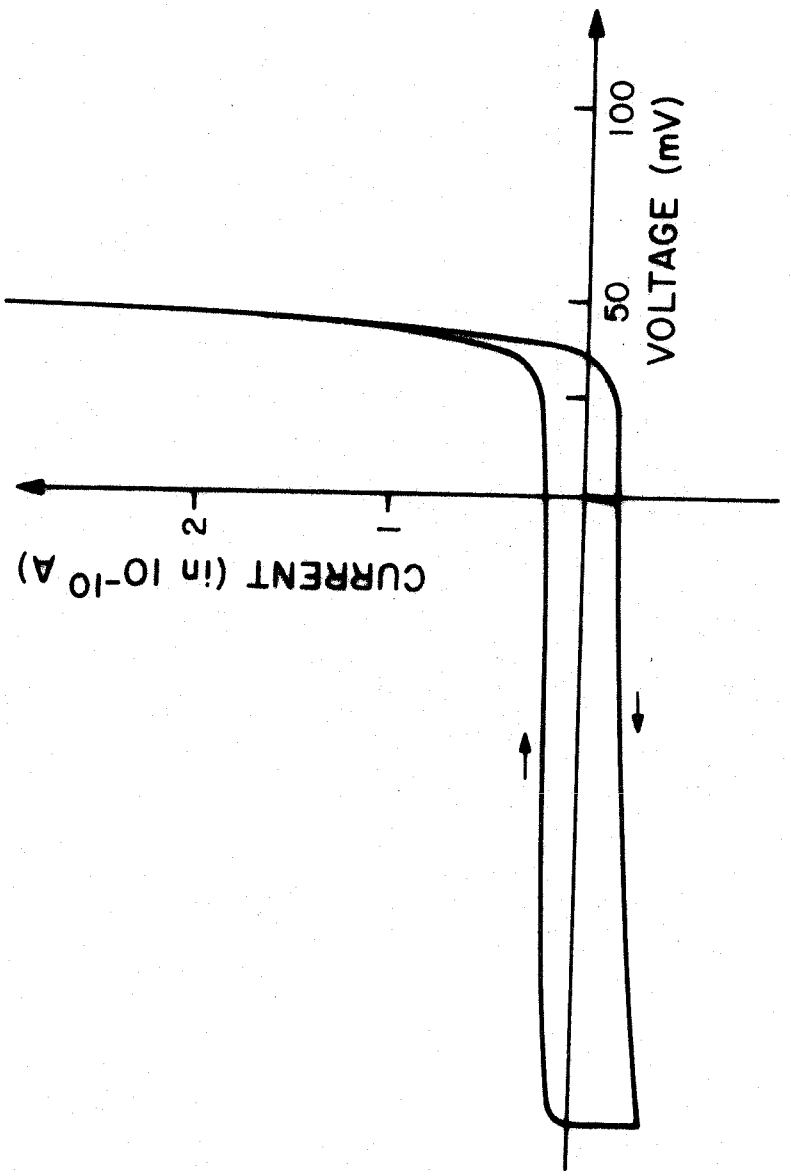

FIG. 15

Fig. 16. Oscilloscope tracing of current vs. time, for a 0.4×10^{-2} cm^2 black PE-decane film in 1.0 M NaCl and 10^{-7} gr/ml alamethicin on test side. The voltage is +145 mV (positive to the alamethicin side). The lowest level to which the current reaches corresponds to the current level of the unmodified lipid membrane. Up to 6 discrete levels are clearly seen.

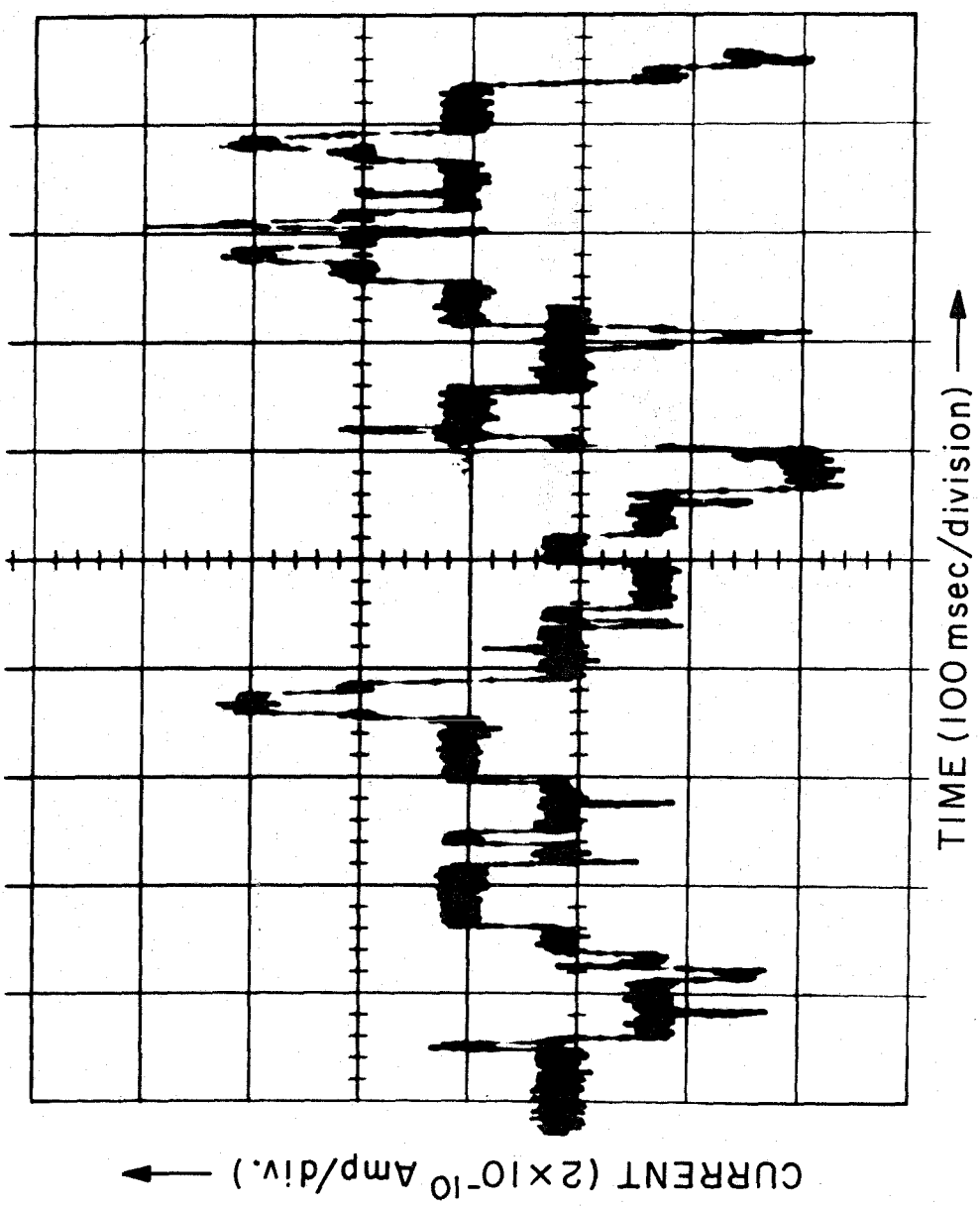

FIG. 16

of the current through a 0.4×10^{-2} cm^2 area of black PE-decane membrane, in 1.0 M NaCl on both sides and 10^{-7} gr/ml alamethicin on the test side only, the voltage being maintained at +145 mV. The lowest current level is identical to that of the unmodified PE-decane membrane at the same voltage and ionic strength medium.

In order to obtain quantitative probability distribution data, one can feed the current information to the step analyser device and obtain directly the distribution of current values sampled at numerous times, during a time period long compared with the duration of a single step. Fig. 17 shows a distribution of the current for a 0.4×10^{-2} cm^2 PE-decane black film in 1.0 M NaCl and 3×10^{-8} gr/ml alamethicin at the test side, with a voltage of +207 mV, taken over a 30 sec period, with a sampling interval of 10 msec. The inspection of the discrete current levels show that the steps that separate them are not equal in magnitude. Fig. 18 shows the difference between consecutive levels obtained from fig. 17. From this it is clear that each level cannot be expressed as with integral multiples of lower levels.

Inspection of the time course of these discrete current fluctuations, such as in fig. 16, shows that in the threshold voltage region the current will remain most of the time in the bare membrane conductance level and at random intervals it will fluctuate rapidly between the characteristic levels. The current level corresponding to the steady state current of the bare membrane, is the most frequent one, showing that under conditions such that not more than a few (~ 5) conductance states can be seen, the membrane spends most of the time at the steady state current of the unmodified film. Beside the bare membrane

Fig. 17. Current distribution of 0.4×10^{-2} cm^2 black PE-decane membrane in 1.0 M NaCl and 3×10^{-8} gr/ml alamethicin on test side. The voltage is clamped at +207 mV. Total time: 30 sec. The ordinate gives the value of the relative probability of finding the current at any value given by the abscissa. Five levels are clearly resolved and they have been labeled 0th, 1st, 2nd, 3rd, and 4th. They are the characteristic states of a patch.

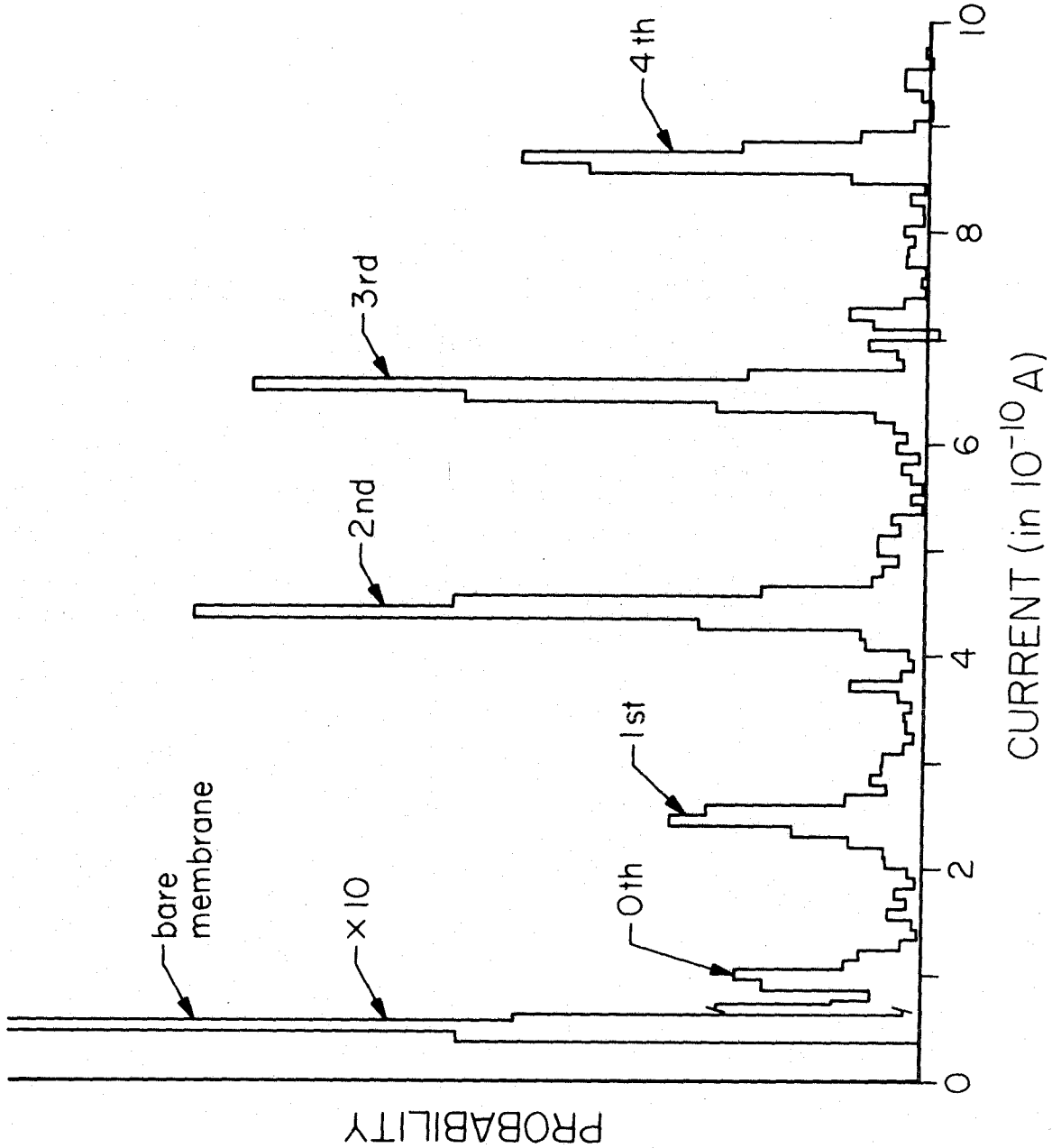
PROBABILITY
bare membrane
x10
0th
1st
2nd
3rd
4th
0
2
4
6
8
10
CURRENT (in 10^{-10} A)

FIG. 17

Fig. 18. The difference in the current of consecutive levels corresponding to the characteristic states of a patch, from fig. 17.

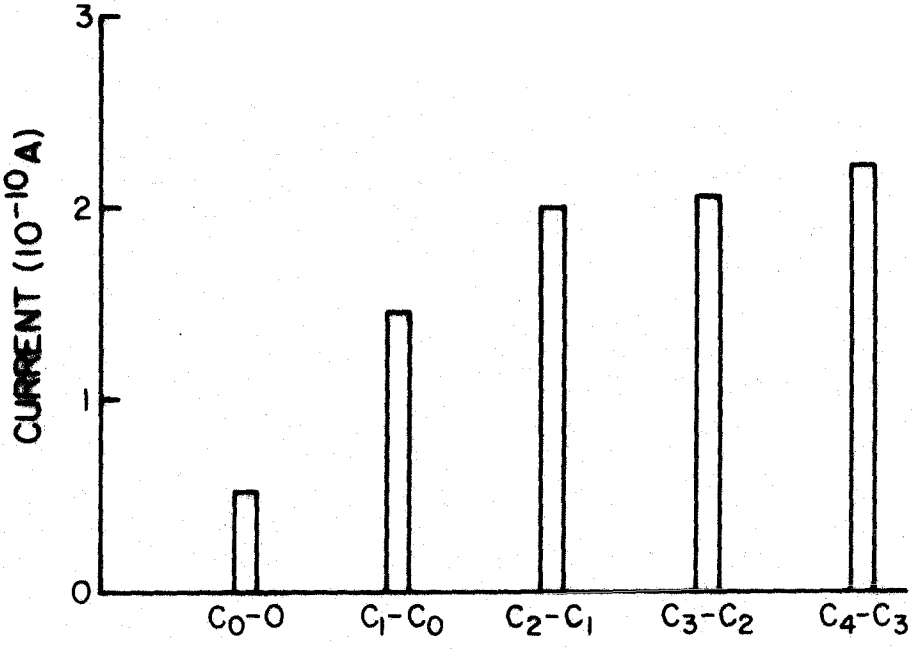

FIG. 18

conductance peak, current peaks corresponding to five other conductance levels can be resolved. They will be labeled zeroeth, first, second, third, and fourth level. It is not always possible to resolve the zeroeth level. Hereafter these conductance levels will be referred to as conductance states of a patch. In section III.2.7 we will give further evidence that these conductance levels indeed represent states of a conductance entity that we will call a patch. These conductance states, therefore, are homologous to the unit channels reported by Gordon and Haydon (1972). In section III.2.8 and in the Discussion we will examine the possibility that the different states of a patch may be actually channels.

III.2.3 Ion Specificity of the Conductance Levels of a Patch

Measurement of the conductance of the various current levels of a patch was accomplished by taking current distributions in the threshold voltage region for 1.0 M solution of different chloride salts, at 2×10^{-8} gr/ml alamethicin on the test side. These current steps were also monitored on the oscilloscope. The results are plotted in fig. 19 and show that the relative conductance of the patch states, in the presence of the different ionic species, correlates well within the relative conductance of bulk solutions of the ions (see Table 1).

III.2.4 The i-V Curve of the Conductance States

In order to measure the current-voltage relation of the several conductance levels of a patch, current distributions as well as oscilloscope tracings were taken for 1.0 M solutions of various kinds of chloride salts.

Fig. 19. The conductance of the first to fourth conductance states of a patch, and the conductivity of bulk, for 1.0 M solutions of LiCl, NaCl, KCl, $CaCl_2$, and Tris-HCl (trihydroxymethylaminomethane hydrochloride). O : first state; □ : second state; ▽ : third state; ◇ : fourth state. ▼ : bulk

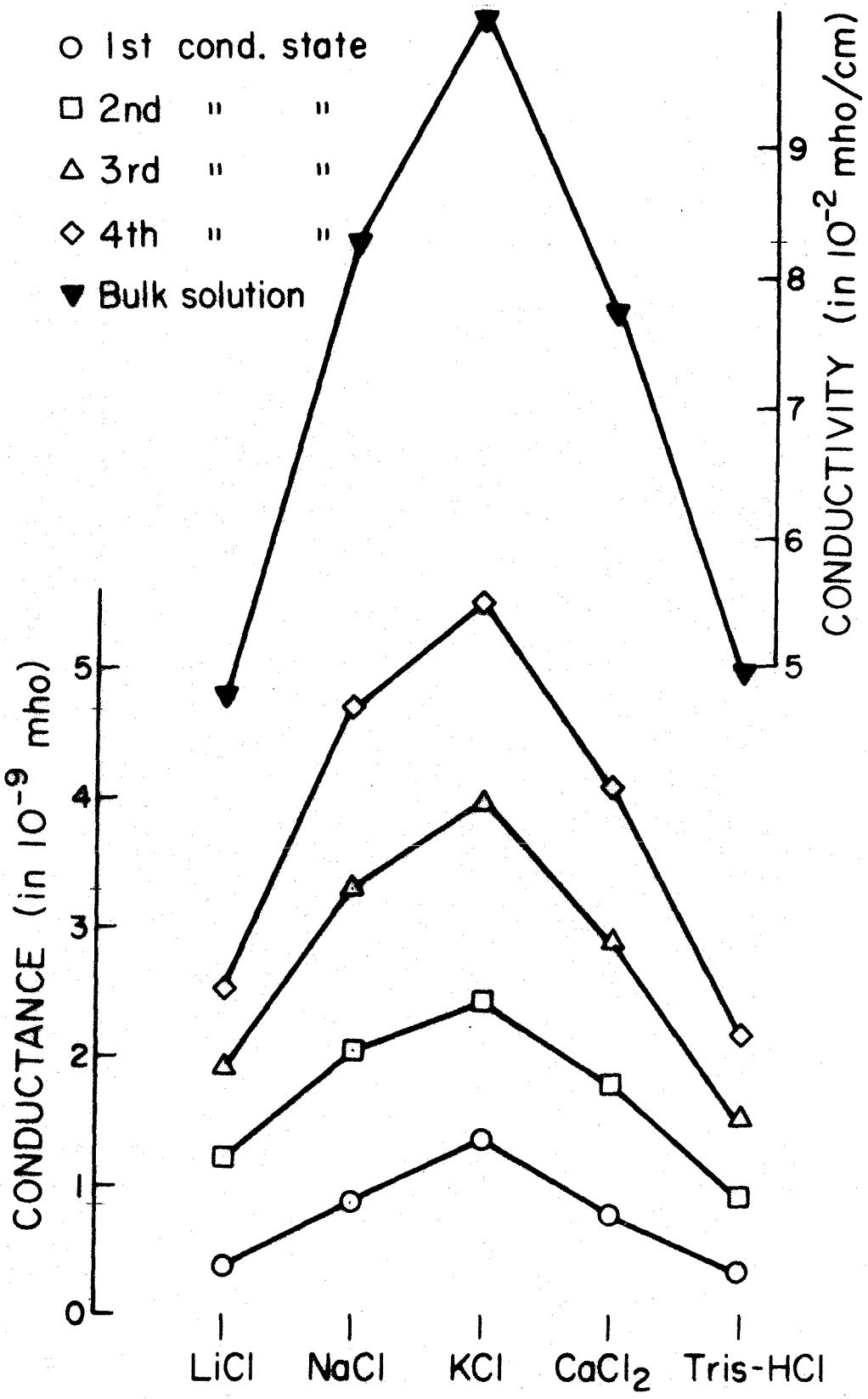
1st cond. state
2nd " "
3rd " "
4th " "
Bulk solution
CONDUCTANCE (in 10^{-9} mho)
CONDUCTIVITY (in 10^{-2} mho/cm)
0
1
2
3
4
5
5
6
7
8
9
LiCl
NaCl
KCl
$CaCl_2$
Tris-HCl

FIG. 19

Individual current steps can be resolved only over a narrow voltage range in the threshold voltage range. Since the voltage at which we find this threshold region, decreases with increasing alamethicin concentration (see Section III.2.12), the alamethicin concentration was increased to bring the threshold voltage gradually down. Overlap between the conductances measured at different alamethicin concentrations, showed that this procedure does not change the conductance levels. Fig. 20 shows the current-voltage characteristic of the conductance levels of a single patch. This is a collection of data taken for 1.0 M NaCl solution in the aqueous phase, and many different alamethicin concentrations, and over several different films (all PE-decane). The scatter from experiment to experiment is not great. The conductance levels of a patch look nearly ohmic. But, data obtained for any one film at a fixed salt concentration show that the conductance levels of a patch increase slightly with voltage. This is shown in fig. 21.

III.2.5 The Dependence of the Conductance States of a Patch on Salt Concentration

Current distributions at threshold voltage were taken for PE-decame black membranes in symmetric solutions of sodium chloride at concentrations ranging from 0.1 M to 1.0 M. The conductance of the first to fourth level is plotted versus the sodium chloride concentration in log-log graph (fig. 22), the conductivity of bulk sodium chloride in the same concentration range is also drawn for comparison. The slopes for all four conductance levels are equal but smaller than that of the bulk solution, suggesting that the decrease in the ionic

Fig. 20. Current-voltage characteristics of the conductance levels of a patch. Collected points from several PE-decane black films in 1.0 M NaCl solution. Symbols as indicated on inset. Notice the nearly ohmic behavior as evidenced by the straight line fit.

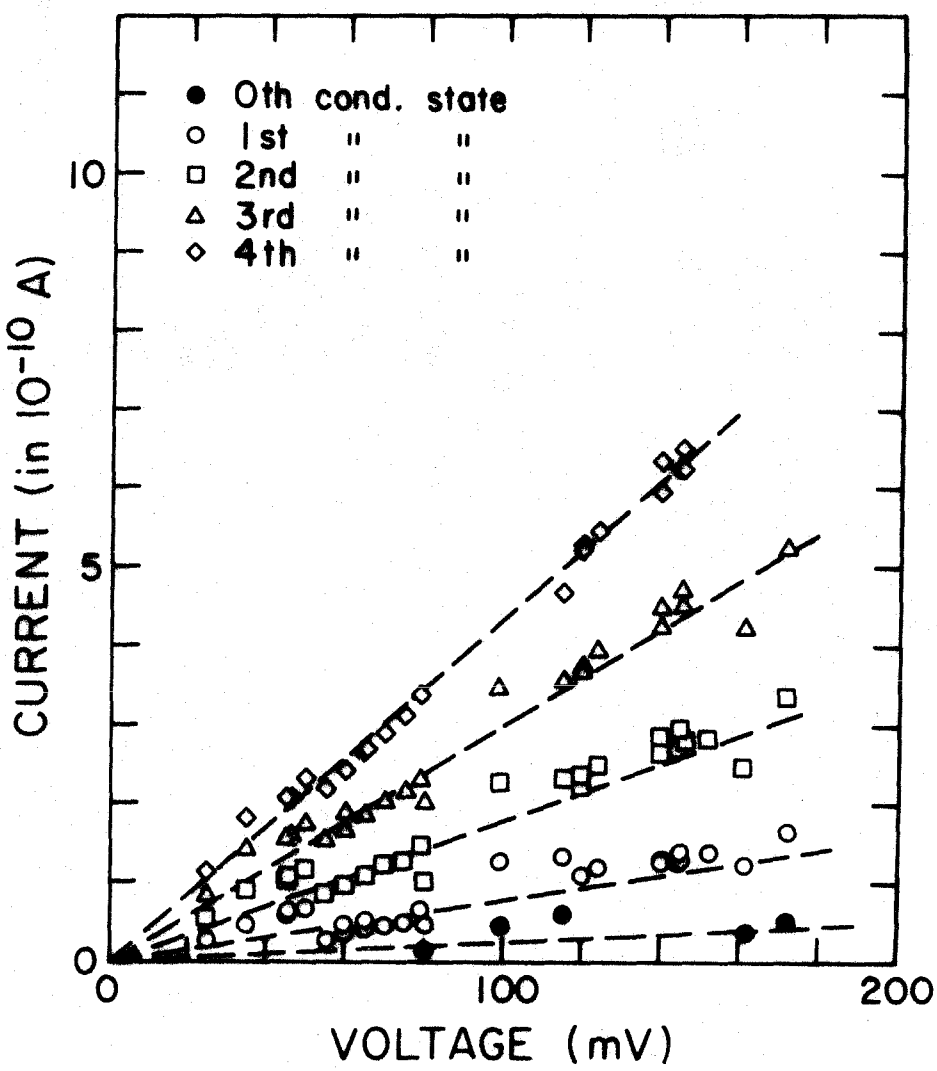
0th cond. state
1st " "
2nd " "
3rd " "
4th " "
CURRENT (in 10^{-10} A)
VOLTAGE (mV)
0
5
10
0
100
200

FIG. 20

Fig. 21. Current-voltage characteristics of the conductance states of a patch. All points were taken on the same PE-decane black film in 1.0 M NaCl solution and alamethicin concentrations from 3 x 10^{-9} gr/ml to 8 x 10^{-8} gr/ml. The slight bend towards the current at high voltages has been emphasized by the lines.

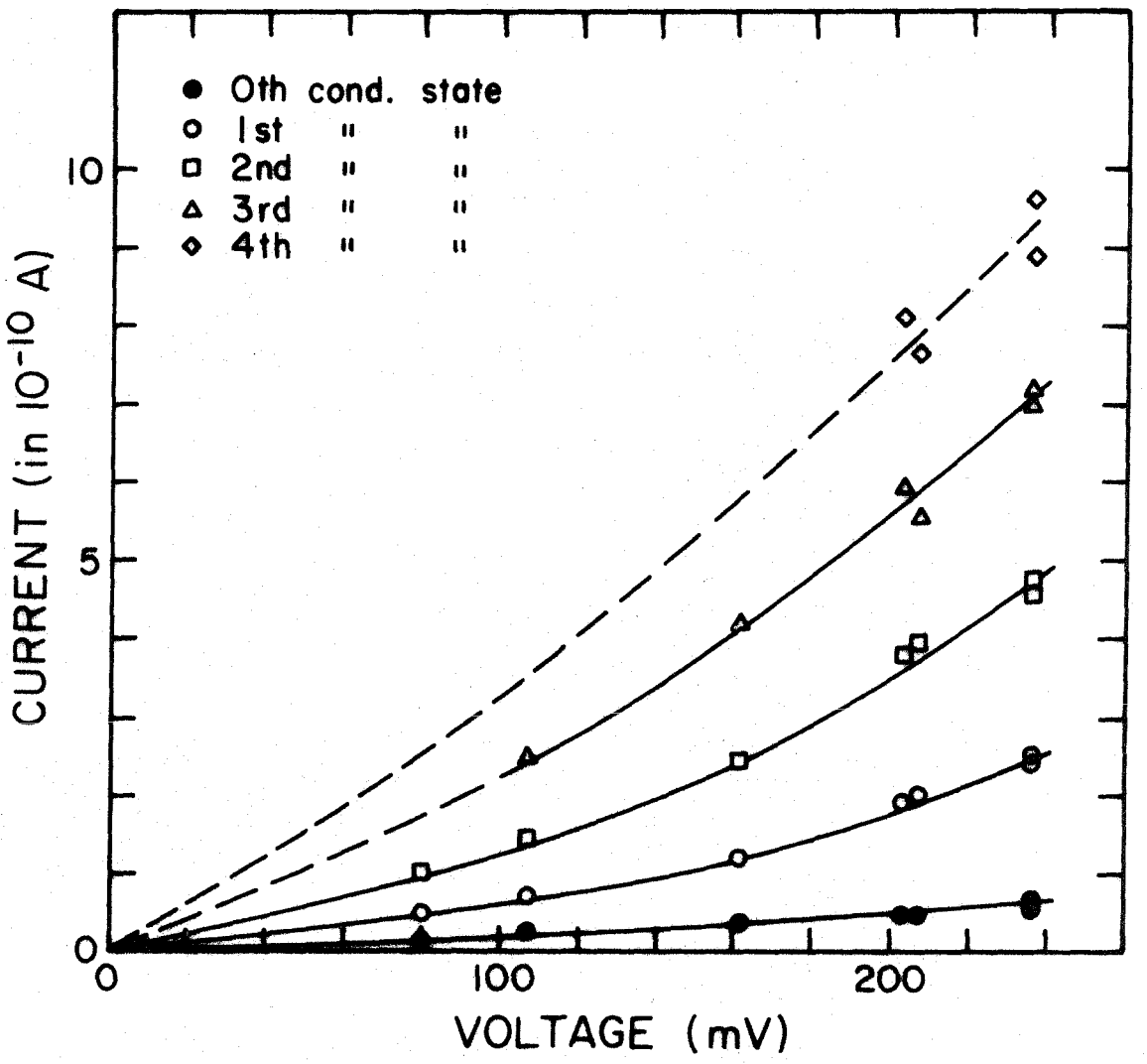
● 0th cond. state
○ 1st " "
□ 2nd " "
△ 3rd " "
◇ 4th " "
CURRENT (in 10⁻¹⁰ A)
10
5
0
0
100
200
VOLTAGE (mV)

FIG. 21

Fig. 22. Log-log graph of the conductance of the characteristic levels of a patch as a function of NaCl concentration (dashed lines). Conductivity of bulk NaCl solution (solid line). Symbols as indicated on inset.

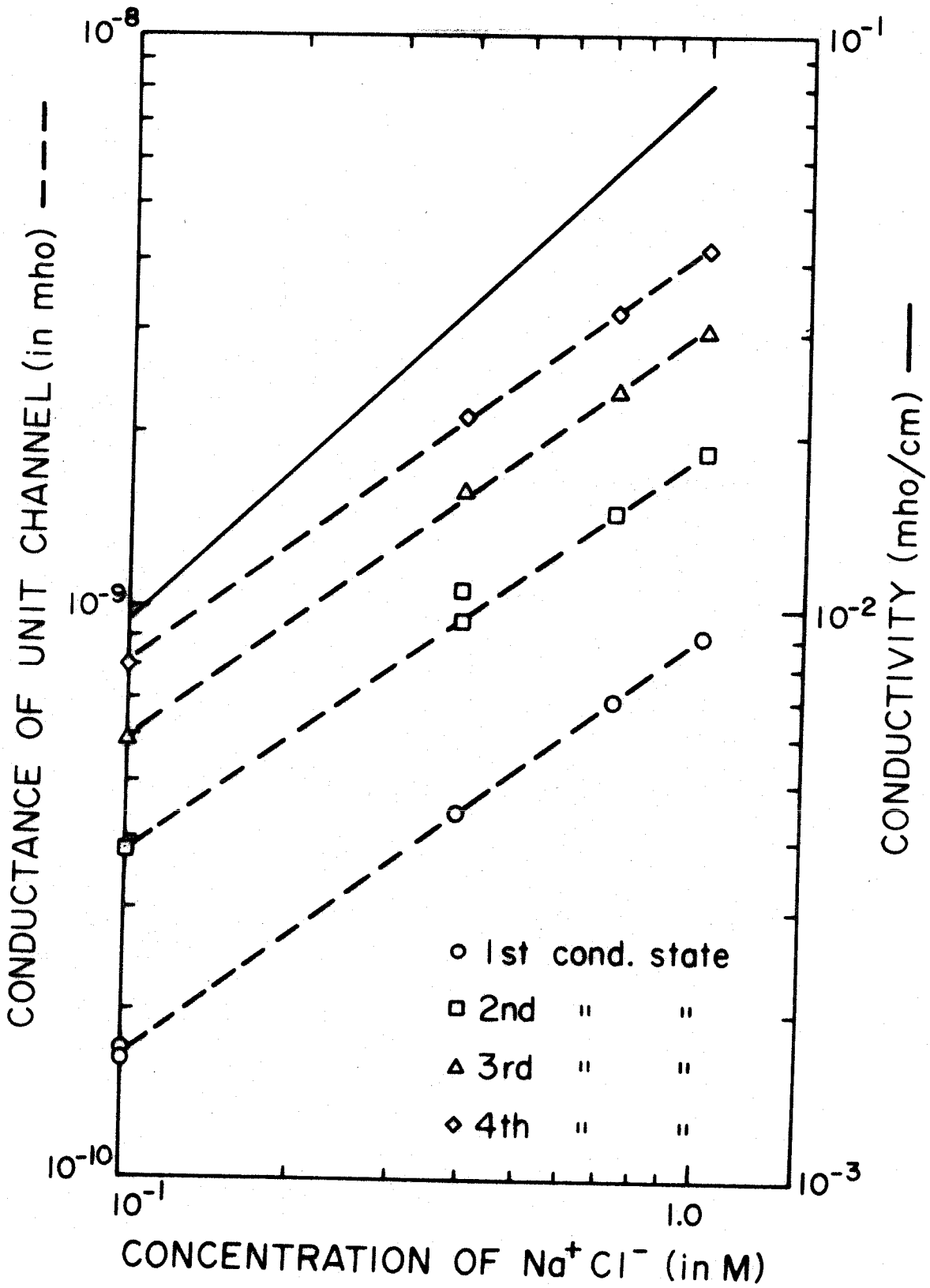
10^{-8}
10^{-9}
10^{-10}
10^{-1}
10^{-2}
10^{-3}
1.0
CONDUCTANCE OF UNIT CHANNEL (in mho) - - -
CONDUCTIVITY (mho/cm) ——
CONCENTRATION OF $Na^+ Cl^-$ (in M)
o 1st cond. state
□ 2nd " "
△ 3rd " "
◇ 4th " "

FIG. 22

dissociation with increasing salt concentration is stronger inside the patch as compared with that of bulk solution. At sodium chloride concentrations lower than 0.1 M, the current steps become too small to be resolved with our equipment.

III.2.6 The Effect of the Viscosity of the Aqueous Solution on the Conductance States of a Patch

Current distributions were taken for 1.0 M NaCl solutions at various concentrations of glycerol. Fig. 23 shows the conductance of the first to fourth level versus the inverse of the viscosity of the glycerol solutions at 23°C. The values for the viscosity of the glycerol solutions in aqueous phase were obtained from the CRC Handbook of Physics and Chemistry. The conductance of the different 1.0 M NaCl in glycerol solutions in bulk is also plotted on the same graph for comparison. It can be seen that there is a very good correlation between the bulk and the states of a patch conductance, and both increase linearly with the inverse of the viscosity, except for small deviations for the 3rd and 4th levels.

III.2.7 Evidence of the Grouping of the Characteristic Conductance Levels into a Patch

Distributions showing more than up to the fourth conductance level can be quantitatively explained in terms of integral multiples of the first five conductance states. Fig. 24 (top) shows a current distribution where levels 1st to 4th, as well as (2nd + 2nd), (2nd + 3rd) or (3rd + 2nd), (3rd + 3rd), (3rd + 4th) or (4th + 3rd), and (2nd + 2nd + 3rd) are resolved. Fig. 24 (bottom) shows the positions of the expected peaks for all possible second order combinations, and their

Fig. 23. Conductance of first to fourth conductance states of a patch in 1.0 M NaCl aqueous solutions with 15%, 30%, and 45%, w/vol glycerol concentrations, versus the inverse of the viscosity at 23°C (dashed lines). Conductivity of bulk solutions (solid line). The corresponding concentrations are indicated on the top scale.

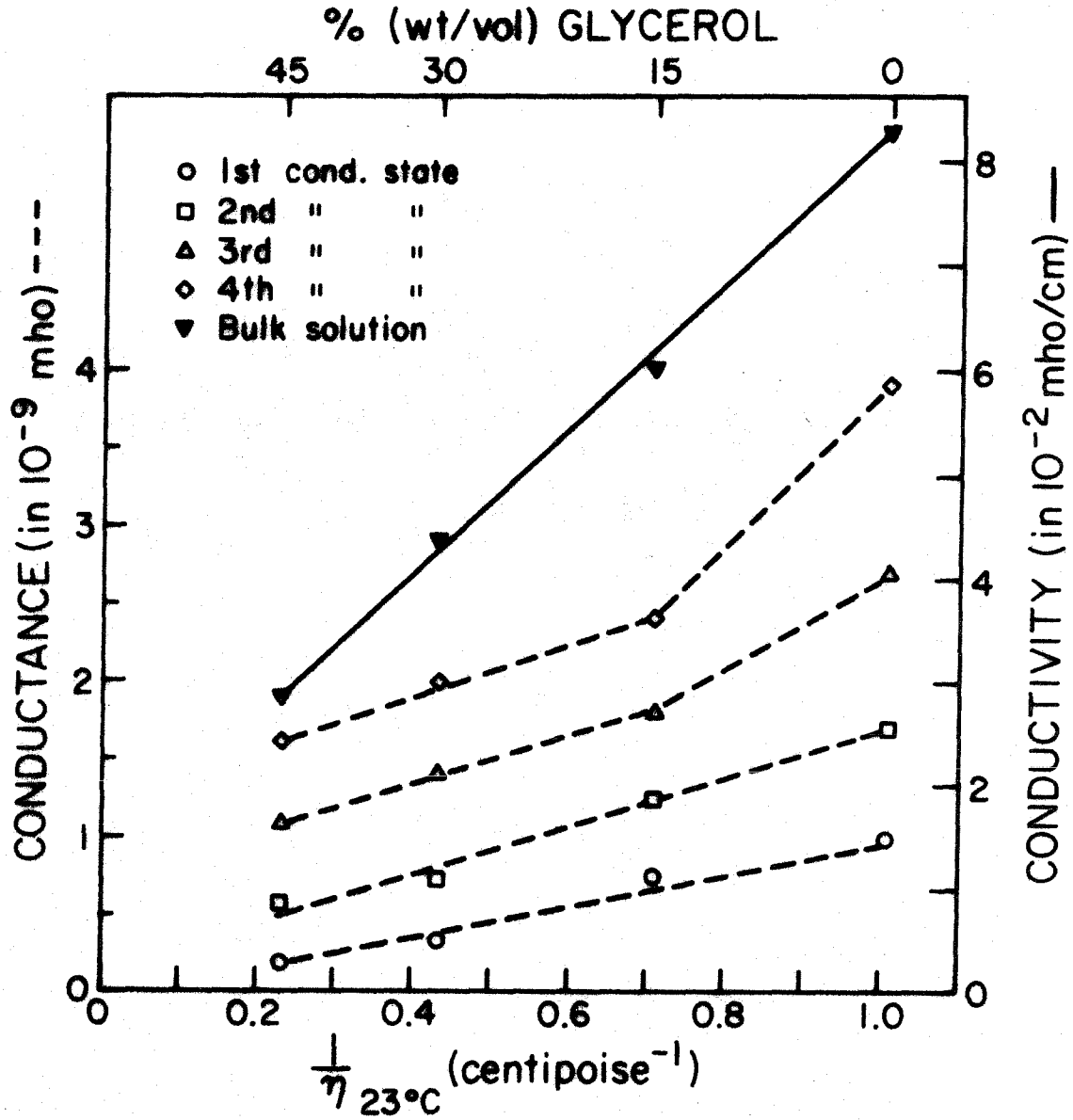
% (wt/vol) GLYCEROL
45
30
15
0
1st cond. state
2nd " "
3rd " "
4th " "
Bulk solution
CONDUCTANCE (in 10^{-9} mho) - - -
CONDUCTIVITY (in 10^{-2} mho/cm) —
0
1
2
3
4
0
2
4
6
8
0
0.2
0.4
0.6
0.8
1.0
$\frac{1}{\eta}_{23°C}$ (centipoise^{-1})

FIG. 23

Fig. 24. (Top) Current distribution for a PE-decane membrane in 1.0 M NaCl and 30% w/v glycerol, taken over a 60 sec. interval at 68 mV. (Bottom) The positions and heights of the 1st to fourth conductance levels are traced in full line. The calculated positions and heights of second order peaks are in dashed lines ($c_{i,j}$ is the peak obtained from the simultaneous occurrence of an i-th state from one patch and a j-th state of a second patch). The positions of a few triplets are also shown (arrows) but their relative expected amplitude has not been calculated. Peaks which are as close as one resolution channel from each other at bottom, actually will give only one peak in the distribution on top.

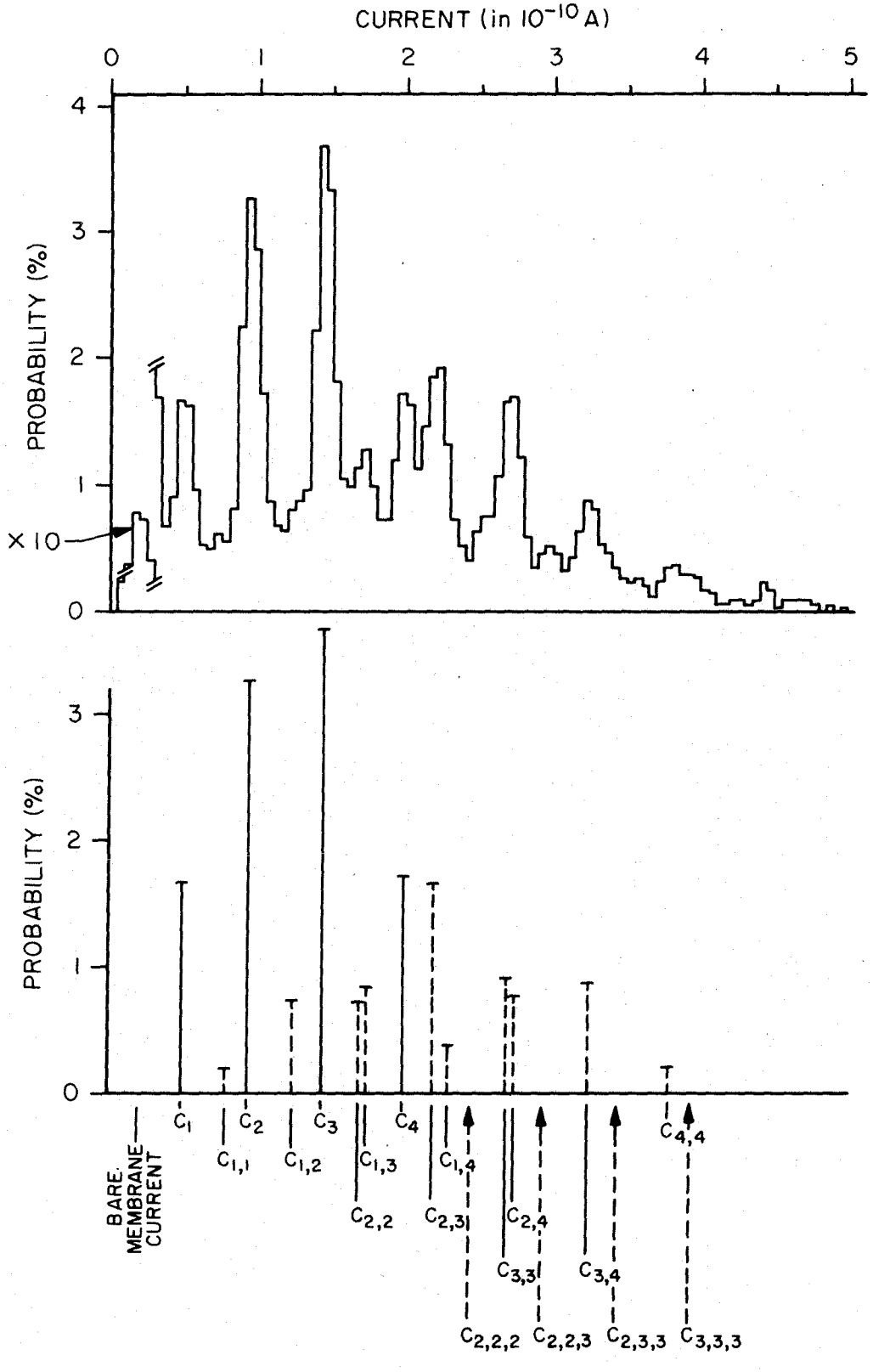
CURRENT (in 10^{-10} A)
0
1
2
3
4
5
PROBABILITY (%)
X 10
BARE MEMBRANE CURRENT
C_1
C_2
C_3
C_4
$C_{1,1}$
$C_{1,2}$
$C_{1,3}$
$C_{1,4}$
$C_{2,2}$
$C_{2,3}$
$C_{2,4}$
$C_{3,3}$
$C_{3,4}$
$C_{4,4}$
$C_{2,2,2}$
$C_{2,2,3}$
$C_{2,3,3}$
$C_{3,3,3}$

FIG. 24

relative amplitudes normalized (see discussion). The positions of some triplets are also shown (arrows) but their amplitudes have not been estimated.

If the voltage is clamped just a few millivolts (ab. 5 mV) beyond the threshold voltage region, and the time course of the current is monitored, one observes that the fluctuations occur over a wider current range, the bare membrane conductance level becomes much less frequent, and the resolution of the characteristic states of a patch diminishes. Under this condition, the current fluctuations within the conductance levels of patch have characteristic times on the order of a few milliseconds in contrast to slower characteristic times on the order of seconds for fluctuations in the number of patches, each involving five conductance levels (fig. 25). In other words, at a constant voltage, slightly higher than the threshold voltage region, the current fluctuates with time as though patches of average conductance that lies between the second and third conductance state, were created, and then disappeared with characteristic times on the order of seconds. Within each patch, five conductance levels, corresponding to the conductance states of a patch (see Sections III.2.2 and III.2.4), fluctuate with characteristic times of the order of milliseconds. Hereafter, the structure capable of five conductance levels as described in Sections III.2.2 through III.2.6 will be defined as a patch.

We have measured the mean conductance of a single patch from current distributions, taken at different voltages. Fig. 26 shows the voltage dependence of the mean conductance state of a patch for membranes made from one PE-decane solution. The results show that the

Fig. 25. Current vs. time on x-y recorder, with a time response of 0.1 sec, for a 0.2×10^{-2} cm^2 area of black PE-decane membrane in 1.0 M KCl solution and 10^{-7} gr/ml alamethicin, at a constant voltage of +190 mV. The width of the fluctuation is smaller than expected because of the time response of the recorder. Notice that when there are in the average more than one patch, the current does not go to bare membrane level very often. For this lapse of time it did not go at all.

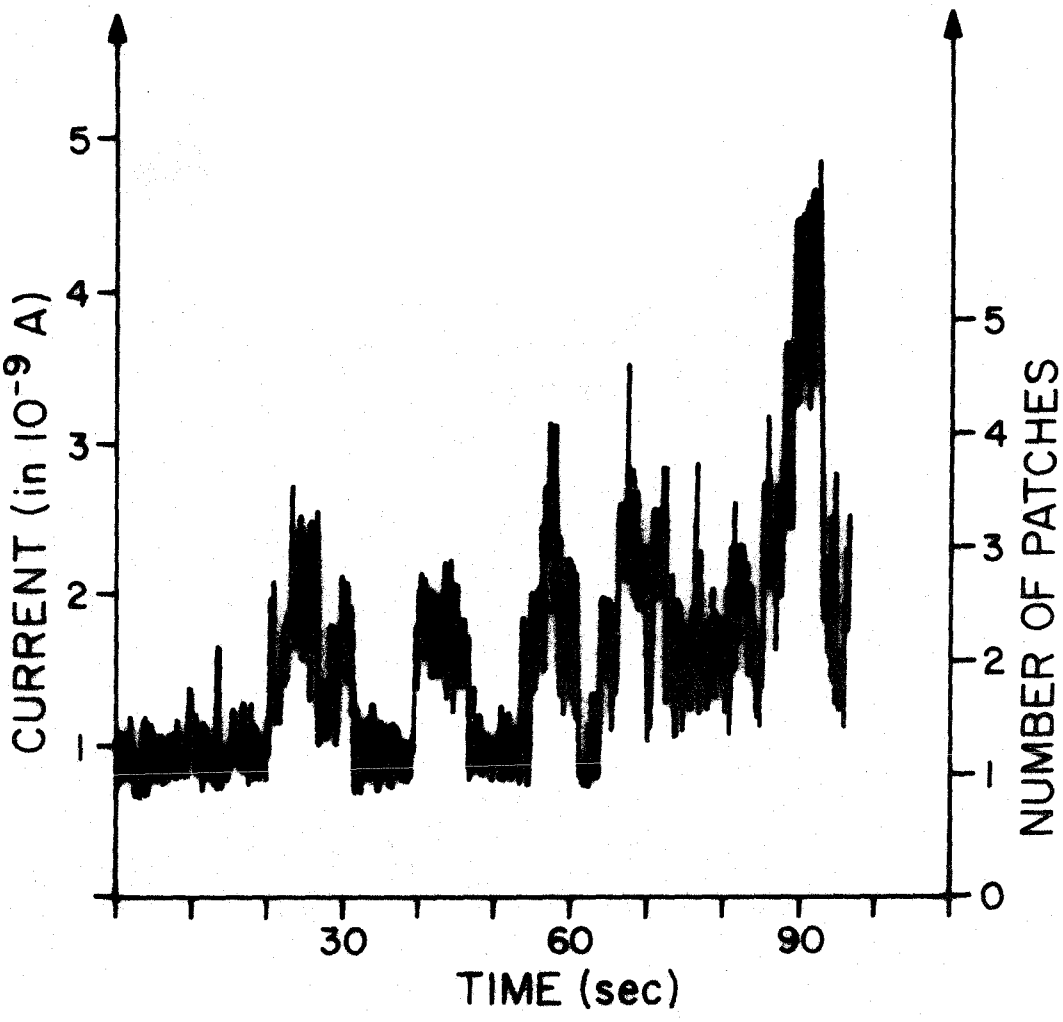
CURRENT (in 10^{-9} A)
1
2
3
4
5
30
60
90
TIME (sec)
0
1
2
3
4
5
NUMBER OF PATCHES

FIG. 25

Fig. 26. The mean patch state calculated from current distributions at different voltages and corresponding alamethicin concentrations.

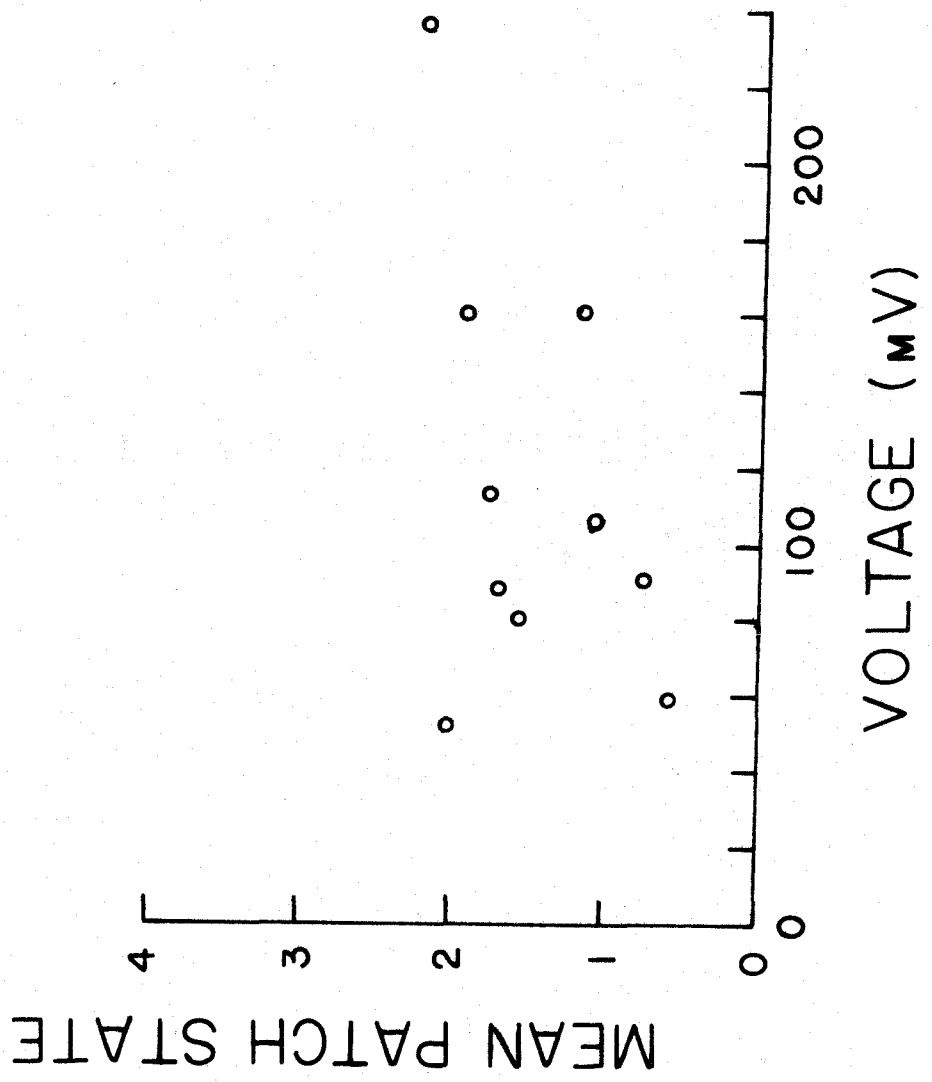

FIG. 26

mean conductance of a patch is practically voltage independent, and lies between the first and second conductance states of a patch.

We have observed that for other batches of PE, the probability distributions of the current levels in a patch give mean patch conductances higher than those shown in fig. 26, namely, between the second and third conductance state of a patch. In this latter case, the single patch mean conductance still remains voltage independent.

III.2.8 The Intra-patch Kinetics

We have measured the time duration of the current steps within a patch in the following manner. We wait until a current step goes up and measure the time to the next current step going down, this we call the "time down" ($t_{\downarrow}$). We repeat this experiment over times long compared with $t_{\downarrow}$ and then plot the distribution of $t_{\downarrow}$. The inverse experiment, which is to wait until a current step goes down and then measure the time to the next step going up is also plotted as a probability density distribution and we refer to it as "time up" ($t_{\uparrow}$). Fig. 27 shows distributions of $t_{\downarrow}$ and $t_{\uparrow}$ for a PE-decane black membrane in 1.0 M NaCl and 8×10^{-8} gr/ml alamethicin in the test side, at +106 mV, taken over a 5 min interval. When these distributions are plotted in log-linear form (fig. 28), they can be fit by a curve of the type:

$$P_{\downarrow}(t) = \frac{1}{\tau_{\downarrow}} e^{-\frac{t}{\tau_{\downarrow}}} \qquad (2a)$$

$$P_{\uparrow}(t) = \frac{1}{\tau_{\uparrow}} e^{-\frac{t}{\tau_{\uparrow}}} \qquad (2b)$$

Fig. 27. Probability density distributions of the transition times of the fluctuations between the conductance states of a patch. PE-decane black membrane in 1.0 M NaCl solution and 8×10^{-8} gr/ml alamethicin on the test side. The voltage is clamped at +106 mV. Total sampling time: 5 min. The probability increase from time 0 to the maximum probability reflects the cut-off level of the low-pass filter.

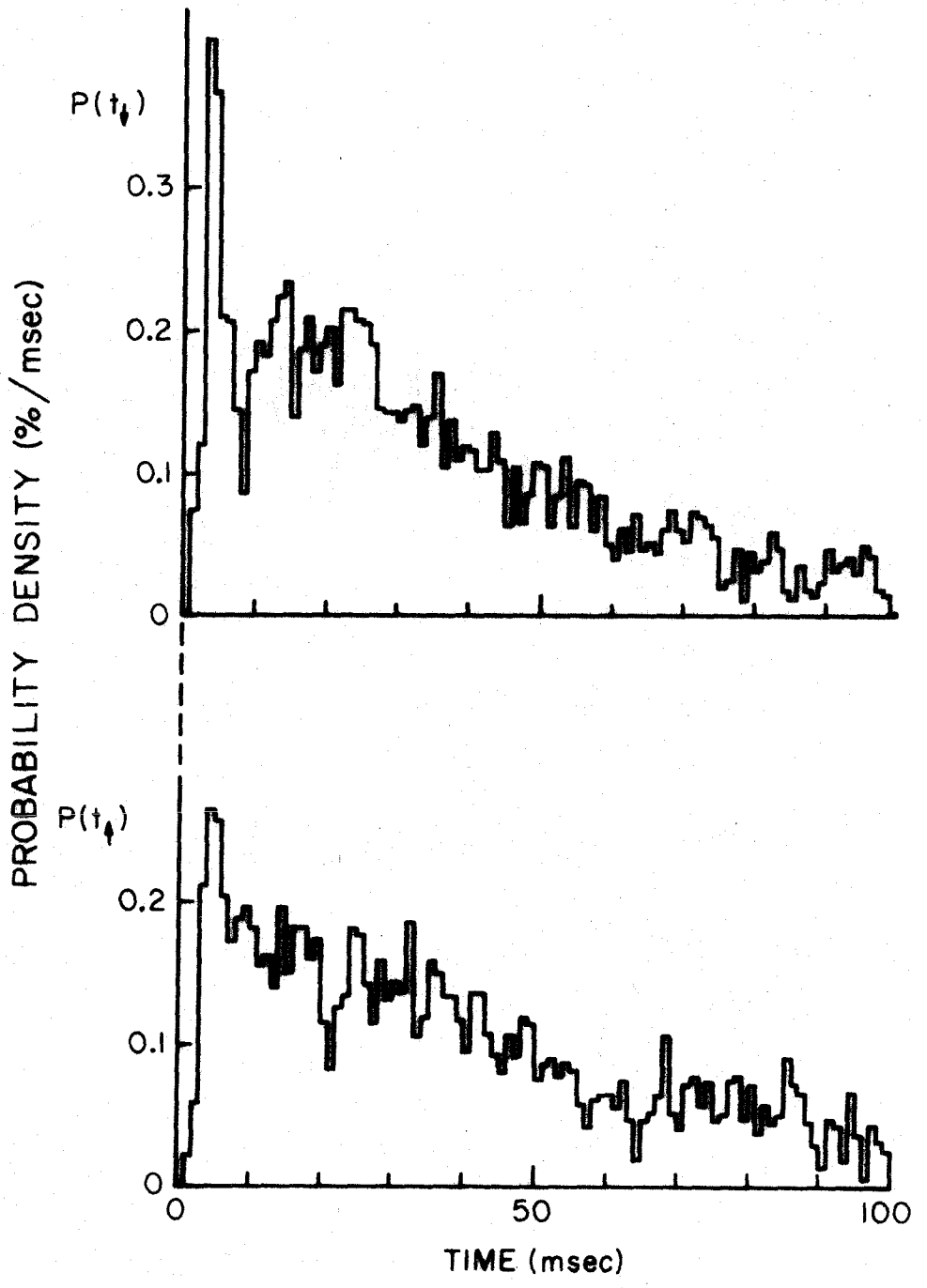
P(t↓)
0.3
0.2
0.1
0
PROBABILITY DENSITY (%/msec)
P(t↑)
0.2
0.1
0
0
50
100
TIME (msec)

FIG. 27

Fig. 28. The same conditions as in fig. 27. All points were plotted on log-linear mode and the straight lines represent a least squares fit of the data.

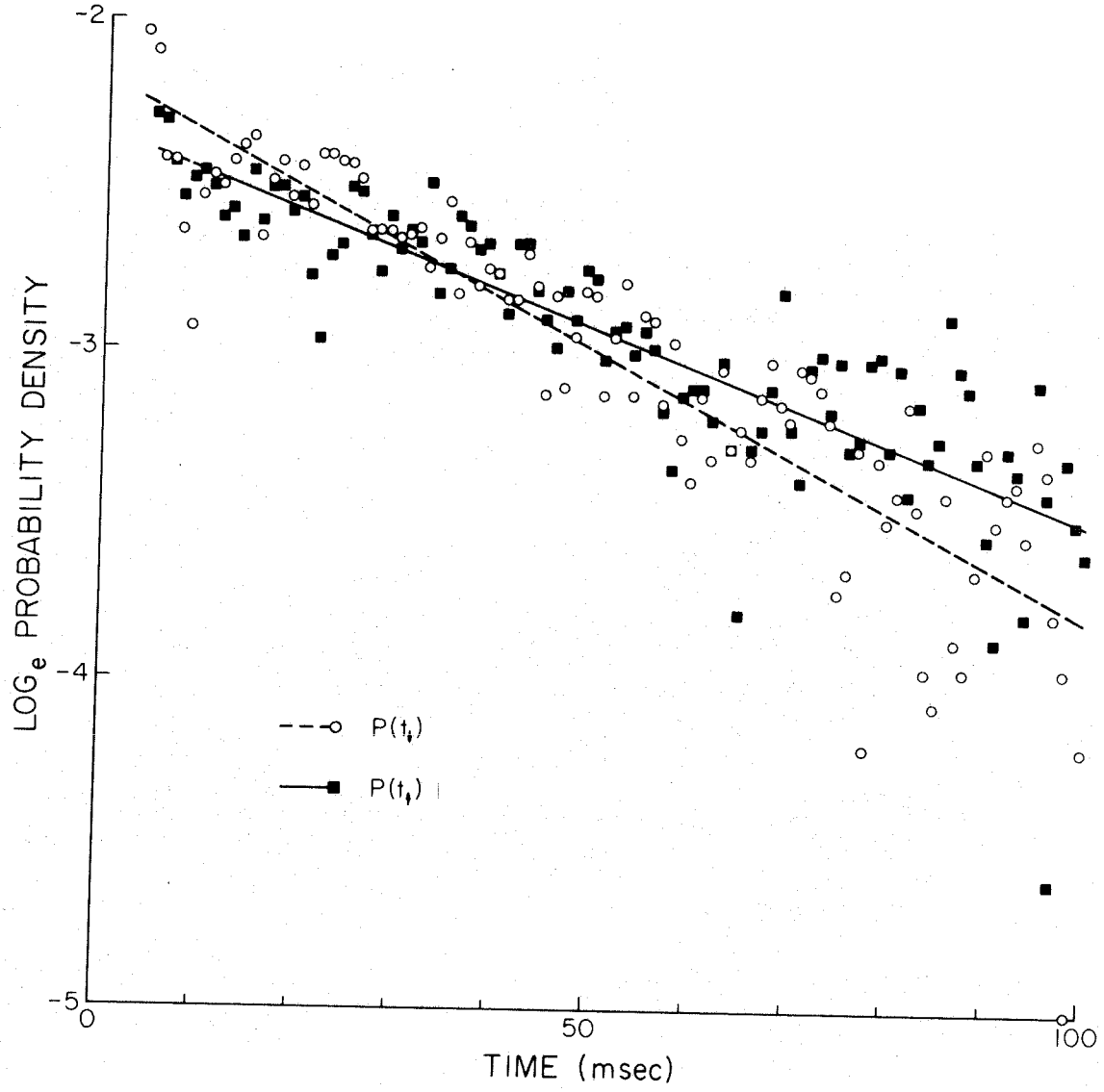

FIG. 28

Thus, we can characterize the probabilities of a step down and a step up by the characteristic times $\tau_{\downarrow}$ and $\tau_{\uparrow}$, respectively.

We have measured the $\tau_{\downarrow}$ and $\tau_{\uparrow}$ as a function of voltage for different threshold voltages. Fig. 29 shows the dependence of these characteristic times on the voltage.

The data shown on fig. 29 were from membranes made from the same PE-decane solution. Both $\tau_{\downarrow}$ and $\tau_{\uparrow}$ decrease as the voltage increases, but this is more pronounced for the $\tau_{\uparrow}$. For membranes made of different batches of PE we have measured shorter characteristic times (in the 3 to 10 m sec range for $\tau_{\downarrow}$ and 3 to 20 m sec range for $\tau_{\uparrow}$), but the exponential nature of the probability distribution is maintained.

It is clear from the description of the "time down" and "time up" experiments that one is computing the distribution of the times spent in any one of the levels before shifting to the next one, up in the case of $\tau_{\uparrow}$, or down in the case of $\tau_{\downarrow}$.

III.2.9 The Inter-patch Kinetics

In the previous sections we have shown that alamethicin interacts with PE-decane black membranes showing discrete conductance levels which group themselves into patches. We also showed that the mean conductance of a single patch was practically voltage independent. The principal voltage effect is, therefore, on the formation of the patches and we must turn to the study of the time course and voltage dependence of the formation of these patches. For this purpose we used a pulse technique and monitored the current response to a voltage step as a function of time.

Fig. 29. The dependence of the characteristic times $\tau_{\downarrow}$ and $\tau_{\uparrow}$ of the intra-patch fluctuations, on the voltage. These points represent data taken for membranes made from the same PE-decane solution but at different alamethicin concentrations. For each voltage value there is a set of $\tau_{\uparrow}$ and $\tau_{\downarrow}$ points.

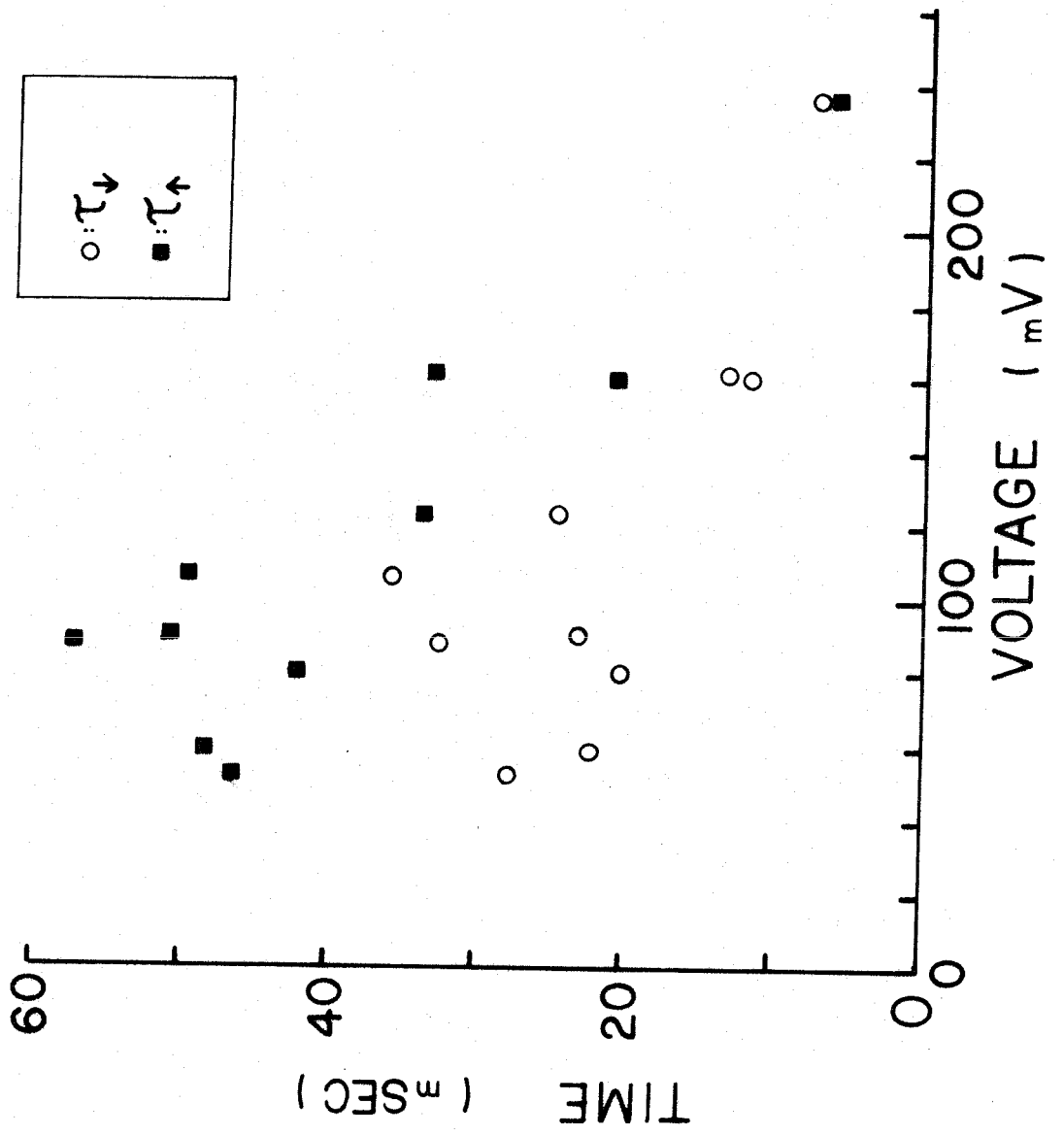

FIG. 29

Fig. 30 shows a series of experiments done on the same membrane at 1.0 M NaCl concentration in the aqueous phase. The magnitude of the voltage pulse was increased successively. It can be seen that the current increases with a constant rate for a few seconds to reach a final state of fluctuations around a mean value. In fig. 31 we have plotted the dependence on voltage of the initial rate of current increase. Fig. 32 shows the average final current versus the voltage. Both the initial rate and the final value are exponentially dependent on the voltage across the membrane.

III.2.10 The Effect of Viscosity of the Aqueous Solution on the Kinetics of the Alamethicin Induced Conductance

The same experiments described in section III.2.9 were done in the presence of 15%, 30%, and 45% w/v glycerol in 1.0 M NaCl concentration in the aqueous phases. The qualitative nature of the kinetics remained the same as described in section III.2.9. The voltage dependence of the initial rate decreased from an e-fold increase every 5.8 mV in no glycerol, to an e-fold increase in 10.8 mV in 30% glycerol. But the dependence of the final average current on voltage remained the same, namely an e-fold increase every 3.3 ± 0.2 mV, from no glycerol to 45% w/v glycerol.

III.2.11 The Steady State Current-voltage Curve of the Alamethicin Doped PE-decane Black Film

An i-V curve analogous to that shown in fig. 15 was plotted on log-linear graph in fig. 33 for a 1.0 M NaCl concentration in the aqueous solutions, and 10^{-6} gr/ml alamethicin at both sides of the membrane. The voltage dependence matches that of the final average

Fig. 30. Time course of the alamethicin induced membrane current. PE-decane membrane in 1.0 M NaCl and 5 x 10^{-7} gr/ml alamethicin. (Top) voltage pulses, 10 sec. duration; 40, 42, 50, 55, and 58 mV. (Bottom) current tracing as followed by x-y recorder with 1/50 sec. time response.

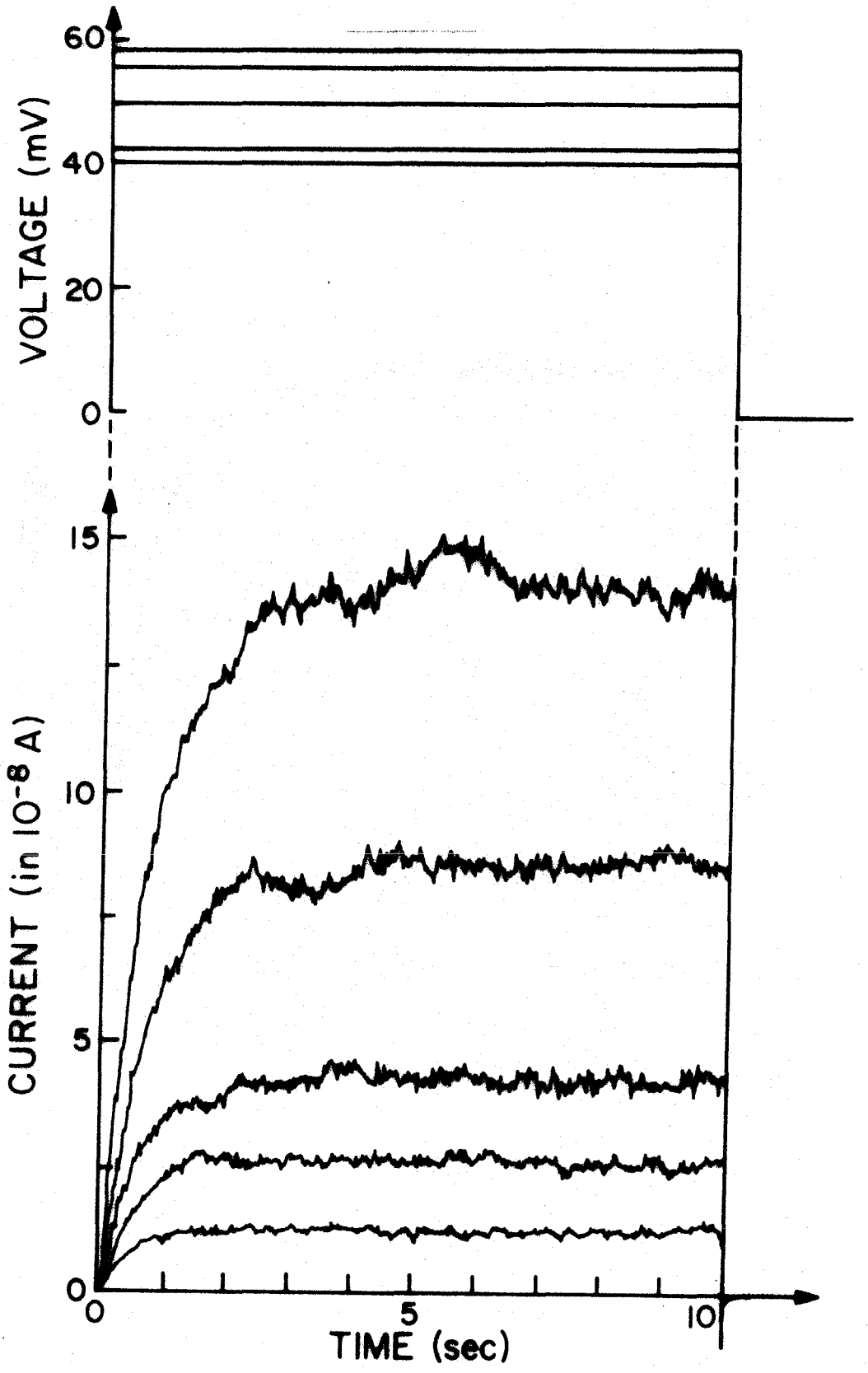

FIG. 30

Fig. 31. The dependence of the initial rate of current increase on voltage for a PE-decane membrane in 1.0 M NaCl and 6.5×10^{-7} gr/ml alamethicin, subjected to a series of voltage pulses.

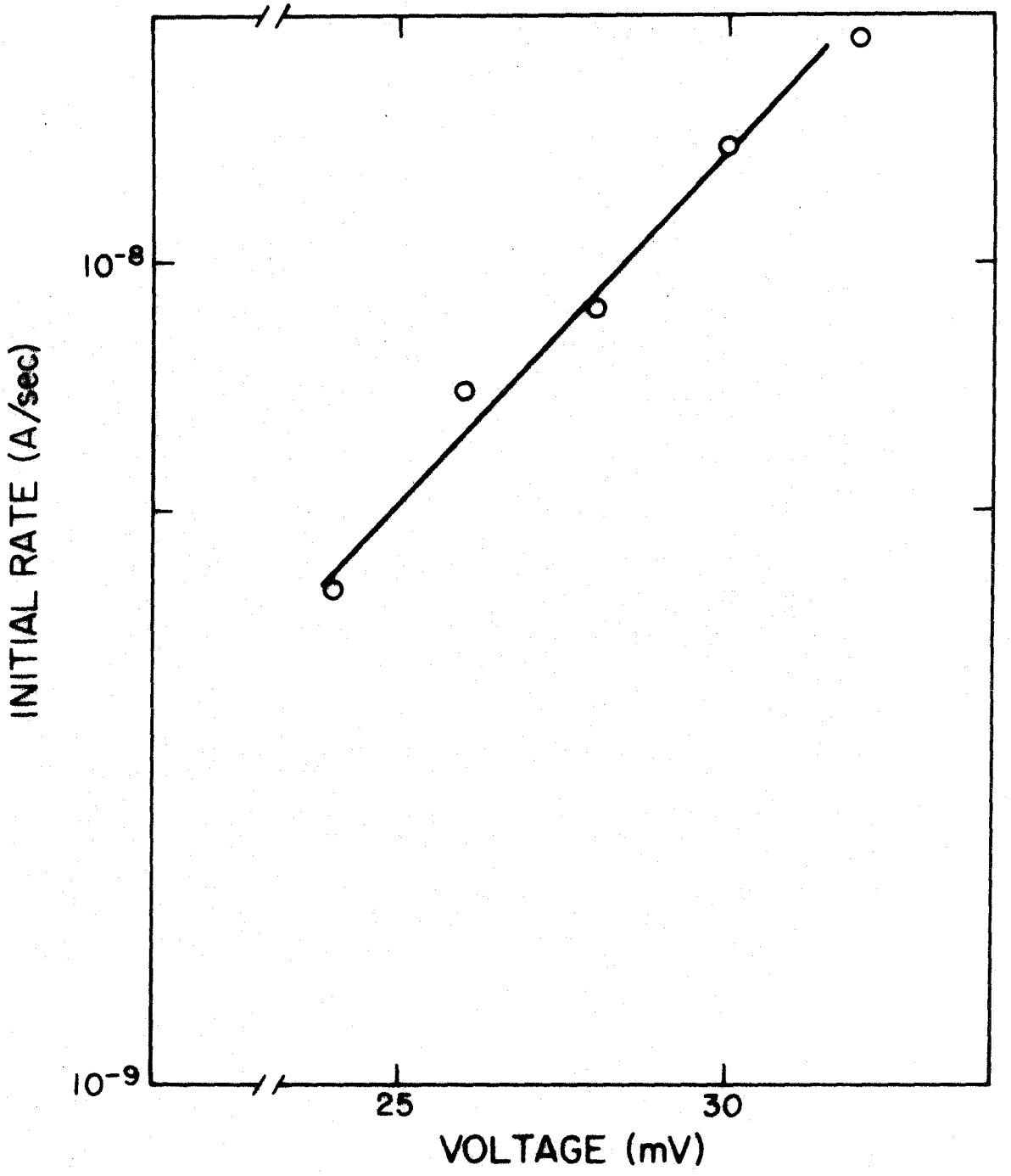

FIG. 31

Fig. 32. The dependence of the final current on voltage, for a PE-decane membrane in 1.0 M NaCl and 8×10^{-7} gr/ml alamethicin, subjected to a series of voltage pulses.

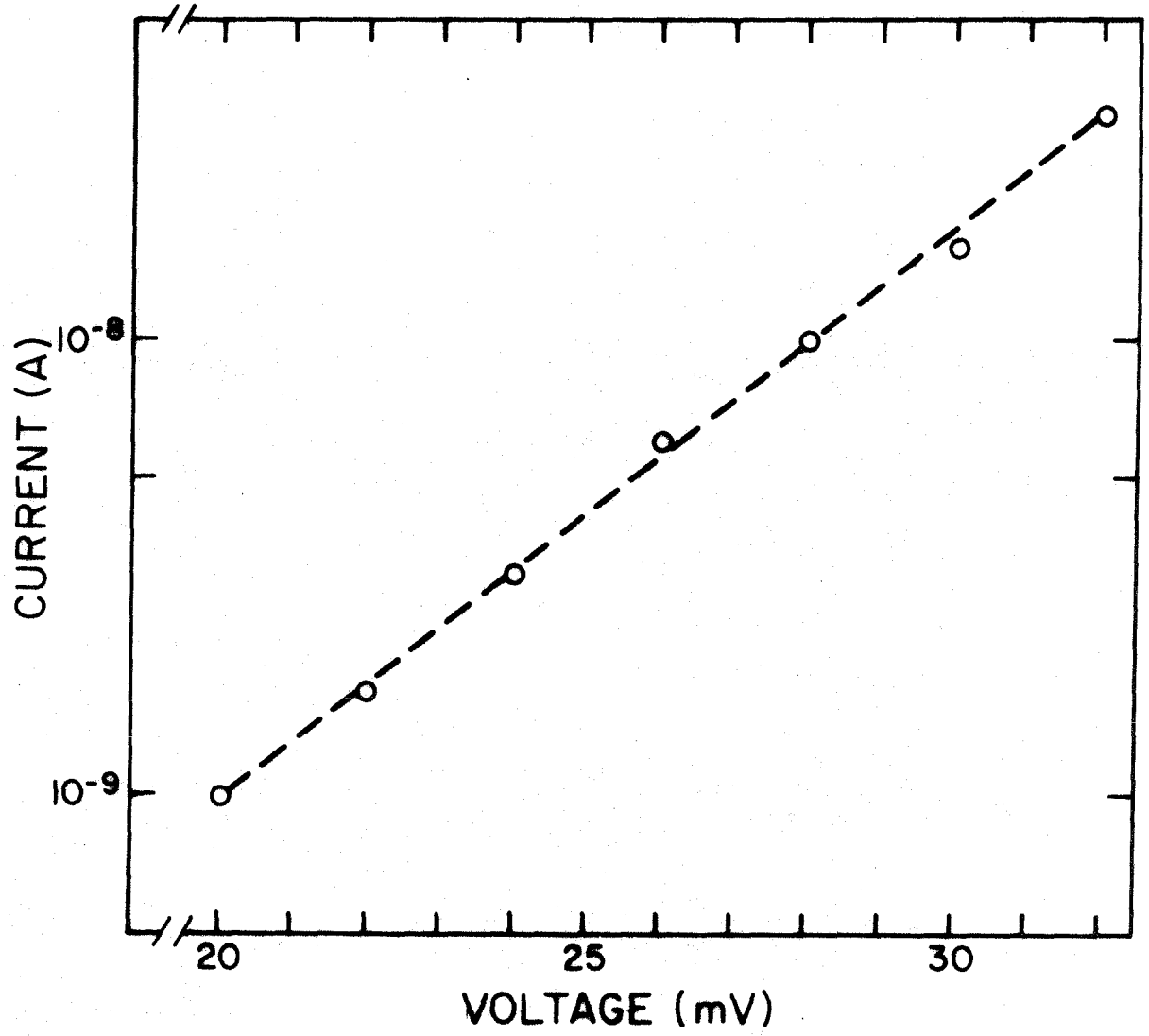

FIG. 32

Fig. 33. i-V curve for a PE-decane membrane in 1.0 M NaCl and 10^{-6} gr/ml alamethicin in both sides. For the negative side, the signs of the current and the voltage should both be negative. The fact that the (+) branch and (-) branch do not coincide is due to small differences in the amount of alamethicin added to each side.

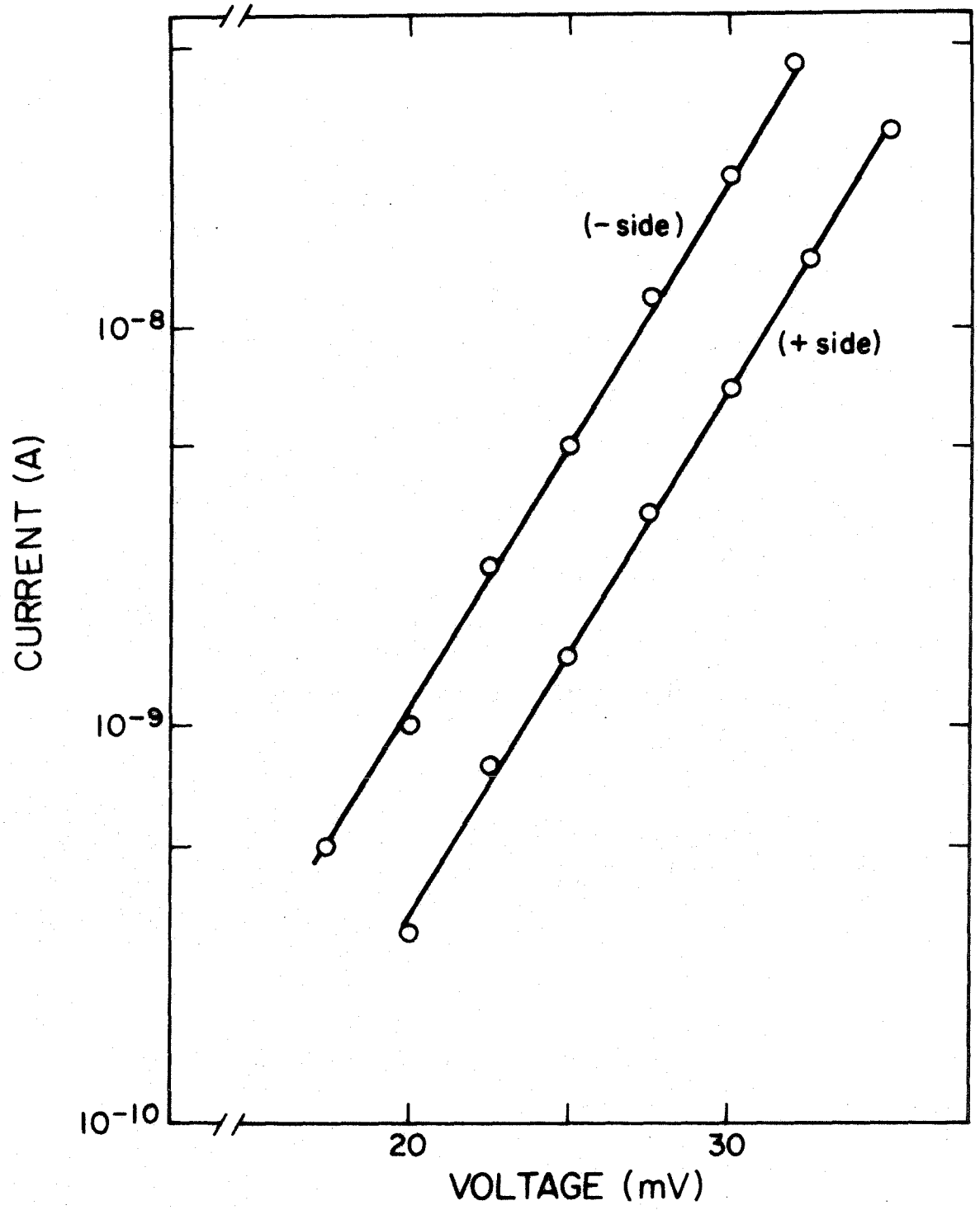

FIG. 33

value of the current shown in section III.2.9, as expected. The i-V curves showed a rate dependent current difference at a given voltage when dV/dt was larger than 1 mV/sec, as expected from the kinetic experiments. Hence to insure that the measurements were made under nearly steady state conditions, the sweep rate was not allowed to exceed 0.45 mV/sec.

III.2.12 The Dependence of the Current on the Concentration of Alamethicin

Current-voltage curves were taken on the same PE-decane black membrane for fixed ionic media and varying amounts of alamethicin in the aqueous phase. Alamethicin was added to one chamber, the test side, in small aliquots of concentrated solution (see Discussion), not larger than 35 $\mu\ell$, and balanced by adding the same amount of the salt solution to the chamber on the other, grounded, side of the membrane. This was followed by 5 min. stirring. Finally the i-V curve was taken. Fig. 34 shows a family of such i-V curves. It can be seen that below the threshold voltage, the conductances are identical, and the currents correspond to bare membrane current, indicating that none of the alamethicin induced conductances was present. The only effect of increasing the alamethicin concentration was to lower the voltage needed to obtain a given number of conductance levels. Since we know that the conductance of the current levels within a patch is very close to ohmic, we can find the voltage, V_n, at which n conductance levels are observed in the average. This is the voltage indicated by the intersection of the experimental i-V curve with the expected i-V curve for n levels. The latter curve is shown in fig. 34 as a dashed line for $n \cong 10$. We

Fig. 34. Family of i-V curves superimposed. PE-decane membrane in 0.1 M NaCl. Alamethicin concentration: (a) 5×10^{-8}, (b) 10^{-7}, (c) 2×10^{-7}, (d) 5×10^{-7}, (e) 10^{-6}, (f) 1.5×10^{-6} gr/ml. Sweep rate of voltage: 12 mV/sec., recorder time response: 1/4 sec. The baseline current (about 10^{-10} A) is the sum of the capacitive charging current and the resistive current of the bare membrane. Dashed line: Expected i-V characteristics of an average of ~ 10 conductance levels.

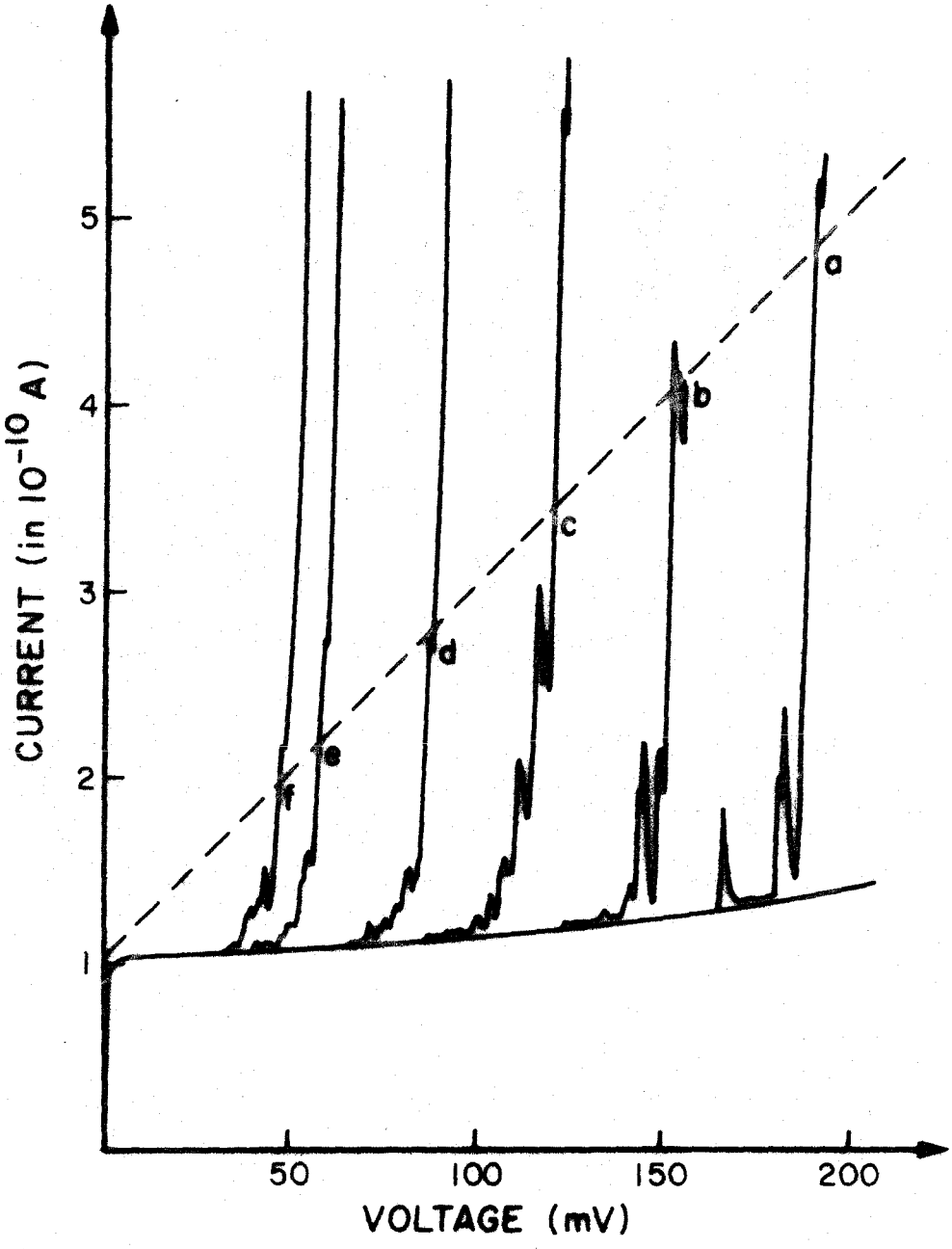

FIG. 34

have observed that under conditions where currents corresponding to not more than up to a few patches, and the current sensitivity is high, V_n will be practically the same for $3 < n < 10$. In other words, at this level of sensitivity, the current increases almost vertically at the onset of the high conductance state. Within the reproducibility of the experiment, moreover, V_n will be effectively the same for $3 < n < 30$. Therefore, we will call this V_n for low values of n, the switching voltage, and denote it by V_s. Fig. 35 shows semilog plots of the concentration of alamethicin in the aqueous phase, versus the switching voltage, for different salts at 0.1 molar concentration. It can be seen that for these salts the switching voltage very closely behaves as:

$$C_{alm} = C_o \, e^{-V_s/36 \text{ mV}} \qquad (3)$$

At very high concentrations of alamethicin, the switching voltage becomes negative. Such a case is shown in fig. 36; the salt concentration was 1.0 M NaCl on both sides of the lipid membrane, and 10^{-5} gr/ml of alamethicin had been added to the test side only. The negative resistance appears because the switching voltage is lower than the zero current voltage, in this case 0 V.

III.2.13 The Effect of the Salt Concentration of the Aqueous Media on the Switching Voltage

As in section III.2.12, families of i-V curves were taken for a black lipid membrane at a fixed alamethicin concentration but with a varying salt concentration in the aqueous phase. Again the concentration is an exponential function of switching voltage. The results are summarized in fig. 37. It can be seen that for all salts measured the

Fig. 35. Log-linear plot of alamethicin concentration versus switching voltage for 0.1 M solutions of different chloride salts. NaCl (x-x), KCl (-o-o), $BaCl_2$ (-·-·).

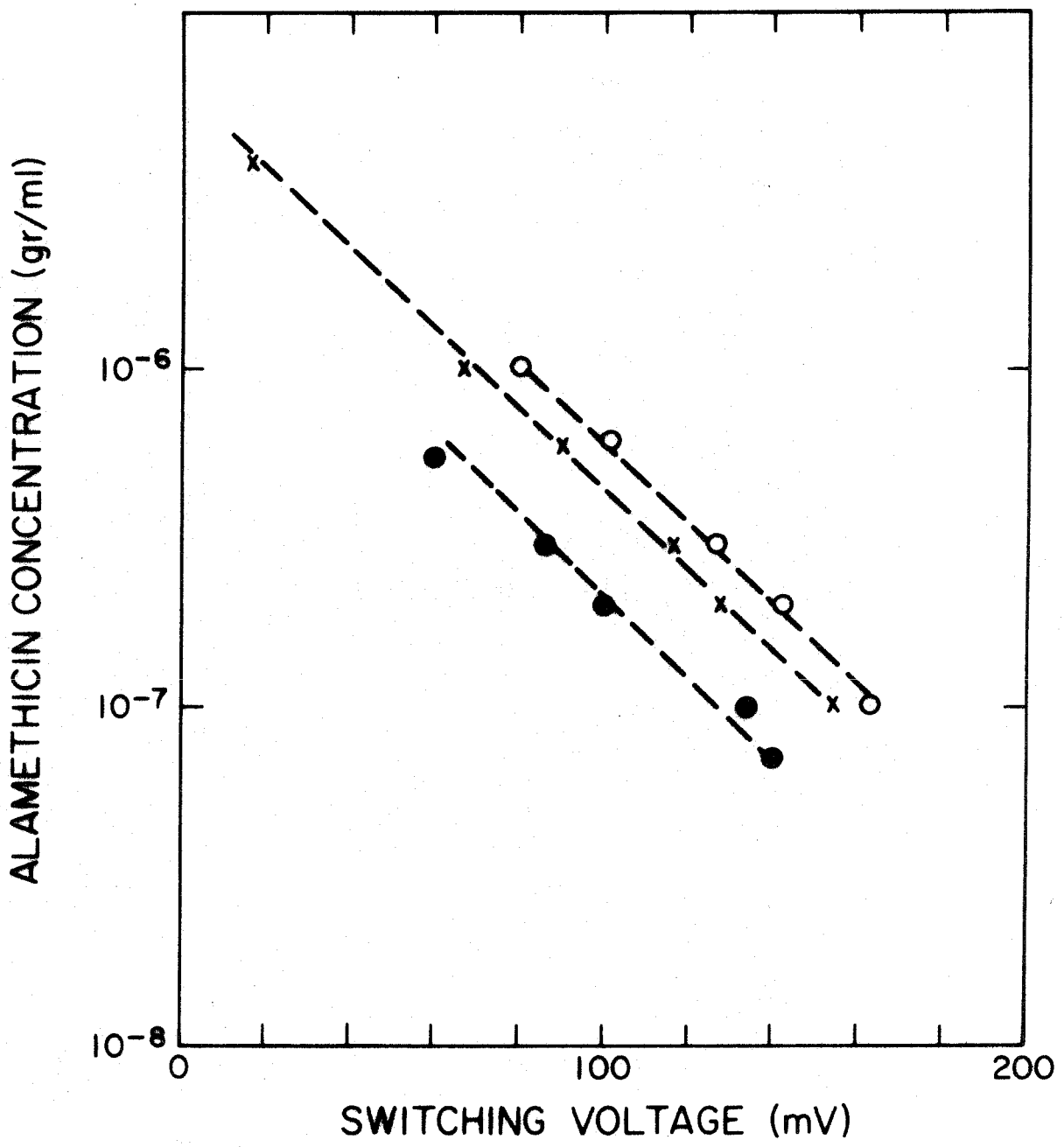
ALAMETHICIN CONCENTRATION (gr/ml)
10-6
10-7
10-8
0
100
200
SWITCHING VOLTAGE (mV)

FIG. 35

Fig. 36. i-V curve of a PE-decame membrane, 0.5 x 10^{-2} cm^2 in area, in 1.0 M NaCl, and 10^{-5} gr/ml alamethicin on one side only (the test side). The negative resistance is due to the fact that the switching voltage is negative, thus lower than the zero current voltage, which is 0.

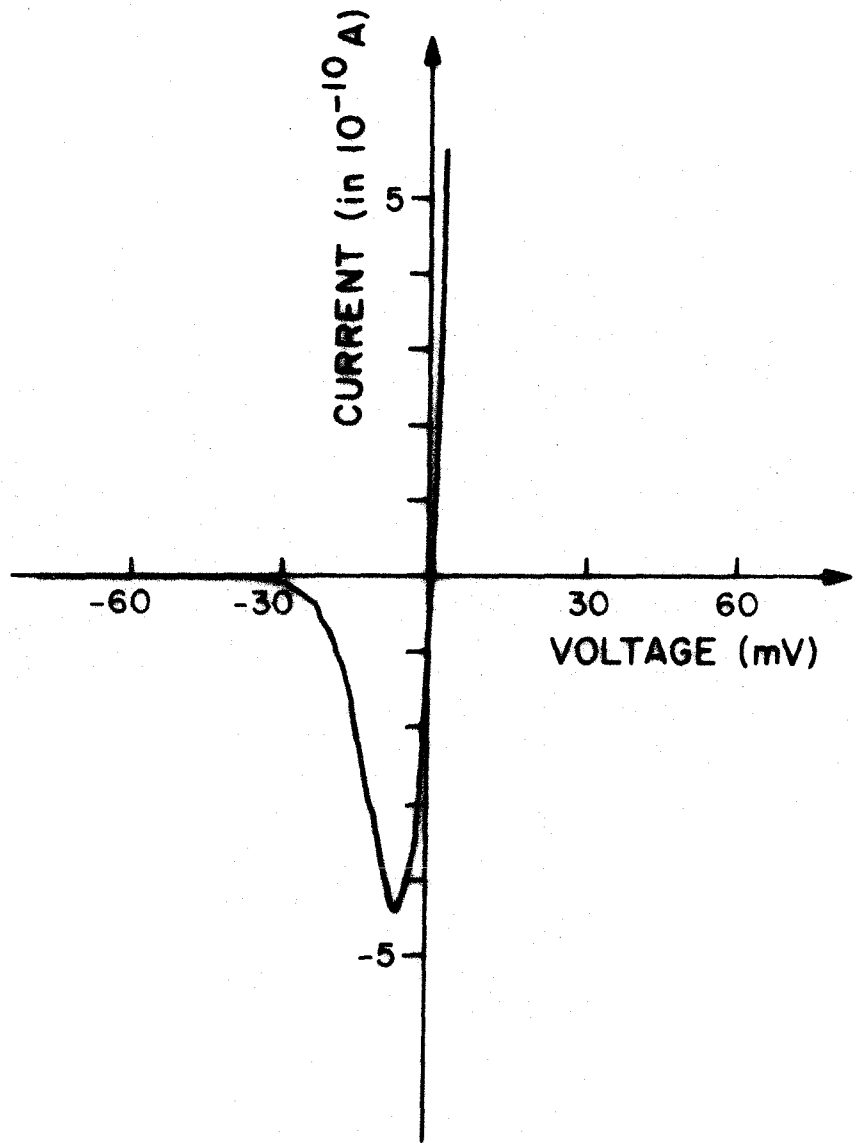

FIG. 36

Fig. 37. Dependence of switching voltage on salt concentration for PE-decane black membranes with alamethicin. (x-x) NaCl; in 2 x 10^{-6} gr/ml alm.; (o-o) KCl, in 10^{-6} gr/ml alm.; (●-●) $CaCl_2$, in 2 x 10^{-7} gr/ml alm.

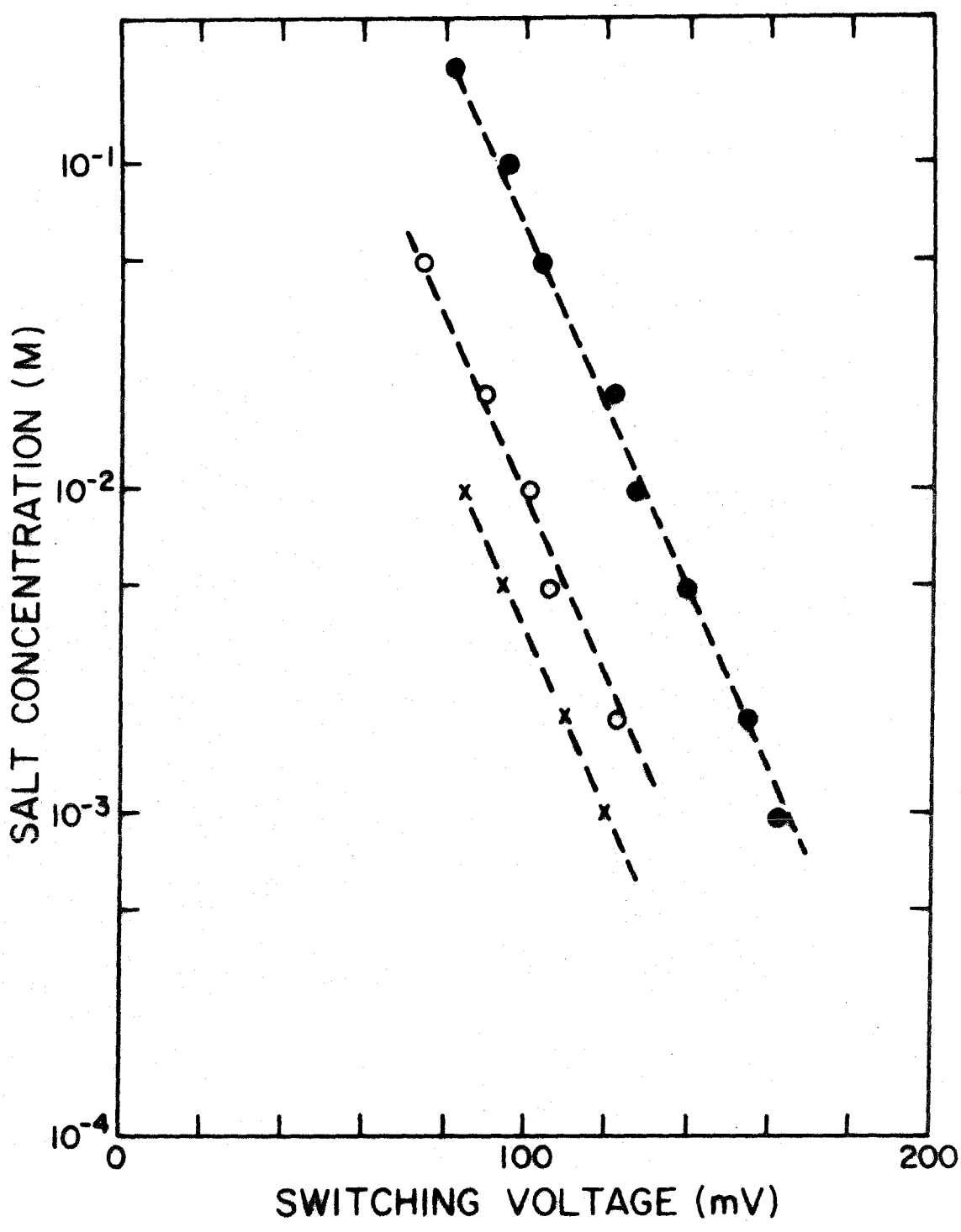
SALT CONCENTRATION (M)
10^{-1}
10^{-2}
10^{-3}
10^{-4}
0
100
200
SWITCHING VOLTAGE (mV)

FIG. 37

switching voltage behaves very much as:

$$C_{salt} = C'_o e^{-V_s/16\ mV} \qquad (4)$$

III.2.14 The Effect of the Surface Charge on the Black Film on the Alamethicin Induced Conductance

Phosphatidyl ethanolamine is a neutral lipid in the pH range of our experiments. More precisely, it is a zwitter-ionic molecule, the positive charge coming from the amino group and the negative one from the phosphate. Black lipid films can also be made from 2% w/v solutions of phosphatidyl glycerol (PG) in n-decane. This lipid bears one negative charge per molecule. Thus, black lipid films made of PG-decane have a negative surface charge. We have studied the interaction of alamethicin with PG-decane black membranes and saw no difference between this result and those found with PE-decane membranes, in terms of steady state current-voltage characteristics, and the dependence of the switching voltage on alamethicin concentration.

III.2.15 The Effect of Alamethicin on the Surface Charge of the Black Lipid Membrane

It has been shown that certain molecules, which act as carriers of particular cations or anions across artificial lipid membranes, can be used as "probes" to detect changes in the surface charge of these films (McLaughlin et al., 1970). We have used the neutral carrier nonactin with PE-decane black films in 0.1 M KCl aqueous solution. At 5×10^{-7} M nonactin concentration in the aqueous medium, the conductivity near zero volts is 2.2×10^{-5} mho/cm^2. The gradual addition of alamethicin up to concentrations of 5×10^{-6} gr/ml in the aqueous phase

does not change the zero volt conductance. The only effect is that at voltages above the V_s for the alamethicin, the current increases as it would be expected by adding the nonactin induced and the alamethicin induced conductance.

III.2.16 The Cation-anion Selectivity of the Alamethicin Modified PE-decane Membrane

We have determined the cation-anion selectivity of alamethicin doped membranes by subjecting the membrane to concentration gradients and measuring resting potentials. In these experiments, we used calomel reversible electrodes to measure the voltage across the membrane, rather than silver-silver chloride, since the latter would develop a Nernst potential due to the chloride gradient, and this voltage would drop across the film. Fig. 38 shows the steady state i-V curve of a PE-decane black membrane, under a 0.5 M to 0.005 M gradient of KCl, 9×10^{-6} gr/ml alamethicin in low-salt side which is the test side, and 6×10^{-7} gr/ml alamethicin in high-salt side. In this case we observe a cationic resting potential of 53 mV, i.e., 26.5 mV per decade of concentration gradient. The negative resistance arises because the switching voltage is lower than the resting potential, as in section III.2.12, fig. 36.

For NaCl the selectivity is also cationic and the resting potential is 13 mV per decade of concentration gradient. In contrast, for $CaCl_2$, there is an anionic resting potential of -26 mV per decade of concentration gradient.

Fig. 38. i-V curve of a PE-decane black membrane in a 100:1 KCl concentration gradient. Low-salt side has 0.005 M KCl and 9×10^{-6} gr/ml alamethicin, and it is the test side. High-salt side has 0.5 M KCl and 6×10^{-7} gr/ml alamethicin. Sweep rate was 0.45 mV/sec., arrows indicate direction of sweep. Negative resistance arises because the switching voltage is lower than the zero current voltage (53 mV). The high conductance at the grounded side is due to the alamethicin present on that side only, the high conductance which generates the negative resistance is due to the alamethicin at the low-salt side. This +53 mV resting potential indicates some cationic selectivity.

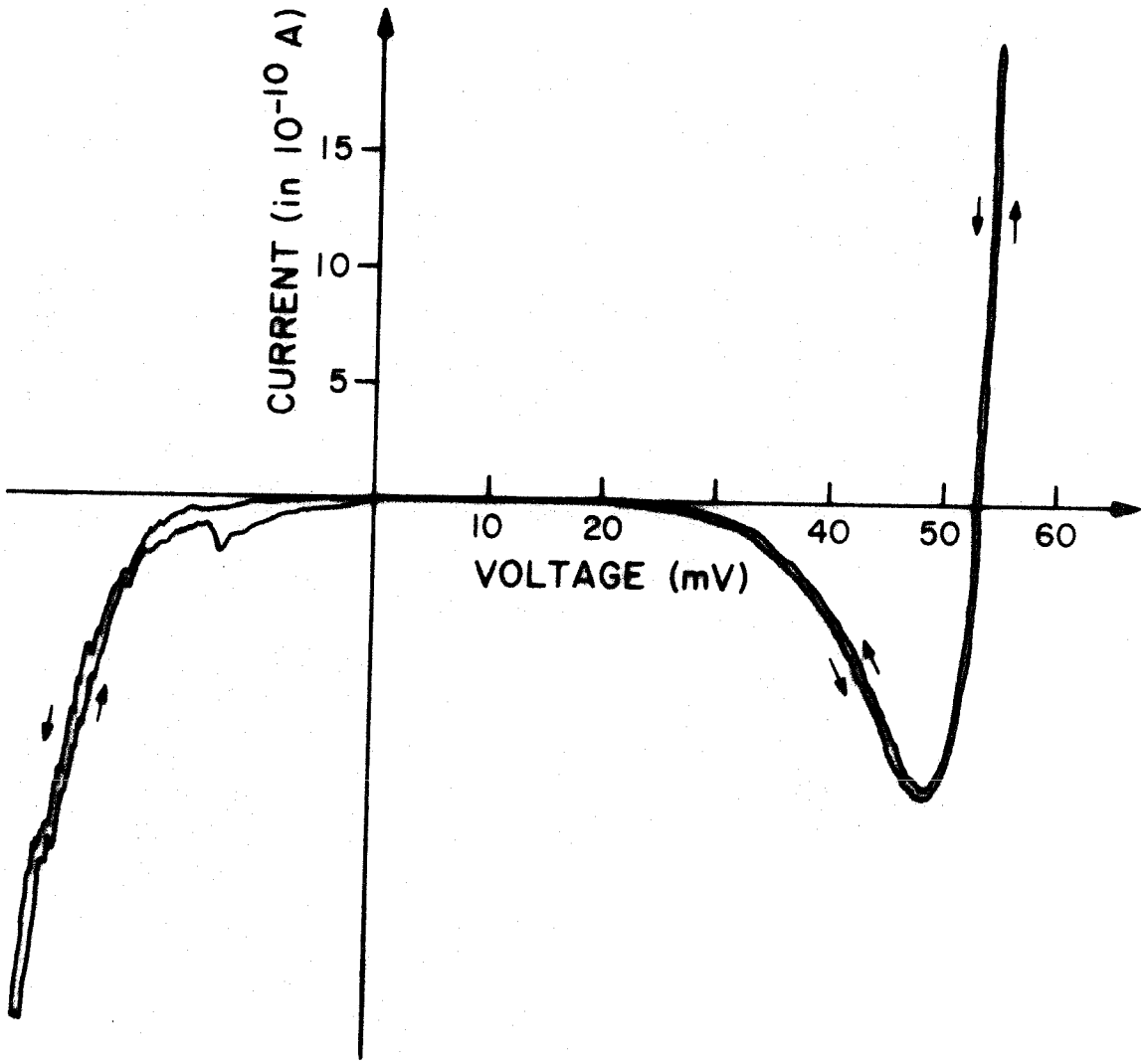

FIG. 38

III.2.17 The Interfacial Nature of the Alamethicin Interaction with PE-decane Black Membranes

As mentioned above, when alamethicin is added to the aqueous medium on one side only of an already formed membrane, the high conductance can only occur when the voltage is positive relative to the switching voltage. In other words, there is a well defined asymmetry acquired by the membrane after the addition of alamethicin on one side only. This suggests that the alamethicin molecules do not diffuse across the membrane appreciably.

If in symmetric salt solutions, alamethicin is added on each side of the membrane at different concentrations, the switching voltages on each side depend only on the alamethicin concentrations on that side.

We have also noticed the independence of the alamethicin induced conductance from each side by studying the inter-patch kinetics. Under symmetrical conditions, that is, equal salt and alamethicin concentration on both sides, the voltage was pulsed for the same length of time and to the same voltage level, in a step pulse. The kinetics of the development of the conductance showed that upon reversal of the voltage sign, the conductance drops to almost bare membrane level, and develops again in the usual manner (fig. 39).

Finally, a three-chambered, two-membrane set-up, shown schematically in fig. 40, was used to further test the strong restriction of the alamethicin molecules to the membrane interface on the side to which the drug was added.

Initially, PE-decane membranes were formed in both septa separat-

Fig. 39. (Top) Symmetric voltage pulses to a PE-decane black film in 1.0 M NaCl and 10^{-6} gr/ml alamethicin on both sides. (Bottom) Current response. The capacitance spikes are large and go off scale.

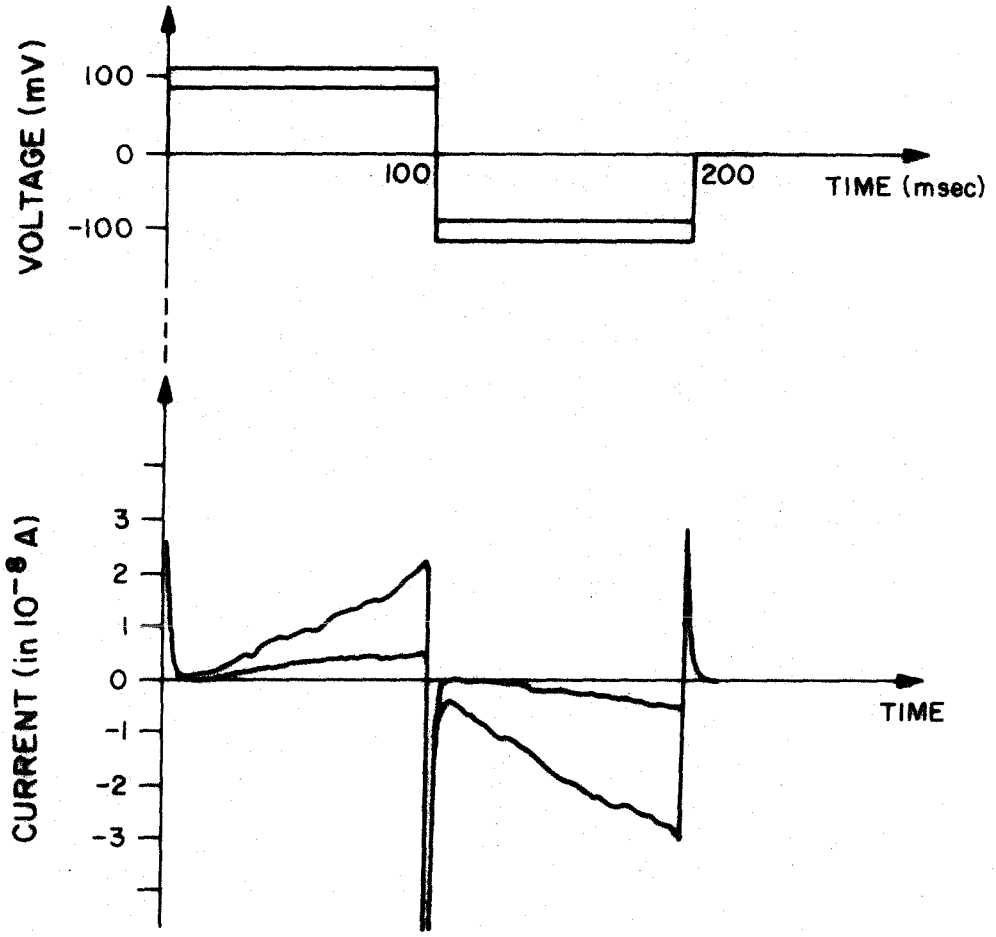
VOLTAGE (mV)
100
0
-100
100
200
TIME (msec)
CURRENT (in 10^{-8} A)
3
2
1
0
-1
-2
-3
TIME

FIG. 39

Fig. 40. Schematic drawing of three chambered, two-membrane, set-up. V is the low impedance voltage source, A is the current measuring apparatus. S is a switch which can short the silver-silver chloride electrodes across either membrane. When S is in position C, then one is measuring the current-voltage characteristics of the membrane between chambers 1 and 2, while the membrane between chambers 2 and 3 is clamped at 0 volts. S in position B gives the opposite situation.

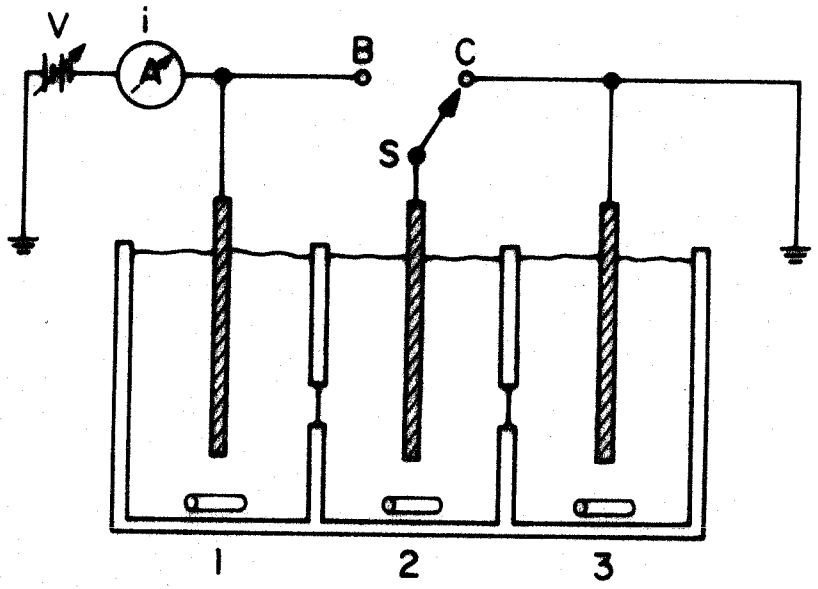

FIG. 40

ing the three chambers, containing 0.1 M KCl solutions. 10^{-6} gr/ml of alamethicin was then added to chamber 1 only. Fig. 41a shows schematically the expected localization of the alamethicin (open circles) and the observed i-V curves of membranes 1,2 and 2,3. High conductance was induced only on membrane 1,2 and only when chamber 1 was positive relative to chamber 2. Subsequently the membrane 1,2 was broken by poking with a small clean Pasteur pipette, and reformed within two seconds, thus allowing practically no inter-chamber diffusion. Fig. 41b shows that high conductance still was only induced on membrane 1,2, but now, either when chamber 1 was positive or negative relative to chamber 2. This is what would be expected if some of the alamethicin on the 1-side of membrane 1,2 had been transferred to the 2-side of the same membrane, during the breaking-respreading operation (see open circles). The chambers were vigorously stirred for 30 min., and i-V curves were taken, the situation remained the same as described in fig. 41b. This strongly suggests that the alamethicin once on the interface stays there.

Fig. 41. Experiment with two membranes in set-up described in fig. 40. (a) Initial conditions: All chambers at 0.1 M KCl, chamber 1 only, 10^{-6} gr/ml alamethicin. i-V curve of membrane 1,2 shows high conductance only when chamber 1 is positive relative to chamber 2. i-V curve of membrane 2,3 just like for bare membrane. (b) Final conditions, after membrane 1,2 has been purposely broken and reformed within a couple of seconds. i-V curve of membrane 1,2 shows alamethicin induced high conductance as though alamethicin had been added from both sides. i-V curve of membrane 2,3 remains in the low conductance state of bare membrane. The conditions described in (b) remain unchanged even after 30 min. of continuous stirring of the solutions. Small open circles stand for alamethicin.

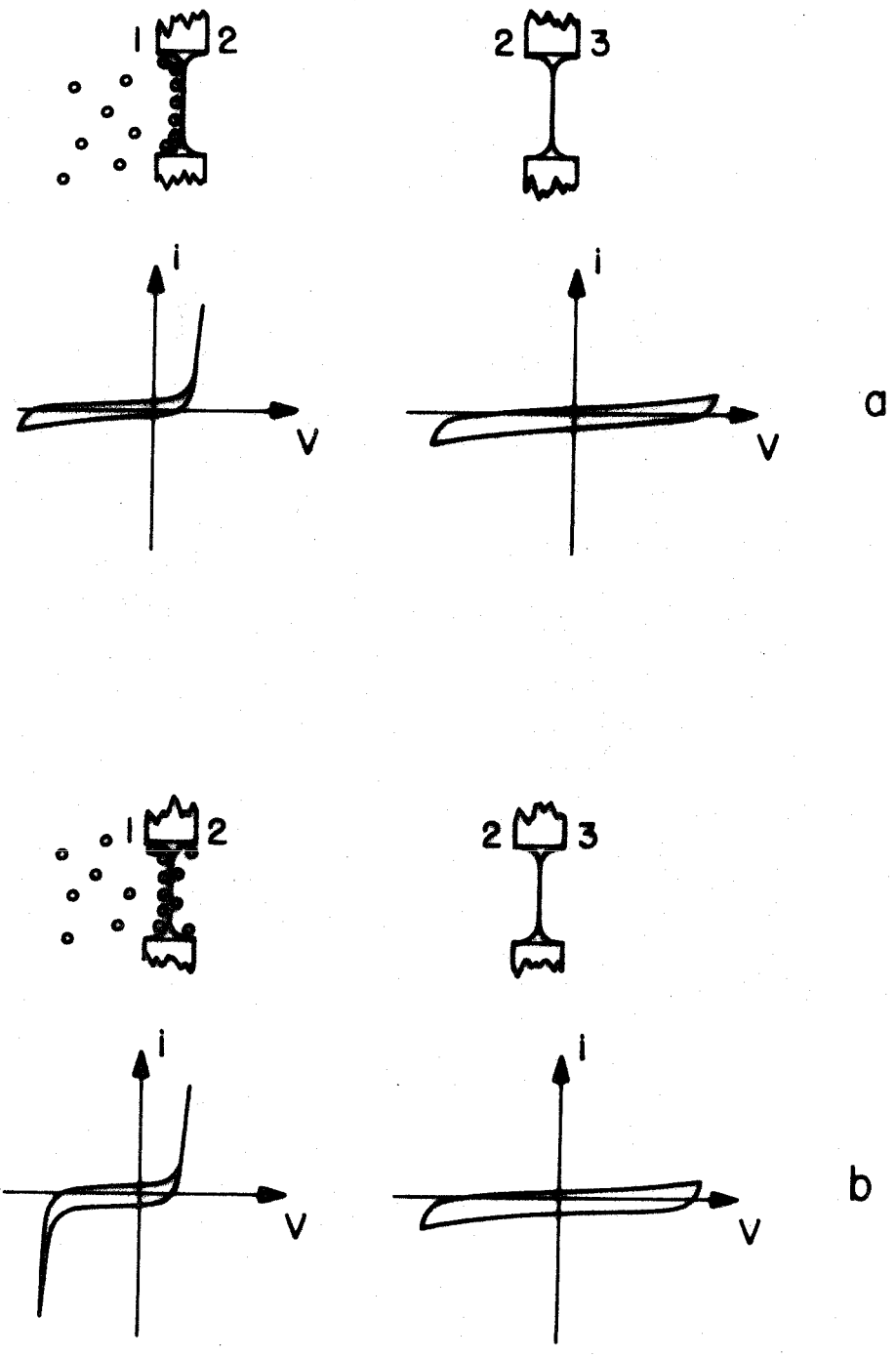

FIG. 41

IV. DISCUSSION

IV.1 General Remarks on the Alamethicin Molecule and its Behavior in the System

The amino acids of the cyclic polypeptide antibiotic alamethicin carry predominantly hydrophobic residues (fig. 2). There is an ionizable carboxyl group, the Glutamine-18 residue, which is titratable and has a pK of 5.5 (Meyer and Reusser, 1967).

Since we have no structural information for alamethicin, beyond its primary structure, the degree of steric constraint imposed is not sufficient to make a unique model, even though the ring closure severely limits the possible conformations. Space filling models of the alamethicin molecule can be built, in which the hydrophobic chains point outward from the center of a planar ring, and the carbonyl groups are directed inward. Alternatively, a model can be built so that one "face" of the ring is largely hydrophobic and the other hydrophilic. Regardless of the particular choice, and many are possible, alamethicin is an amphipathic molecule, and thus we expect it to have surface active properties.

A striking feature of the alamethicin ring is the relative flexibility of the Glutamine-18 residue. It readily bridges the ring and it is conceivable that both its α-carboxyl and γ-amide groups, together with the γ-amide group of the Glutamine-6 residue provide a chelating site, the flexibility of which could account for the relatively poor cation selectivity.

Not unexpectedly, from its peculiar structure, alamethicin forms lipid soluble complexes with alkali metals, over a wide pH range,

suggesting the relatively little influence of the state of ionization of the carboxyl on the complex formation (Pressman, 1968). Likewise, alamethicin is soluble in aqueous solvents, with a tendency to form micelles (see below), and more so at high pH. It would seem then that in alkali metal salt solutions, it forms complexes that are either neutral or positively charged.

The dependence on the high power of the alamethicin concentration of its induced conductance (see section III.2.12) strongly suggests that an aggregate may be responsible for the ionic translocation.

McMullen and Stirrup (1971) have indeed shown that alamethicin forms micelles even within aqueous solutions. This being the case, it becomes important to know the concentration range where the amount of the monomeric form is directly proportional to the amount of alamethicin present. The critical micellar concentration (cmc) is the upper boundary for this concentration range. Alamethicin in 0.05 M NaCl and pH 8.0 solution has a cmc of 2.4×10^{-6} M ($\sim 4.1 \times 10^{-6}$ gr/ml).

Practically all of our experiments have been done at alamethicin concentration below this measured cmc. Since we did not control the pH in most of them and the salt concentrations used were higher, it is conceivable that the cmc might be lower for our conditions. The relevant experiments on the dependence of switching voltage on alamethicin concentration (see section III.2.12) were done at 0.1 M NaCl close to (a factor of two) the condition at which McMullen and Stirrup (1971) measured their cmc. Further, those experiments gave the same results whether or not the solution was buffered to pH 7.9 by 0.005 M Tris.

Alamethicin is highly surface active, and lowers the interfacial tension between 0.05 M KCl, pH 8.0 aqueous solution and decane from ~ 50 dynes/cm by ~ 30 dynes/cm at the cmc. This reflects a very highly amphipathic characteristic of the monomeric molecule. Thus, the alamethicin molecules partition preferentially to the surfaces rather than remaining in solution. In other words, at dilutions below cmc there would be an equilibrium in the aqueous phase between the monomers and the micelles, very favorable for the former, and most of the monomers would be at the interfaces (water-air, water-container) forming a monolayer of a density dependent on the concentration of the alamethicin.

It is relevant, thus, to estimate the upper limit of the alamethicin concentration range necessary to cover all surfaces involved, with a monolayer. The surface area spanned by one alamethicin molecule is ~ 200 $\mathring{A}^2$ (Chapman et al., 1969). The total surface of a typical experimental chamber is 25 cm^2 when it contains 7 ml of solution. It would require a concentration of about $5 \cdot 10^{-7}$ gr/ml of alamethicin to completely cover all interfaces with a monolayer. This is higher than most of our actual experimental concentrations.

Therefore, we propose that the addition of alamethicin to the aqueous phase is followed by the adsorption of most of the molecules to the interfaces, among them, that between the bilayer and water. This is in agreement with the experiments discussed in section III.2.17.

In their description of the experiments on surface tension between aqueous and decane phases, McMullen and Stirrup (1971) observed a decrease in the presence of the adsorbed film, as a function of alamethicin concentration, beyond the cmc. This finding suggests that the

micelles themselves are significantly amphiphathic, and, thus, that they too prefer the interface.

One important difference between our observations and those of all other groups that have reported on alamethicin-black lipid films interactions, is that in our system, alamethicin does not diffuse appreciably across the membrane, as evidenced by the asymmetry of the current-voltage characteristics when alamethicin is added only on one side of the bilayer (sections III.2.1, III.2.17), whereas in all others, it must diffuse, since the i-V curves are only slightly asymmetric, and this asymmetry disappears as the alamethicin concentration is increased on one side only. The possibility that alamethicin might be carried through the membrane by the current must be discarded also, since far too many moles of charge move through the membrane, and thus, if alamethicin were permitted to go along with each charge, the lateral asymmetry would be gradually destroyed.

The main difference between our system and all others lies in the fatty acids of the phospholipids used. While we have used bacterial PE and bacterial PG, both having fully saturated hydrocarbon chains, other groups have used a variety of lipids, but in all cases containing unsaturated fatty acids.

It is possible that the alamethicin solubility in the oily phase of the membrane is higher for unsaturated hydrocarbons than for saturated ones, thus accounting for the observed difference. Likewise, the long-range effects of alamethicin on the mobility of the fatty acid chains observed by Hauser et al. (1971) could also be a consequence of a higher solubility of the antibiotic in the lipids they used.

At any rate, we think that this difference is an asset to our system. It is clear that in the other systems reported, there is a zero volt conductance which depends on the alamethicin concentration (Cherry et al., 1972) and is voltage independent for low voltage ranges. Although no detailed studies have been made, it is quite likely that these conductances come about as a consequence of a carrier mechanism. Therefore, the system we chose had the clear advantage of experimentally providing us with the "pure" voltage dependent conductance effect of alamethicin, not "contaminated" with a superimposed background current due to a carrier effect.

IV.2 Alamethicin Produces Pores in the Black Lipid Film

The discreteness of the ionic conductance induced by alamethicin in PE-decane black films has been shown in section III.2.2. The data show that ions are translocated through the membrane by pores of relatively fixed conformation which connect the aqueous phases on both sides of the membrane.

When acting in a channel fashion, alamethicin cannot act as a carrier of the ions in a way similar to that of nonactin (see Introduction). The mobility of the alamethicin-cation complex needed to account for the observed fluxes would be too high. Consider the lowest discrete conductance state ($\sim 2.5 \times 10^{-10}$ mho) in 1.0 M NaCl. At, say, 100 mV, the current flowing would be $\sim 2.5 \times 10^{-11}$ A or $\sim 1.6 \times 10^{8}$ ions/sec. If we assume that the thickness to be spanned is about 40 Å, then we would require a mobility of at least 5×10^{-4} $cm^2/(sec\ volts)$. This value is much too high for a carrier molecule the size of alamethicin since it is

much higher than the mobility of free ions in aqueous solution.

Assuming, on the other hand, that we are dealing with a pore, 40 Å long and that the mobility of the ions inside the pore is similar to that in bulk solution, we can get an estimate of the diameter of such a pore by using the relation

$$G = \sigma \frac{A}{\ell} \qquad (4)$$

where

G : conductance of the pore ($\sim 2.5 \times 10^{-10}$ mho)

σ : conductivity in bulk ($\sim 8.3 \times 10^{-2}$ mho/cm)

A : area of cross section of pore ($\pi d_p^2/4$)

ℓ : length of pore (~ 40 Å)

d_p : diameter of pore

and thus obtain $d_p \sim 4$ Å.

As shown in section III.2.3, the relative conductances of the discrete states for a number of different salts correlate well with their relative conductivities in bulk. The ratios of the different conductances relative to those of KCl are summarized in table 1. This correlation is in agreement with the pore model.

The ohmic nature of the conductance of the discrete levels has been described in section III.2.4. This behavior would be expected for a transmembrane hole.

The conductance dependence on the salt concentration, for the different states of the patch, is in agreement with the postulated pore mechanism. There is, though, a systematic difference between the conductance in bulk and that in the alamethicin pore, namely that in bulk

solution, the conductance increases practically linearly with concentration, whereas in the alamethicin pore the conductance g_p is of the form:

$$g = [NaCl]^{.71} \qquad (5)$$

for the first to fourth conductance states, in the concentration range 0.1 M to 1.0 M (fig. 22).

From the classical theory of dissociation we know that for a uni-univalent salt

$$\Lambda_m = F\,\alpha(\mu^+ + \mu^-) \qquad (6)$$

where Λ_m is the molar conductance, F is the Faraday constant
α is the dissociation constant
μ^+ and μ^- are the mobilities of the Na^+ and Cl^- ions, respectively.

Therefore, if we wanted to fit the pore conductance data with the simple classical theory we would have to invoke that either the dissociation constant or the mobilities are proportional to the 0.71 power of the salt concentration. Such a requirement, for the dissociation constant, would not be unrealistic since the pore is fairly small (similar effects occur even in bulk solution at high ionic strength).

Since we know too little about the physical structure of the alamethicin pore, the deviations from bulk, such as observed, are not inconsistent with the pore mechanism. A detailed explanation must remain an open problem.

As mentioned in the Introduction, the Conductance of the Gramacidin A pore follows a relation $g_p = [KCl]^{0.5}$.

Consequently, it is our belief that the conductance states of a patch are, in effect, various states of an asymmetric pore across the bilayer, formed by the interaction of alamethicin with the membrane.

IV.3 The Alamethicin Channels Are Composed of Cooperative Subunits that Form a Patch

We have shown that the onset of the alamethicin induced membrane conductance occurs in discrete steps (see section III.2.2). If the voltage is clamped at a value where only a few conductance steps can be seen (~ 5) and the current is monitored as a function of time, the first striking observation is that most of the time the current remains at the level corresponding to the conductance of the bare membrane, while at random intervals the current goes for a while into rapid fluctuations between five resolvable current levels (fig. 16), it then returns to the bare membrane level, and repeats the cycle again. This behavior is the first suggestion of grouping, since it is apparent that once the first current step appears it is always followed by rapid fluctuations through all the conductance states.

When the sizes of the conductance steps are measured (fig. 18), it is observed that for the five resolvable levels there is a reproducible pattern. The conductance of any one level is never a simple sum of lower levels. This is an indication that there is no common denominator for these levels. If the conductance steps were independent pores, the levels should be close to integer multiples of the first level. Therefore, we are led to believe that either we are dealing with groups of pores cooperating in such a way as to give this characteristic pattern or that we are dealing with <u>one</u> pore capable of existing in several

different states (for instance, one pore with five different diameters lined by various numbers of alamethicin molecules). Either way, one conceives of these conductance steps as being states of a cooperative unit. This unit we have called a patch.

The strongest evidence for the existence of a patch as a separate entity comes from the current distributions of more than 5 current levels (fig. 24, section III.2.7). In such cases it is possible to quantitatively explain both position and amplitude of all peaks in terms of combinations of the basic five levels of a patch.

Fig. 24 (top) shows a current distribution where ten discrete current levels can be resolved. At the bottom in the same figure, we have retraced in solid lines the first to fourth conductance levels of a single patch (in this case the zeroth level was not resolved), both their positions and amplitudes. They are labeled c_1, c_2, c_3, and c_4, with their relative probabilities p_1, p_2, p_3, and p_4. By adding pairwise the currents of each of these levels (above the current of the bare membrane), we have determined the positions where peaks resulting from simultaneous occurrence of levels from two patches should be found. We labeled these positions $c_{i,j}$, where i,j represent the levels of each patch. This procedure locates almost all peaks in the top figure. To locate the remaining peaks we have looked for combinations involving three simultaneous patches, and they have, indeed, proven to fit the data correctly. As for the expected amplitudes we assumed that the patches were statistically independent. The relative probabilities for the combined peaks would be given by

$$\left.\begin{aligned} p_{1,1} &= \pi_2\, p_1^2 \\ p_{1,2} &= \pi_2\, 2p_1p_2 \\ p_{1,3} &= \pi_2\, 2p_1p_3 \\ &\vdots \\ p_{4,4} &= \pi_2\, p_4^2 \end{aligned}\right\} \qquad (7)$$

where π_2 is the probability of there being two patches. The factor 2 appears for all $p_{i,j}$ with $i \neq j$ because there are two ways one can observe the simultaneous state i and state j depending from which of the two patches each of them comes. But for $i = j$, there is only one way it can happen, namely, both patches being in the same state.

In order to eliminate π_2 from eq. (7), we chose $p_{3,4}$ as given by the experimental data and normalized the amplitudes of the other second order peaks relative to its value.

The fact that they fit the data very well is an indication that, first, we are indeed dealing with a characteristic set of states of a unit called a patch, and, second, that these patches are statistically independent, thus not cooperative and therefore consisting of entities far removed from each other in the membrane (hence the name patch).

IV. 4 The Voltage Dependence of the Conductance Results from the Voltage Dependence of the Rates of Formation and Destruction of Patches

In section III.2.9, we showed that the kinetics of the onset of high conductance following a voltage pulse has a linear initial rate and reaches a saturation value. Both the initial rate and the

saturation value are strongly voltage dependent.

A simple kinetic theory that fits our data and that is easily interpretable in terms of patches can be developed.

Let us call n the number of patches, and $\bar{g}_p$ the average conductance of a single patch. Let μ be the probability of forming a patch per unit time, and λ the probability per unit time--for a patch to be destroyed.

Then, we can write, for the average number of patches:

$$\frac{d\bar{n}}{dt} = \mu - \lambda \bar{n} \tag{8}$$

integrating, we get for the initial conditions $\bar{n}(0) = 0$

$$\bar{n}(t) = \frac{\mu}{\lambda} (1 - e^{-\lambda t}) . \tag{9}$$

The steady state average current, $\bar{I}$, is given by

$$\bar{I} = \bar{n} \bar{g}_p V \tag{10}$$

where V is the voltage across the membrane therefore

$$\bar{I} = \bar{g}_p V \frac{\mu}{\lambda} (1 - e^{-\lambda t}) \tag{11}$$

To fit eq. (11) with our data (for a particular alamethicin and salt concentration), we compare separately the findings on the steady state currents and those on the rates with which the steady states are approached.

The steady state data (section III.2.9, fig. 32) require

$$\bar{I} = \bar{g}_p V \frac{\mu}{\lambda} = 2.3 \times 10^{-9} \; e^{\frac{V}{3.3}} \tag{12}$$

The rate data (section III.2.9, fig. 31) require

$$\frac{d\bar{i}}{dt} = \bar{g}_p V \mu = 6.7 \times 10^{-8} \; e^{\frac{V}{5.8}} \tag{13}$$

Dividing (12) into (13) we obtain:

$$\lambda = 29 \times e^{-\frac{V}{7.7}} . \tag{14}$$

Since $\bar{g}_p \sim 2 \times 10^{-9}$ mho, eq. (13) gives

$$\mu = 3.3 \times 10^{-2} \; \frac{e^{\frac{V}{5.8}}}{V} . \tag{15}$$

In eq. (8) through (15), V is in (mV), $\bar{i}$ is in (mA), $\bar{g}_p$ is in (mho) μ and λ are in (sec^{-1}), t is in (sec), and $\bar{n}$ is the average number of patches (dimensionless units). Eq. (14) and (15) have two coefficients each. We have not done experiments over a wide range of alamethicin concentrations to directly show the dependence of these coefficients on the drug concentration. Nevertheless, we have always found the same exponential factors where sometimes the preexponential coefficients have been different. Thus, we suspect that the exponential only contains the voltage dependence.

Our model assumes statistically independent patches. With the interpretation that μ is the probability of forming a patch per unit time and λ is the probability for a patch to be destroyed per unit time, the probability distribution of the patches, should be Poissonian, that is the probability of there being n patches, P(n), should be:

$$P(n) = \frac{\bar{n}^n e^{-\bar{n}}}{n!} \qquad (16)$$

where $\bar{n}$ is given by eq. (9).

We stated earlier that the identity of these patches is maintained up to levels of a few thousand patches. To show this, we consider the fluctuations in the number of patches as reflected by fluctuations in the current. One can show that the mean square value of the measured membrane conductance should be given by (see Appendix 2)

$$\overline{G^2} = \bar{n}\,\overline{\gamma^2} + (\overline{n^2} - \bar{n})\,\bar{\gamma}^2 \qquad (17)$$

where γ is the conductance of a single patch and $\bar{\gamma}$ the mean conductance of a patch, $\overline{\gamma^2}$ the mean of the square of the conductance, and n the number of patches. If n follows a Poisson distribution,

$$\overline{n^2} - \bar{n}^2 = \bar{n}$$

and

$$\overline{G^2} = \bar{n}\,\overline{\gamma^2} + \bar{n}^2\,\bar{\gamma}^2 .$$

We see immediately that

$$\sigma_G^2 = \overline{G^2} - \bar{G}^2 = \bar{n}\,\overline{\gamma^2} .$$

The mean conductance $\bar{G}$ (see Appendix 2) is given by

$$\bar{G} = \bar{n}\,\bar{\gamma}$$

so that

$$\frac{\sigma_G^2}{\bar{G}} = \frac{\overline{\gamma^2}}{\bar{\gamma}} .$$

Both $\bar{\gamma}$ and $\overline{\gamma^2}$ can be directly calculated from current distributions of the states of one patch, for any voltage (section III.2.7). To measure $\sigma_G^2/\bar{G}$, we have taken current distributions at several voltages, with the number of patches roughly up to 600. In these cases, the discrete states of a patch are not resolved. Table 2 shows the values obtained for $\sigma_G^2/\bar{G}$ at various voltages, and corresponding average number of patches, for 1.0 M NaCl and for 0.05 M NaCl. We have also added the calculated value of $\overline{\gamma^2}/\bar{\gamma}$ from current distribution (for 0.05 M NaCl we have extrapolated from the results of section III.2.6).

Thus, in summary, for 1.0 M NaCl

$$\frac{\sigma_G^2}{\bar{G}} = (3.20 \pm 0.27) \times 10^{-9} \text{ (mho)}$$

$$\frac{\overline{\gamma^2}}{\bar{\gamma}} = (3.05 \pm 0.20) \times 10^{-9} \text{ (mho)}$$

and for 0.05 M NaCl

$$\frac{\sigma_G^2}{\bar{G}} = (2.24 \pm 0.52) \times 10^{-10} \text{ (mho)}$$

$$\frac{\overline{\gamma^2}}{\bar{\gamma}} = (2.55 \pm 0.30) \times 10^{-10} \text{ (mho) (extrapolated).}$$

We conclude that the value of the fluctuations is in sufficiently good agreement with the predicted value, so that the concept of a patch can be considered valid even at current levels so high that discrete steps cannot be resolved.

The data above were taken at conductance levels corresponding to about 10-600 patches. Since the kinetic data provides us with the same voltage dependence of the patch formation from values corresponding to the range 5-3000 patches, we believe that it is unlikely that another mechanism is operating at higher levels.

IV.5 The Conductance and the Rate of Formation of Patches are High Power Functions of the Alamethicin and Salt Concentrations

In section III.2.12 we showed that the dependence of the switch-voltage on the alamethicin concentration is given by

$$\ell n \frac{C_{ala}}{C_m} = - \frac{V_s}{V_m} \qquad (18)$$

Where C_{ala} is the alamethicin concentration, V_s is the switching voltage, V_m and C_m are constants.

On the other hand, we have shown in the previous section that the steady state conductance from the kinetic experiments (section III.2.9) is given by

$$g = g_o e^{\frac{V}{V_o}} \qquad (19)$$

where g_o is independent of the voltage, and fixed for a given alamethicin concentration. V_o is a constant which we have measured to be 3.3 ± 0.2 mV over a wide range of alamethicin and salt concentrations.

In order to obtain the dependence of the conductance on the alamethicin concentration, we take eq. (19) and evaluate at the switching voltage, namely

$$g_s = g_o e^{\frac{V_s}{V_o}} \tag{20}$$

by eliminating V_s from (20) and (18) we obtain

$$g_o = g_s\left(\frac{1}{C_m}\right)^{\frac{V_m}{V_o}} \cdot C_{ala}^{\frac{V_m}{V_o}} . \tag{21}$$

Therefore, (,,) gives us the functional form of the dependence of conductance on alamethicin concentration, namely

$$g \sim C_{ala}^{V_m/V_o} . \tag{22}$$

From fig. 35, we can measure V_m. It is 36 mV. Therefore,

$$g \sim C_{ala}^{11 \pm 1} . \tag{23}$$

A completely analogous derivation can be done to obtain the functional dependence of the conductance on the salt concentration, since the switching voltage as a function of salt concentration has the same functional relation as the dependence on the C_{ala} (section III.2.13). Since the slope, as measured from fig. 37, for the salts (NaCl, KCl, and $BaCl_2$) is 16 mV, we obtain

$$g \sim C_{salt}^{4.9 \pm 0.5} . \tag{24}$$

Thus, we propose that

$$g \sim C_{ala}^{11 \pm 1} \cdot C_{salt}^{4.5 \pm 0.5}\, e^{\frac{V}{3.3 \pm 0.2}} \tag{25a}$$

gives the conductance of a PE-decane film, V in millivolts.

Likewise, from (18) and the voltage dependence of the probability of forming a patch, per unit time (eq. (15)) we show that

$$\mu \sim C_{ala}^{6.2 \pm 0.5} \cdot C_{salt}^{2.6 \pm 0.5} . \qquad (25b)$$

Therefore, it seems clear that both the conductance and the rate μ are very strongly dependent on the alamethicin concentration.

IV.6 The Fluctuations Within the States of a Patch Are Nearly Independent of Voltage

As can be seen from fig. 26 and section III.2.7, the mean conductance of a patch is practically voltage independent. One feature of the intrapatch fluctuations is that the mean differs for different batches of PE. Nevertheless, for any one membrane forming solution, the mean is reproducible. Typically the mean state of a patch varies from 1.5 to 3.0, thus all distributions observed are peaked at some intermediate state, never at an extreme.

Likewise, the characteristic time constants, $\tau_{\uparrow}$ and $\tau_{\downarrow}$, (section III.2.8, fig. 29) are not voltage dependent, at least up to 140 mV. Again, we have observed variations on the values of $\tau_{\uparrow}$ and $\tau_{\downarrow}$ for different batches of PE, but the qualitative nature of the voltage dependence, namely that there is a trend towards slightly shorter $\tau_{\uparrow}$ and $\tau_{\downarrow}$ only at high voltages, is maintained. Typically, these characteristic times are shorter than 60 msec, and can be as short as a fraction of a millisecond.

The observation that the distribution of the $\tau_{\uparrow}$ and $\tau_{\downarrow}$ can be fitted by one exponential decay (section III.2.8, fig. 28) for each,

suggests the possibility that this mechanism arises from some simple model. We have tried two models.

First, if we assume that the states of a patch have equal transition probabilities for a transition up, regardless of the state (the highest state excluded) and equal probabilities for a transition down, regardless of the state (the lowest state excluded), then the probability distributions of finding the patch in a given state are monotonic and will peak in the lowest or highest state depending on whether $\tau_{\uparrow}$ is smaller or larger than $\tau_{\downarrow}$. Since this is in contradiction with our observed distributions, this model can be excluded.

Another simple model would be to consider that the states of a patch arise from the simultaneous occurrence of statistically independent fluctuations of subunits, each with two states "on" and "off."

Consider the general case, of n subunits. If the probabilities for "on" and "off" transitions have characteristic times τ_{on} and τ_{off}, then the probability of finding any one of these subunits in the "on" state is

$$p = \frac{1}{1 + \frac{\tau_{off}}{\tau_{on}}} \quad . \tag{26}$$

The aggregate of n subunits has n+1 states. State i is defined by any i out of the n subunits in the "on" state, all the others in the "off" state. The probability, π_i, of being in the state i is given by the binomial distribution

$$\pi_i = \frac{n!}{(n - i)!\, i!}\, p^i (1 - p)^{n-i} \quad . \tag{27}$$

We calculate the probability per time unit $P_\uparrow$ that from any state i (except the highest) there occurs an upward transition to state i+1, and similarly the probability per time unit $P_\downarrow$, from any state (except for the lowest) there occurs a downward transition. We obtain

$$P_\downarrow = \frac{np}{1-(1-p)^n} \cdot \frac{1}{\tau_{on}} =: \frac{1}{\tau_\downarrow} \tag{28}$$

$$P_\uparrow = \frac{n(1-p)}{1-p^n} \cdot \frac{1}{\tau_{off}} =: \frac{1}{\tau_\uparrow} \tag{29}$$

(26), (28), and (29) imply

$$\frac{\tau_\uparrow}{\tau_\downarrow} = \frac{1-p^n}{1-(1-p)^n} \tag{30}$$

and the average state should be

$$\bar{g} = np \, . \tag{31}$$

Since $\tau_\uparrow$, $\tau_\downarrow$ and $\bar{g}$ are experimentally measurable quantities in our system, we can insert the observed values and solve (30), (31) for n and p. $\frac{\tau_\uparrow}{\tau_\downarrow} \sim 2$ and $\bar{g} \sim 1.5$ give no solutions for the system (30), (31).

Alternatively, if we postulate that n=4, since we only observe five states in a patch, then (31) => p = .375 (30) => $\tau_\uparrow/\tau_\downarrow \sim 1.15$ in contradiction to observed values which are around 2. Therefore this simple model must be excluded as well. Although detailed analyses of other models which would invoke some sort of cooperativity between the states have not been evaluated it would be possible to get a fit, due

to the number of parameters that would have to be varied. We propose to leave this elaboration an open question subject to further investigation.

REFERENCES

Andrews, D. M., E. D. Manev, and D. A. Haydon (1970).

"Composition and Energy Relationships for Some Thin Lipid Films, and the Chain Conformation in Monolayers at Liquid-Liquid Interfaces." Special Discussion of the Faraday Soc., 1:46-56.

Bangham, A. D. (1968).

"Membrane Models with Phospholipids." From "Progress in Biophysics and Molecular Biology." J.A.V. Butler and D. Noble, Ed., Pergamon Press.

Barfort, P., E. R. Arguilla, and P. A. Vogelhut (1968).

"Resistance Changes in Lipid Bilayers: Immunological Applications." Science, 160:1119-112.

Bean, R. C., W. C. Shepherd, H. Chan, and J. T. Eichner (1969).

"Discrete Conductance Fluctuations in Lipid Bilayer Protein Membranes." J. Gen. Physiol., 53:741.

Bean, R. C. (1972).

"Multiple Conductance States in Single Channels of Variable Resistance Lipid Bilayer Membranes." J. Membrane Biol., 7:15-28.

Boheim, G. (1972).

"Erregbarkeit Schwarzer Lipid-Membranen." Thesis, RWTH Aachen, Germany.

Burge, B. W. and J. H. Strauss, Jr. (1970).

"Glycopeptides of the Glycoprotein at Sindbis Virus." J. Mol. Biol., 47:449-466.

Branton, D. (1969).

"Membrane Structure." Ann. Rev. of Plant Physiol., 20:209-238.

del Castillo, J., A. Rodriguez, C. A. Romero and V. Sanchez (1966).

"Lipid Films as Transducers for Detection of Antigen-Antibody and Enzyme-Substrate Reactions." Science, 153:185.

Chapman, D., R. J. Cherry, E. G. Finer, H. Hauser, M. C. Phillips, and G. G. Shipley (1969).

"Physical Studies of Phospholipid/Alamethicin Interaction." Nature, 224:692-694.

Chapman, D. (1970).

"The Chemical and Physical Characteristics of Biological Membranes." In "Membranes and Ion Transport." Ed. by E. E. Bittar. Wiley-Interscience, Publ.

Cherry, R. J., D. Chapman, and D. E. Graham (1972).

"Studies on the Conductance Changes Induced in Bimolecular Lipid Membranes by Alamethicin." J. Membrane Biol., 7:325-344.

Delbrück, M. (1971).

"Lipid Bilayers as Models of Biological Membranes." From "The Neurosciences, Second Study Program: F. A. Schmitt, ed. Rockefeller Univ. Press, N.Y.

Duax, W. L., H. Hauptman, C. M. Weeks, and D. A. Norton (1972).

"Valinomycin Crystal Structure Determination by Direct Methods." Science, 176:911-914.

Ehrenstein, G., H. Lecar, and R. Nossal (1970).

"The Nature of the Negative Resistance in Bimolecular Lipid Membranes Containing Excitability Inducing Material." J. Gen. Physiol.,

55:119.

Eisenman, G., S. M. Ciani, and G. Szabo (1968).

"Some Theoretically Expected and Experimentally Observed Properties of Lipid Bilayer Membranes Containing Neutral Molecular Carriers of Ions." Federation Proc., 27:1289-1309.

Eng, L. F., F. C. Chao, B. Gerstl, D. Pratt, and M. G. Tavaststjerna (1968).

"The Maturation of Human White Matter Myelin. Fractionation of the Myelin Membrane Proteins." Biochem., 7:4455.

Fettiplace, R., D. M. Andrews, and D. A. Haydon (1971).

"The Thickness, Composition, and Structure of Some Lipid Bilayers and Natural Membranes." J. Membrane Biol., 5:277-297.

Finer, E. G., H. Hauser, and D. Chapman (1969).

"Nuclear Magnetic Resonance Studies of Interactions of Phospholipids with Cyclic Antibiotics." Chem. Phys. Lipids, 3:386-392.

Finkelstein, A. (1970)

"Weak Acid Uncouplers of Oxidative Phospharylation: Mechanism of Action on Thin Lipid Films." Biochim. Biophys. Acta, 205:1.

Finkelstein, A., and A Cass (1968).

"Permeability and Electrical Properties of Thin Lipid Membranes." J. Gen. Physiol., 52:145s-172s.

Frye, L. D. and M. Edidin (1970).

"The Rapid Intermixing of Cell Surface Antigens after Formation of Mouse-Human Heterokaryons." J. Cell. Sci., 7:319-333.

Goodal, M. C. (1970).

"Structural Effects in the Action of Antibiotics on the Ion Permeability of Lipid Bilayers: III. Gramicidins "A" and "S," and Lipid Specificity." Biochim. Biophys. Acta, 219:471.

Goodal, M. C. (1972).

"Structural Effects in the Action of Antibiotics on the Ion Permeability of Lipid Bilayers: IV. Mechanism of Autocatalytic Behavior." Biochim. Biophys. Acta, in press.

Gordon, L. G. M., and D. A. Haydon (1972).

"The Unit Conductance Channel of Alamethicin." Biochim. Biophys. Acta, 255:1014-1018.

Gotlib, V. A., E. P. Buzhinsky, and A. A. Lev (1968).

"Nature of the Cationic Specificity of Bimolecular Phospholipid Membranes with Valinomycin Introduced into Them." Biophysics (USSR), Eng. Trans., 13:675-680.

Hall, J. E., C. A. Mead, and G. Szabo (1972).

"A Barrier Model for Current Flow in Lipid Bilayer Membranes." J. Membrane Biol., accepted for publication.

Harris, E. J. (1968).

"Some Responses of Artificial Membranes and Mitochondria to Permeability Modifying Substances." From: "Membrane Models and the Formation of Biological Membranes." Ed. by L. Bolis and B. A. Pethica. North Holland, Amsterdam, publ.

Hauser, H., E. G. Finer, and D. Chapman (1970).

"Nuclear Magnetic Resonance Studies of the Polypeptide Alamethicin and Its Interaction with Phospholipids." J. Mol. Biol., 53:419-433.

Haydon, D. A. (1970).

"The Organization and Permeability of Artificial Lipid Membranes." From "Membrane and Ion Transport." Ed. by E. E. Bittar. Wiley-Interscience, Publ.

Haydon, D. A. and S. B. Hladky (1972).

"Ion Transport Across Lipid Membranes." Quart. Rev. Biophys., 5:505.

Hille, B. (1970).

"Ionic Channels in Nerve Membranes." Progr. Biophys. Mol. Biol., 21:1-32.

Hladky, S. B. and D. A. Haydon (1972).

"Ion Transfer across Lipid Membranes in the Presence of Gramicidin A. I: Studies of the Unit Conductance Channel." Biochim. Biophys. Acta, 274:294-312.

Hladky, S. B. and D. A. Haydon (1970).

"Discreteness of Conductance Change in Bimolecular Lipid Membranes in the Presence of Antibiotics." Nature, 225:41.

Hodgkin, A. L., A. F. Huxley, and B. Katz (1952).

"Measurement of Current-Voltage Relations in the Membrane of the Giant Axon of Loligo." J. Physiol., 116:424-448.

Hodgkin, A. L. and A. F. Huxley (1952).

"A Quantitative Description of Membrane Current and Its Application to Conduction and Excitation in Nerve." J. Physiol., 116:449-472.

Hopfer, U., A. L. Lehninger, and W. S. Lennarz (1970).

"The Effect of the Polar Moiety of Lipids on Bilayer Conductance Induced by Uncouplers of Oxidative Phosphorylation." J. Membrane Biol., 3:142-155.

Hopfer, U., A. L. Lehninger, and T. E. Thompson (1968).
"Protonic Conductance Across Phospholipid Bilayer Membranes Induced by Uncoupling Agents for Oxidative Phosphorylation." Proc. Nat. Acad. Sci., 59:484.

Huang, O. (1969).
"Studies on Phosphatidylcholine Vesicles. Formation and Physical Characteristics." Biochemistry, 8:344.

Huebner, J., and L. J. Bruner (1972).
"Apparatus for Measurements of the Dynamic Current Voltage Characteristics of Membranes." J. Phys. E. Sci. Instrum., 5:310.

Ivanov, V. T., I. A. Leone, N. D. Abdulaev, L. B. Senyavina, E. M. Popov, Y. A. Ovchinikov, and M. M. Shemyakin (1969).
"The Physicochemical Basis of the Functioning of Biological Membranes: The Conformation of Valinomycin and its K^+ Complex in Solution." Biochem. Biophys. Res. Comm., 34:803-811.

Kenner, G. W. and R. C. Sheppard (1958).
"α-Aminoisobutyric Acid, β-Hydroxyleucine, and γ-Methylproline from the Hydrolysis of a Natural Product." Nature, 181:48.

Kilbourn, B. T., J. D. Dunitz, L. A. R. Pioda, and W. Simon (1967).
"Structure of the K^+ Complex with Nonactin, a Macrotetrolide Antibiotic Possessing Highly Specific K^+ Transport Properties." J. Mol. Biol., 30:559-563.

Krasne, S., G. Eisenman, and G. Szabo (1971).
"Freezing and Melting of Lipid Bilayers and the Mode of Action of Nonactin, Valinomycin, and Gramicidin." Science, 174:412-415.

Kushnir, L. D. (1968).

"Studies on a Material which Produces Excitability in Bimolecular Lipid Membranes. I. Production, Isolation, Gross Identification and Assay." Biochim. Biophys. Acta, 150:285.

Läuger, P., W. Lesslauer, E. Marti, and J. Richter (1967).

"Electrical Properties of Bimolecular Phospholipid Membranes." Biocheim. Biophys. Acta, 135:20-32.

Läuger, P. and G. Stark (1970).

"Kinetics of Carrier-mediated Ion Transport Across Lipid Bilayer Membranes." Biochim. Biophys. Acta, 211:458.

Lea, E.J.A. and R. C. Croghan (1969).

"The Effect of 2,4-Dinotrophenol on the Properties of Thin Phospholipid Films." J. Membrane Biol., 1:225.

Liberman, E. A. and V. P. Topaly (1968).

"Selective Transport of Ions Through Bimolecular Phospholipid Membranes." Biochim. Biophys. Acta, 163:125-136.

Liberman, E. A., E. N. Mochova, V. P. Skulachev, and V. P. Topaly (1968).

"Effect of Uncoupling Agents of Oxidation Phosphorylation in Bimolecular Phospholipid Membranes." Biofizika, 13:188.

McLaughlin, S.G.A., G. Szabo, G. Eisenman, and S. M. Ciani (1970).

"Surface Charge and the Conductance of Phospholipid Membranes." Proc. Natl. Acad. Sci., 67:1268-1275.

McLaughlin, S. (1972).

"The Mechanism of Action of DNP on Phospholipid Bilayer Membranes." J. Membrane Biol., accepted for publication.

McMullen, A. I. (1970).

"Some Properties of the Ion Gating Polypeptide Alamethicin." Biochem. J., 119:108.

McMullen, A. I. and J. A. Stirrup (1971).

"The Aggregation of Alamethicin." Biochim. Biophys. Acta, 241:807-814.

Meyer, C. E. and F. Reusser (1967).

"A Polypeptide Antibacterial Agent Isolated from Trichoderma viride." Experimentia, 23:85-86.

Moore, C. and B. C. Pressman (1964).

"Mechanism of Action of Valinomycin on Mitochondria." Biochim. Biophys. Res. Comm., 15:562.

Mueller, P., D. O. Rudin, H. T. Tien, and W. C. Wescott (1962).

"Reconstitution of Cell Membrane Structure in vitro and Its Transformation into an Excitable System." Nature, 194:979.

Mueller, P. and D. O. Rudin (1963).

"Induced Excitability in Reconstituted Cell Membrane Structure." J. Theoret. Biol., 4:268-280.

Mueller, P. and D. O. Rudin (1967).

"Development of K^+-Na^+ Discrimination in Experimental Bimolecular Lipid Membranes by Macrocyclic Antibiotics." Biochem. Biophys. Res. Comm., 26:398.

Mueller, P. and D. O. Rudin (1968).

"Action Potentials Induced in Bimolecular Lipid Membranes." Nature, 217:713-719.

Mueller, P. and D. O. Rudin (1969).

"Translocators in Bimolecular Lipid Membranes: Their Role in Dissipative and Conservative Bioenergy Transductions." From "Current Topics in Bioenergetics," Vol. 3, Academic Press.

Myers, V.B. and D. A. Haydon (1972).

"Ion Transfer Across Lipid Membranes in the Presence of Gramicidin A. II: The Ion Selectivity." Biochim. Biophys. Acta, 274:313-322.

Pagano, R. and T. E. Thompson (1967).

"Spherical Lipid Bilayer Membranes." Biochim. Biophys. Acta, 144: 666.

Payne, J. W., R. Jakes, and B. S. Hartley (1970).

"The Primary Structure of Alamethicin." Biochem. J., 117:757-766.

Phillips, M. C., R. M. Williams, and D. Chapman (1969).

"On the Nature of Hydrocarbon Chain Motions in Lipid Liquid Crystals." Chem. Phys. Lipids, 3:234-244.

Pinkerton, M., L. L. Steinrauf, and P. Dawkins (1969).

"The Molecular Structure and Some Transport Properties of Valinomycin." Biochem. Biophys. Res. Comm., 35:512-518.

Pressman, B. C. (1968).

"Ionophorous Antibiotics as Models for Biological Transport." Fed. Proceed., 27:1283-1288.

Reusser, F. (1967).

"Biosynthesis of Antibiotic U-22,324, a Cyclic Polypeptide." J. Biol. Chem., 242:243-247.

Rouser, G., G.J. Nelson, S. Fleischer, and G. Simon (1968).
"Lipid Composition of Animal Cell Membranes, Organelles and Organs." From "Biological Membranes" , Ed. by D. Chapman. Academic Press.

Rouser, G. (1971).
"Structure of Cellular Membranes and Regulation of Their Lipid Composition." From: "Chemistry and Brain Development." Ed. by R. Paoletti and A. N. Davison. Plenum Press.

Sarges, R. and B. Witkop (1964).
"Formyl, a Novel NH_2-Terminal Blocking Group in a Naturally Occurring Peptide. The Identity of seco-Gramicidin with Desformyl-gramicidin." J. Amer. Chem. Soc., 86:1861.

Sheetz, M. P., and S. I. Chan (1972).
"Effect of Sonication on the Structure of the Lecithin Bilayer." Biochemistry, accepted for publication.

Sheetz, M. P. (1972).
"Proton Magnetic Resonance Studies of Membrane Systems." Ph.D. thesis, California Institute of Technology.

Singer, S. J. and G. L. Nicolson (1972).
"The Fluid Mosaic Model of the Structure of Cell Membranes." Science, 175:720-731.

Stark, G., B. Ketterer, R. Benz, and P. Läuger (1971).
"The Rate Constants of Valinomycin-mediated Ion Transport through Thin Lipid Membranes." Biophys. J., 11:81.

Stoeckenius, W. and D. M. Engelman (1969).

"Current Models for the Structure of Biological Membranes." J. of Cell Biology, 42:613.

Tosteson, D. C., T. E. Andreoli, M. Tieffenberg, and P. Cook (1968).

"The Effects of Macrocyclic Compounds on Cation Transport in Sheep Red Cells and Thin and Thick Lipid Membranes." Cell Membrane Biophys., 51:373s-384s.

Urry, D. W. (1971).

"The Gramicidin A Transmembrane Channel: A Proposed $II_{(L,D)}$ Helix." Proc. Nat. Acad. Sci., 68:672-676.

Urry, D. W., M. C. Goodal, J. D. Glickson, and D. F. Mayers (1971).

"The Gramicidin A Transmembrane Channel: Characteristics of Head-to-Head Dimerized $II_{(L,D)}$ Helices." Proc. Nat. Acad. Sci., 68:1907-1911.

White, S. (1970).

"Thickness Changes in Lipid Bilayer Membranes." Biochim. Biophys. Acta, 196:354-357.

White, S. H. (1972).

"Analysis of the Torus Surrounding Planar Lipid Bilayer Membranes." Biophys. J., 12:439.

Yguerrabide, J. and L. Stryer (1971).

"Fluorescence Spectroscopy of an Oriented Model Membrane." Proc. Nat. Acad. Sci., 68:1364-1368.

TABLES

Table 1. Conductance ratios for 1.0 M solutions of different chloride salts, in bulk and as observed for the conductance levels of a patch, from fig. 19.

Table 2. Calculated $\sigma_G^2/\overline{G}$ from current distributions at several voltages and corresponding number of patches. The values of $\overline{\gamma^2}/\overline{\gamma}$ obtained from the single patch distribution are also given.

Table 1

Conductance State	Conductance ratios relative to KCl				
	LiCl	NaCl	KCl	$CaCl_2$	Tris-HCl
1st	.26	.65	1	.58	.23
2nd	.50	.83	1	.73	.38
3rd	.48	.83	1	.74	.38
4th	.46	.87	1	.76	.41
Bulk solution	.48	.83	1	.77	.49

Table 2

A. 1.0 M NaCl, 6×10^{-7} gr/ml alamethicin

Voltage (mV)	$\frac{\sigma_G^2}{\bar{G}}$ (mho)	No. of patches
24	3.25×10^{-9}	57
26	2.16×10^{-9}	109
28	3.48×10^{-9}	164
30	3.71×10^{-9}	264
34	3.38×10^{-9}	664

$\left\langle \frac{\sigma_G^2}{\bar{G}} \right\rangle = 3.20 \pm 0.27 \times 10^{-9}$ mho

$\langle \overline{\gamma^2}/\bar{\gamma} \rangle = 3.05 \times 10^{-9}$ mho

—o—

B. 0.05 M NaCl, 2×10^{-6} gr/ml alamethicin

Voltage (mV)	$\frac{\sigma_G^2}{\bar{G}}$ (mho)	No. of patches
67.5	1.00×10^{-10}	10
67.5	3.13×10^{-10}	8.1
70	2.25×10^{-10}	20
70	2.23×10^{-10}	20
72	2.63×10^{-10}	31

$\left\langle \frac{\sigma_G^2}{\bar{G}} \right\rangle = 2.24 \pm 0.52 \times 10^{-10}$ mho

$\langle \overline{\gamma^2}/\gamma \rangle = 2.55 \times 10^{-10}$ mho (extrapolated)

APPENDIX 1

THE OPERATION OF THE STEP ANALYSER DEVICE

The special circuit shown in Fig. 10 allows the Princeton Applied Research Waveform Eductor (TDH-9) to be used essentially as a multichannel analyser which is capable of measuring both amplitude and time distributions. We will consider briefly the operation of the Waveform Eductor and then describe how the special circuit enables it to measure each type of distribution.

The Waveform Eductor consists basically of 100 memory capacitors which are gated sequentially to the incoming signal by a ring counter driven by a clock. The clock's square wave is externally available. In addition, the instrument generates a gate pulse at the beginning of the sequential sweep, and a ramp voltage whose amplitude is proportional to the number of the memory capacitors then gated to signal input. The ramp amplitude at the 100^{th} channel is 5 volts.

In addition, it is possible to vary the time constant of the memory capacitors by switching in different series resistances, and to vary the length of time taken for one sweep.

It is possible to initiate the sweep either internally, with a variable delay between the beginning of a new sweep and the end of the last one, or by triggering on an external signal.

We have inserted a diode in series with the input signal so that the capacitors will always charge if the input voltage is greater than the stored voltage. We always operate in a regime where the input

voltage is much greater than the stored voltage, to insure that the response is linear.

With this background, we can proceed to a description of the operation of our special circuit. We will consider first the amplitude distribution application.

From the signal-in jack the signal is amplified by a factor of 10 and filtered simultaneously by a variable cut-off low-pass filter.

The output of this first amplifier goes to the input of a sample and hold consisting of an FET gate, a 1.0 mf'd capacitor and an analog device 142B operational amplifier. The acquisition time of this circuit element is less than μsec.

The FET is made conducting during the gate pulse supplied by the TDH-9, at the beginning of the sweep. Consequently, the voltage sampled at the beginning is held throughout the sweep and continuously compared to the value of the ramp. When the ramp voltage exceeds the voltage sampled, the output of the comparator C1(LM 311) goes from zero to +5 volts.

When the mode switch S4 is in the P(A) position, the output of the LM 311 is applied to J-input of the first of a pair of J-K flip-flops. The first flip-flop has the property that when a clock pulse is applied to the clock input (CLK), the output (Q) takes the value it had before the clock, if the input is 0, and goes to logical 1, if the input is 1. The second flip-flop has the property that it passes the value of the input to the output, after a clock pulse. The net effect of the two flip-flops is to insure that there will be one and only one time immediately following the switch of the LM 311 from low to high, when

the J input to the second flip-flop (J2) and its $\overline{Q}$ output have the same value. These values are ANDed together by NAND gate plus inverter combination formed by G4 and I4. The output of this gate is ANDed together with a pulse triggered by the clock from the PAR with a duration controlled by the SN74121 monostable multivibrator, T1. This insures that the output at the "signal-out" jack will be synchronous with the gating of one and only one memory capacitor in the TDH-9 and the amount of charge stored on the capacitor will be constant for each cycle. Consequently, after many repetitions of the above cycle, with a variable amplitude wave applied to the input, the TDH-9 will have stored in its memory capacitors an amplitude probability distribution.

The voltage on a given memory capacitor will be proportional to the number of pulses it received during the measuring time. The number of pulses it received is determined by the number of times the ramp voltage just exceeded the sampled voltage, when that particular capacitor's gate is open. Consequently, the amplitude whose probability is measured by a given capacitor is proportional to the number of the capacitor, with capacitor 100 corresponding to an amplitude of 5 volts, the maximum amplitude of the ramp.

Distributions in time, instead of amplitude, may be built up in a similar manner.

Amplifier A2 differentiates the incoming signal and applies a negative going pulse to the Schmidt trigger input of the monostable multivibrator T2. The positive pulse is applied through A3 to the Schmidt trigger input of T1. Both Schmidt triggers act as level

detectors and produce an output pulse of fixed length and amplitude, when the input reaches 2 volts. Two NAND gates, G1 and G2, are wired in such a way that: (1) with both the inputs from T1 and T2 high, a situation which prevails most of the time, the output of G2 can be either high or low, G1 will be in the opposite state. (2) If G2 is low and the input to T2 triggers an output pulse from T2 to G2, G2 will go high, driving G1 low.

A subsequent pulse from T1 will drive G1 high and return G2 to the low state. Consequently, the output of the "reconstructed-waveform" jack will track a square wave input at the "signal-in" jack, assuming the differentiated signal pulses from A2 and A3 are large enough to trigger the multivibrators T1, and T2. It should be noted at this point, that if G2 or G1 is high, an output pulse from T1 or T2, respectively, will have no effect on the output state of either G1 or G2. We, thus, have circuitry which will go up once on the receipt of positive transition and will stay up, regardless of the number of subsequent positive transitions, until a negative transition occurs.

By using the external trigger mode of the TDH-9, it is possible to measure a distribution of times between positive and negative transitions, negative and positive transitions, positive and positive or negative and negative transitions. This can be accomplished by triggering the sweep on the desired type of initial transition using S3. The desired type of final transition is then determined by S4, which insures that the type of transition desired will be indicated by a zero to positive transition at the input of the first J-K flip-flop. The output of the pulse to the TDH-9 then follows in exactly the manner

described before. But now, the number of the channel which receives the pulse is proportional to the time between the triggering of the sweep and the second transition. Consequently, after many sweeps, a distribution of times is built up.

APPENDIX 2

DERIVATION OF EQ. (17), SECTION IV.4

If n is the number of patches and γ_i the conductance of the i-th patch, then the conductance of the system, G, is given by

$$G = \sum_{i=1}^{n} \gamma_i$$

since all patches are identical, all γ_i have the same mean, $\bar{\gamma}$.

For a fixed n

$$\bar{G}_n = n\,\bar{\gamma}$$

and if n is allowed to vary,

$$\bar{G} = \bar{n}\,\bar{\gamma}$$

to obtain $\overline{G^2}$ we note that

$$G_n^2 = (\gamma_1 + \gamma_2 + \cdots + \gamma_n)(\gamma_1 + \gamma_2 + \cdots + \gamma_n)$$

$$G_n^2 = (\gamma_1^2 + \gamma_2^2 + \cdots + \gamma_n^2) + (\gamma_1\gamma_2 + \gamma_1\gamma_3 + \cdots + \gamma_n\gamma_{n-1})$$

but, since γ_i and γ_j are the conductances of independent patches

$$\overline{G_n^2} = n\overline{\gamma^2} + (n^2 - n)\,\bar{\gamma}^2$$

and letting n vary $\quad \overline{G^2} = \bar{n}\,\overline{\gamma^2} + (\overline{n^2} - \bar{n})\,\bar{\gamma}^2.$